# THE MEASUREMENT AND ANALYSIS OF EARTH MOTION RESULTING FROM UNDERGROUND ROCK FAILURE

by

Noel C. Joughin

A Thesis presented to the Faculty of Engineering of the University of the Witwatersrand, Johannesburg

For the Degree of Doctor of Philosophy

August, 1966

# THE MEASUREMENT AND ANALYSIS OF EARTH MOTION RESULTING FROM UNDERGROUND ROCK FAILURE

## SUMMARY

The seismic method was used to investigate the effects of underground rock failure. This method is particularly attractive since, in principle, it is possible to locate the focus of a violent rock failure, to determine the quantity of energy radiated by the failure, and to determine the mechanism of the failure. The considerations in the design of a seismic network are given and the method of interpreting the data is also described.

The seismic network was installed at the Harmony Gold Mine in the Orange Free State, and consisted of nine seismometers linked by means of cable to a 16-channel tape-recorder. The network operated continuously, and the tape-recordings were processed on a replay machine at the Bernard Price Institute of Geophysical Research.

The accuracy with which seismic events could be located was $\pm$ 100 feet with 90 percent confidence. During the first year of recording, 3100 seismic events were located ranging in magnitude from $10^3$ ft.-lbs. to $10^8$ ft.-lbs. of radiated energy.

It was found that there were two distinct groups of seismic events. 95 percent of the events occurred at an elevation between the reef plane and a weak band of rock 300 feet above the plane, in which case 85 percent were above advancing faces and 10 percent above worked-out areas. The remaining 5 percent occurred in a confined group near

/ a dolerite ....

a dolerite sill at an elevation of about 2400 feet above the reef plane. The seismic observations were compared with some earlier strain measurements in the Ventilation Shaft. This comparison showed that the elevation of the seismic events coincided with the elevation of regions where measured extensional strains in the rock exceeded the original compressive strain in the rock. It was concluded that rock failure was limited to a zone extending to a height of approximately 300 feet above the excavation and that the zone extended laterally as the faces advanced, except that rock failure also occurred in a confined region at the dolerite sill.

A large proportion of the seismic events and damage due to rock failure occurred near those faces which were most highly stressed. Energy must be released when the size of the mine excavation increases. The energy release per unit area was compared with damage due to rock failure, seismicity and the stope labour requirements. All these factors showed a marked increase as the energy release rate increased. It was concluded that the rate of energy release is a significant parameter in predicting the magnitude of problems arising from rock failure and that these problems are easily manageable when the rate of energy release is less than $10^8$ ft.-lbs. per fathom$^2$.

There was no difference in the behaviour of seismic events of different size, except that all the events of magnitude $10^7$ ft.-lbs. and $10^8$ ft.-lbs. occurred at dykes. Although blasting triggered a large number of events, more than 50 percent occurred well outside blasting time, and the rate at which seismic events occurred fluctuated quite widely, even when the rate of mining was nearly constant.

/ The ....

The total amount of energy radiated by the seismic events was four orders of magnitude less than the calculated amount of energy released by mining.

Only a small fraction of the damage was accompanied by seismic activity, which implies that the damage was due to falls of rock which had been fractured before the rockfalls occurred. The only manner in which this type of damage can be reduced is to reduce the extent of the fracturing, by reducing the energy release rate, or by improving the type of support in the stopes.

Current theories show that some rock types can fail violently or non-violently, depending on the manner in which the rock is loaded. It is shown that these theories may explain the stable development of the fracture zone; however, the large quantities of energy that are dissipated stably can only be dissipated by friction in the fracture zone; a relatively small fracture zone is required to dissipate this energy.

Studies of the mechanism of the seismic events showed that the mechanism was some form of volumetric collapse. The mechanism of some of the seismic events could, therefore, be a sudden growth in the fracture zone, the collapse of fractured rock near the face or in worked-out areas, or the sudden failure of a volume of rock slightly removed from the excavation. The mechanism of the seismic events near the dolerite sill was not clearly resolved; it could, however, have been a shear movement.

/ APPENDIX 1.

# THE MEASUREMENT AND ANALYSIS OF EARTH MOTION RESULTING FROM UNDERGROUND ROCK FAILURE

by

Noel C. Joughin

A Thesis presented to the Faculty of Engineering of the University of the Witwatersrand, Johannesburg

For the Degree of Doctor of Philosophy

August, 1966

## DECLARATION BY CANDIDATE

I, Noel Cain Joughin, hereby declare that this Thesis is my own work and that the material herein has not been submitted by me for another degree at any other University.

N. C. Joughin

# THE MEASUREMENT AND ANALYSIS OF EARTH MOTION RESULTING FROM UNDERGROUND ROCK FAILURE

## SUMMARY

The seismic method was used to investigate the effects of underground rock failure. This method is particularly attractive since, in principle, it is possible to locate the focus of a violent rock failure, to determine the quantity of energy radiated by the failure, and to determine the mechanism of the failure. The considerations in the design of a seismic network are given and the method of interpreting the data is also described.

The seismic network was installed at the Harmony Gold Mine in the Orange Free State, and consisted of nine seismometers linked by means of cable to a 16-channel tape-recorder. The network operated continuously, and the tape-recordings were processed on a replay machine at the Bernard Price Institute of Geophysical Research.

The accuracy with which seismic events could be located was $\pm$ 100 feet with 90 percent confidence. During the first year of recording, 3100 seismic events were located ranging in magnitude from $10^3$ ft.-lbs. to $10^8$ ft.-lbs. of radiated energy.

It was found that there were two distinct groups of seismic events. 95 percent of the events occurred at an elevation between the reef plane and a weak band of rock 300 feet above the plane, in which case 85 percent were above advancing faces and 10 percent above worked-out areas. The remaining 5 percent occurred in a confined group near

/ a dolerite ....

a dolerite sill at an elevation of about 2400 feet above the reef plane. The seismic observations were compared with some earlier strain measurements in the Ventilation Shaft. This comparison showed that the elevation of the seismic events coincided with the elevation of regions where measured extensional strains in the rock exceeded the original compressive strain in the rock. It was concluded that rock failure was limited to a zone extending to a height of approximately 300 feet above the excavation and that the zone extended laterally as the faces advanced, except that rock failure also occurred in a confined region at the dolerite sill.

A large proportion of the seismic events and damage due to rock failure occurred near those faces which were most highly stressed. Energy must be released when the size of the mine excavation increases. The energy release per unit area was compared with damage due to rock failure, seismicity and the stope labour requirements. All these factors showed a marked increase as the energy release rate increased. It was concluded that the rate of energy release is a significant parameter in predicting the magnitude of problems arising from rock failure and that these problems are easily manageable when the rate of energy release is less than $10^8$ ft.-lbs. per fathom$^2$.

There was no difference in the behaviour of seismic events of different size, except that all the events of magnitude $10^7$ ft.-lbs. and $10^8$ ft.-lbs. occurred at dykes. Although blasting triggered a large number of events, more than 50 percent occurred well outside blasting time, and the rate at which seismic events occurred fluctuated quite widely, even when the rate of mining was nearly constant.

/ The ....

The total amount of energy radiated by the seismic events was four orders of magnitude less than the calculated amount of energy released by mining.

Only a small fraction of the damage was accompanied by seismic activity, which implies that the damage was due to falls of rock which had been fractured before the rockfalls occurred. The only manner in which this type of damage can be reduced is to reduce the extent of the fracturing, by reducing the energy release rate, or by improving the type of support in the stopes.

Current theories show that some rock types can fail violently or non-violently, depending on the manner in which the rock is loaded. It is shown that these theories may explain the stable development of the fracture zone; however, the large quantities of energy that are dissipated stably can only be dissipated by friction in the fracture zone; a relatively small fracture zone is required to dissipate this energy.

Studies of the mechanism of the seismic events showed that the mechanism was some form of volumetric collapse. The mechanism of some of the seismic events could, therefore, be a sudden growth in the fracture zone, the collapse of fractured rock near the face or in worked-out areas, or the sudden failure of a volume of rock slightly removed from the excavation. The mechanism of the seismic events near the dolerite sill was not clearly resolved; it could, however, have been a shear movement.

/ APPENDIX 1.

CONTENTS

FIGURES



/ ....

/ ....

# THE MEASUREMENT AND ANALYSIS OF EARTH MOTION RESULTING FROM UNDERGROUND ROCK FAILURE

## INTRODUCTION

Rockbursts have been a part of South African gold mining for more than a half-century. With the passage of time, mining methods have been evolved which have alleviated the severity of rockbursts. However, as mines become deeper, this problem threatens to become very serious. It has become obvious that empirical methods will not provide a satisfactory solution and intensive research has been launched at a better understanding of the rockburst mechanism.

In early 1963, when this study was commenced, the theories that had been proposed and the more relevant observations which had been published are as follows. The concept of a fracture dome was popular amongst most mining engineers. There was no uniformity in this theory; one form was that the rock in the dome is heavily fractured and is held up by Voussoir arches, and another was that the dome is a region in which strata separation occurs, so that the hangingwall develops into a number of beams (Biccard Jeppe).[1] There was been considerable discussion on the extent of this fracture zone; some believed that it extends right through to surface and others that it extends only a few tens of feet into the hangingwall. Denkhaus[2] attempted to predict the shape of the fracture dome by using the theory of elasticity and a maximum tensile and shear stress as a failure criterion. He concluded that the height of the fracture dome would be of the same magnitude as the span of the excavation. Barcza and von Willich[3] reported some strata movement measurements made at Harmony Gold Mine which showed the extent to which

/ movements ....

movements occurred in the hangingwall. These measurements were considered by Denkhaus, Hill and Roux[4] to demonstrate "an almost classical development of the fracture dome". Wiggill[5] introduced the concept of "macroplastic flow" into the fracture dome theory. In this concept the rock behaves according to some of the soil mechanics laws and, in addition, exhibits time dependent properties. Rockbursts were classified broadly into two categories, namely, intradosal and extradosal, i.e., bursts originating inside and outside the fracture zone respectively. Pretorius[6] has given a good description of some factors influencing the different types of rockburst. Ultrasonic techniques were used by Lutsch and Szendrei[7] to determine the extent of the fracture zone surrounding stope faces. They were able to detect fracture planes at a distance of 10 feet into the rock, and showed that the fracture intensity decreased with distance into the rock.

In an investigation into Witwatersrand Earth Tremors, Gane, Seligman and Stephen[8] found that these tremors had their origins close to mine workings. A more intensive underground seismic investigation by Cook[9] revealed that the majority of seismic events occur within 100 feet of the working face and that there were many more seismic events than manifestations of damage. Between 1963 and 1966, a change in thought became evident, the emphasis was taken off the fracture dome and turned to a small fracture zone around the excavation with the remainder of the rock being continuous and nearly elastic. Hoek[10] has demonstrated that rock behaves elastically up to fracture and that the modified Griffith theory is an adequate failure criterion under static load conditions. Ortlepp and Nicoll[11] and Ryder and Officer[12] have shown that the movements in the rock around an excavation are satisfactorily predicted by

/ elasticity ....

elasticity theory applied to a continuous rock mass. The development of electrical analogues based on elasticity theory have given additional impetus to the present popularity of this theory. Furthermore, publications by Cook[13,14,15] have led to a better understanding of the basic mechanics of rock failure and rockbursts.

The seismic technique promises to be the most fruitful observational method of attack on the rockburst problem, since it allows measurements of rock movements deep within the rock mass to be made. It has three very attractive features; it enables the focus of a violent event to be located, it enables a quantitative determination of the kinetic energy radiated by the event to be made and it is theoretically possible to determine the movements that take place at the focus. Following on the successful seismic experiment at East Rand Proprietary Mines, Limited (E.R.P.M.) it was decided to set up a second one at a different mine. The Harmony Gold Mine was selected because it was prone to rockbursts and earth tremors and the geological environment differed from that at E.R.P.M. There was also the fear that Harmony might encounter a severe rockburst problem because preliminary strength tests showed that the quartzite there was stronger than at E.R.P.M. It was thought that rock failures at Harmony might, therefore, be more violent than those at E.R.P.M.

The E.R.P.M. seismic network was designed to locate events occurring near one longwall stope. Harmony is a comparatively new mine and the worked-out area is much smaller. The new seismic network was, therefore, able to cover the entire mine so that the overall rock movement pattern could be discerned without losing too much location accuracy. In addition, this network was arranged to operate continuously.

/ CONSIDERATIONS ....

CONSIDERATIONS IN THE DESIGN OF THE SEISMIC NETWORK.

The most versatile method of recording, storing and manipulating data is by means of tape-recorders. For seismic networks, the tape-recorders must be multi-channelled to accommodate all the seismometers and time signals. The time signals take the form of a sequence of coded pulses which give the time of day at any instant. For location purposes, the most convenient type of record is a visual one, consequently the tape-recorders must drive a photographic oscillograph. It was desirable to do all data processing at the Bernard Price Institute in Johannesburg, therefore it was necessary to operate a record deck at the Harmony Mine and a re-play deck in Johannesburg.

Seismometer Layout:

When a failure or explosion occurs in rock, waves travel out radially from the disturbance. In solid, homogeneous rock there are two modes of wave propagation, namely, compressional and shear. The compressional, or P, wave travels faster than the shear, or S wave. If at a point remote from the source, the difference in times of arrival of the P and S waves can be measured, then the distance from the source to the measuring point can be calculated. For this to be done the velocities of the P and S waves must be known. In practice it is not easy to determine when the S wave arrives because it is usually obscured by the coda of the P wave, especially when the P-S interval is short. Alternatively, if there are two measuring points and the direction of the source is known, the distance of the source can be calculated using the difference in times of arrival of the P waves at the two measuring points. Consider two measuring points $S_1$ and $S_2$ separated by a distance 2d, the locus of a source point which produces a constant difference in the times of arrival (delay time) at $S_1$ and $S_2$, is a hyperbola.

/ Figure 1. ....

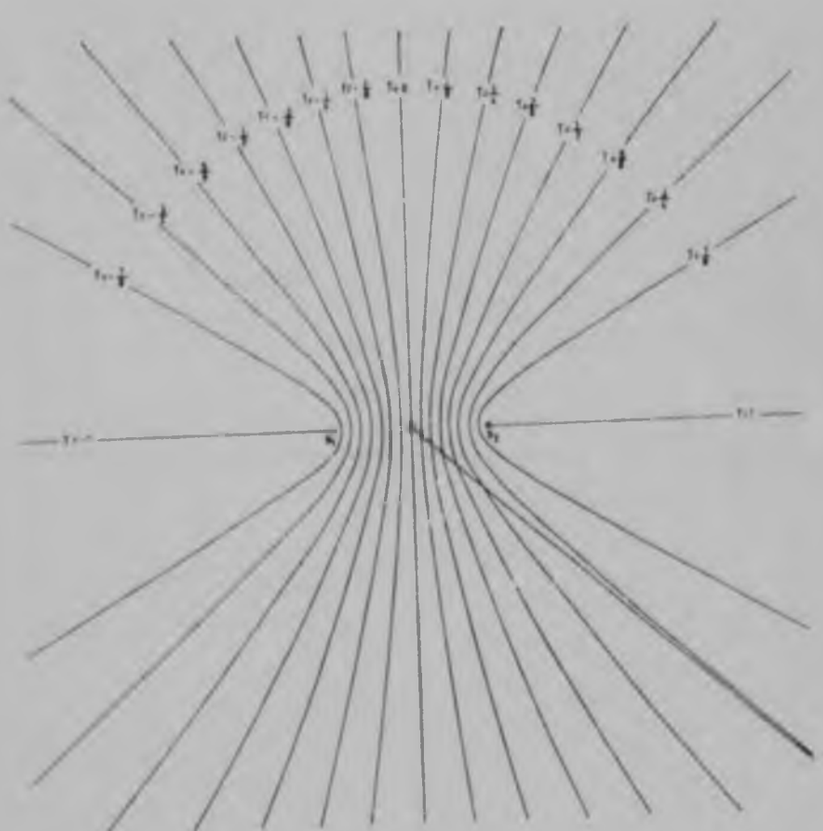

FIGURE 1 A FAMILY OF HYPERBOLAS CORRESPONDING TO DIFFERENT DELAY TIMES, T, BETWEEN SEISMOMETERS $S_1$ AND $S_2$.

Figure 1 shows a family of hyperbolas for different delay times. The curves are for equal increments in delay time, where the delay time is in dimensionless form

$$\text{Delay Time} = \frac{\alpha\, t}{2d} = T$$

$\alpha$ = P wave velocity

t = delay time in seconds

The spacing between the hyperbolas is a measure of the accuracy with which a source point can be located. Imagine a source point which can lie anywhere along a radial line from O and making an angle $\theta$ with the line $S_1S_2$. Along the line $\theta = 0$, between $S_1$ and $S_2$ the hyperbolas are normal to the radial line and are closely spaced, the resolution is best here: outside $S_1$ and $S_2$ the line is coincident with the hyperbola for T = 1, and the resolution is zero. The radial line is coincident with the hyperbola T = 0 when $\theta = 90^{\circ}$ and the resolution is again zero. In general, the resolution is best at small angles and close to the origin; the hyperbolas all become asymptotic to radial lines so that at large distances the resolution tends to zero. From Figure 1, it can be seen that three measuring points are required to obtain a unique location in a two-dimensional space, and that for good resolution, the three measuring points should lie at the corners of an equilateral triangle which encloses the source. Similarly in three dimensions, four measuring points are required to provide a unique solution, and the optimum configuration of the four points is at the corners of a tetrahedron which encloses the source. Additional measuring points surrounding the source will greatly improve the accuracy of the location. A co-planar array of measuring points will have a very poor resolution and ambiguity in a direction normal to the plane.

In selecting the sites for seismometers on the mine, the object was to enclose as much of the mine workings as possible, with tetrahedral arrays of seismometers. ....

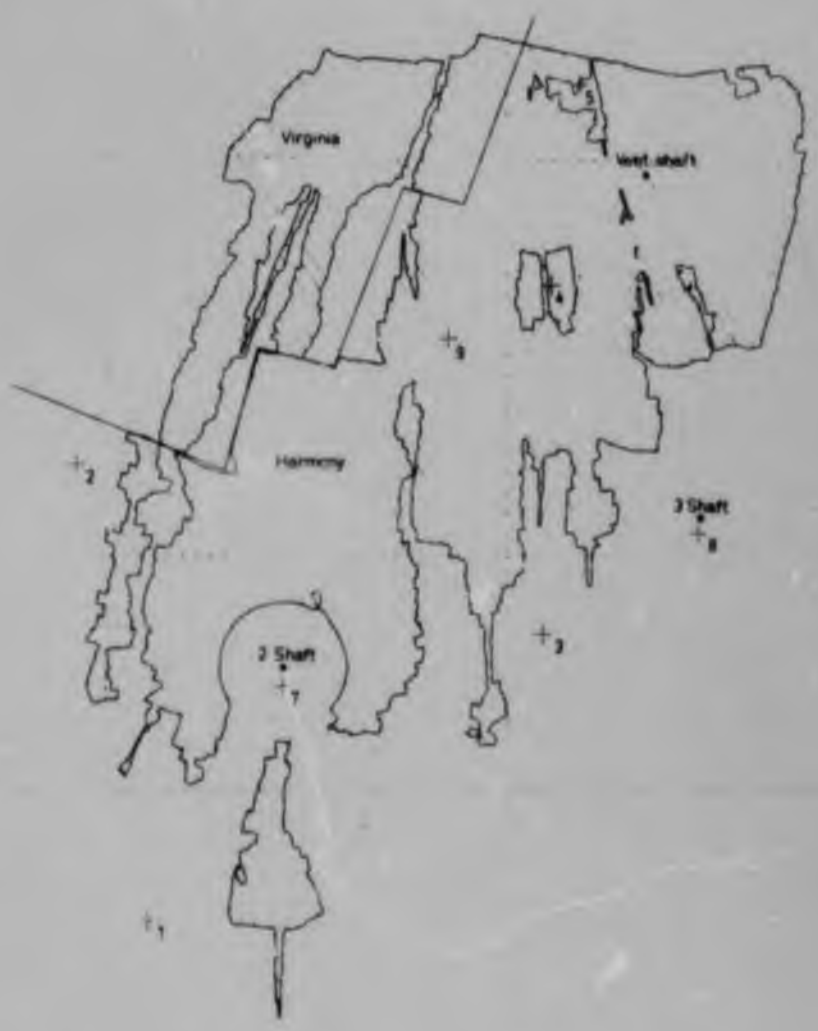


FIGURE 2 PLAN OF HARMONY ON A GRID OF 5000 FEET, SHOWING THE POSITIONS OF SEISMOMETERS 1 TO 9 AND THE BOUNDARY OF THE VIRGINIA PORTION.

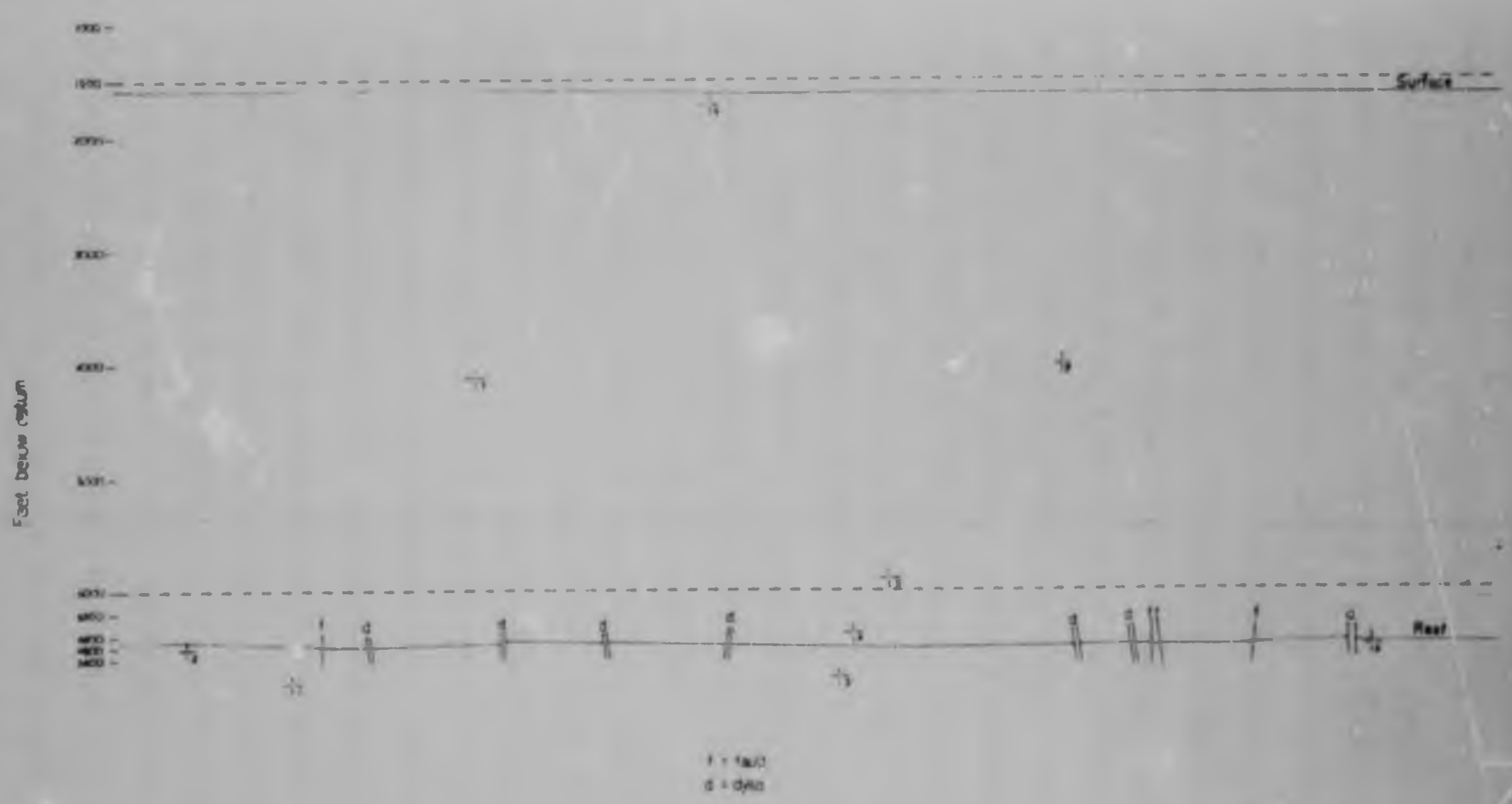


FIGURE 3 A VERTICAL SECTION THROUGH HARMONY SHOWING THE POSITIONS OF SEISMOMETERS 1 TO 9, THE SURFACE AND THE REEF PLANE.

Figure 2 and Figure 3 show the plan position and elevation of the selected seismometer sites. Seismometers 1, 2, 3, 4, 5 and 6 were all situated in haulages below the reef plane, 7 and 8 were in intermediate pump-stations half-way up shafts, and 9 was on surface. Seismometers 1, 2, 3, 7; 3, 4, 6, 8; and 2, 3, 5, 9 form three overlapping tetrahedral arrays. All the seismometers were rigidly fixed in the ends of diamond-drill holes 100 feet long, to reduce noise from activity in the haulages and to minimize wave scattering effects from the haulages. The surface seismometer was fixed in sandstone 100 feet below surface. All the seismometers were vertical except 1, 4 and 5, which detect only horizontal motion. This array also covered a portion of the neighbouring Virginia Mine. All the seismometers were linked to the tape-recorder by means of twin conductor screened cable. All the cable was carried in standard electrical conduit for protection against theft and mechanical damage. The conduit provided extra screening which was an advantage since all the cables were in close proximity with high voltage power cables. The tape-recorder was situated underground at the 17 level station, 3 shaft, so that it would not be necessary to bring a large number of cables up the shaft to surface. It was necessary to use existing telephone wire in the shafts to link the surface seismometer and the seismometers in the pump stations to the tape-recorder. This resulted in a large amount of cross-talk from telephone bell bringing, and a small amount of cross-talk between seismometers 8 and 9 which used the same telephone cable. The cross-talk from the bells was of no consequence since it rarely occurred at the same time as a seismic event. Altogether 100,000 feet of cable was used to join the seismometers to the recorder.

The seismometers were Hall-Sears, Model HS-1 with a natural frequency of 4.5 c/s. They have a sensitivity of

/ 0.5 volts ....

0.5 volts per inch per second with a 1000 ohm load. The frequency response of the seismometers is shown in Appendix 4.

Recorder Design:

The sensitivity requirements of the recording system are two-fold.

a) The first motions of the seismic events must be sharp and clear for good accuracy and for first motion studies. This implies that the recorder must have a good high frequency response and high sensitivity.

b) For energy determination and mechanism studies by means of spectral analysis, the widest possible bandwidth and low distortion are required. The most serious form of distortion is saturation distortion, therefore this requirement implies a low sensitivity. Another form of distortion which sometimes occurs in seismic amplifiers when the signal level becomes high, is blocking.

The seismic experiment at E.R.P.M. revealed that the magnitudes of the seismic events that could be satisfactorily located ranged from $10^3$ ft.-lbs. to $10^9$ ft.-lbs., and that most energy was carried in the 20 c/s to 100 c/s frequency range. The range in the energy of the events to be expected is $10^6$. Since the energy is proportional to the square of the particle velocity and since seismometers are sensitive to particle velocity, the range in output from the seismometer will be $10^3$ or 60 db. It was also found that the first motion of a $10^3$ ft.-lb. event at a distance of a few thousand feet from the seismometer caused an output of 10 μV from the seismometer. The lower limit to the bandwidth was set by the seismometer which had a cut-off just below 4.5 c/s. The upper limit was set by attenuation of seismic waves in rock; over a distance of 4000 feet, the

/ attenuation ....

attenuation of a 1000 c/s wave is 20 db more than that of a low frequency wave, there was clearly no point in attempting to record waves of nigher frequency.

Finally, the recorder was situated underground and it was convenient to give it attention only once a day and therefore the tape had to play for 24 hours. The re-play machine had to run at a higher speed than the record machine so that the tapes could be played back in a normal working day. A re-play speed four times higher than the record speed was selected; this had the advantage that the output from the re-play heads was four times higher; however, the signal frequency was also four times higher, and this posed difficulties in transcribing to a visual record. The longest 1.5 mil tape available was 5000 ft. long, so that the record speed had to be 0.6 ins. per sec.

The specifications of the recording system were:

a) Record speed 0.6 ins/sec.
b) Re-play speed 2.4 ins/sec.
c) At least 10 channels
d) Dynamic range of 60 db.
e) Sensitive to 10 μV signal input.
f) Frequency response from 4 to 1000 c/s.
g) Blocking must not occur in the amplifiers.
h) Compromise between high sensitivity and cut-off distortion.

No standard tape-recorders were available with these specifications and the cost of modifying standard machines was found to be prohibitive. Consequently machines had to be designed and built. The basic features of this design were kept similar to those of the recorder at E.R.P.M., so that tapes recorded at E.R.P.M. could be processed on the new equipment if necessary. The tape transport system was identical with the E.R.P.M. system, except for a change in

/ the tape ....

the tape tensioning arrangement. The record-replay heads were also identical with the E.R.P.M. recorder; they were E.M.I. 16-track heads for a one inch tape. The record-replay characteristic of these heads was 20 db down at 4 c/s and 1000 c/s record frequency, when the tape speed was C.6 in/sec. on record and 2.4 in/sec. on replay. Since the desired bandwidth was 4 c/s to 1000 c/s, it was not possible to make use of modulation techniques because an even larger bandwidth would have been necessary.

In general, sophisticated techniques are required to obtain a signal to noise ratio of 40 db. at low tape speeds, therefore a dynamic range of 60 db could be attained by using two channels, one with a gain 30 db less than the other, and each having a signal to noise ratio of at least 30 db. The E.R.P.M. recorder used D.C. Biasing which resulted in a signal to noise ratio of 30 db. A.C. biasing could have provided an improvement in the signal to noise ratio and a slight improvement in the linearity at the expense of more complex electronic circuiting and a poorer high frequency response. A.C. Biasing is more critical to adjustments while D.C. biasing is more prone to low frequency noise caused by dust particles on the tape. D.C. biasing was selected for the Harmony recorder since it provided the adequate signal to noise ratio of 30 db and a total harmonic distortion of less than 5 percent.

There were 16 tracks available, nine were allocated to high sensitivity channels for each seismometer, six to low sensitivity channels for selected seismometers, and one to time signals.

Blocking of the amplifiers was circumvented by not using capacitors as coupling elements between the amplifier stages. Since a good low frequency response was required, the amplifier stages were direct coupled. The imput and output

/ signal ....

signal levels on the record and replay sides were identical, so that the record and replay amplifiers were made identical, except for equalization in the replay amplifiers. The first two stages were differential amplifiers which have good linearity and good stability. The final stages were a common emitter stage and a driver stage for driving the 3 ohm heads, in the case of the recorder, and 15 ohm galvanometers, in the case of the replay deck. A circuit diagram is shown in Appendix 4.

On installing the recorder in the mine, two difficulties arose. The first difficulty, which was anticipated, was that 50 c/s pickup from the mine power supply necessitated the first stage of the amplifier being placed at the seismometer. The second difficulty was the appearance of a slowly varying D.C. voltage on the cable from the seismometers to the recorders. The source of this voltage was never identified; however, it appeared to be related to underground electric locomotives. This voltage upset the operation of the direct coupled amplifier stages, and coupling transformers had to be introduced at each end of the cable.

The oscillograph used was a Hall-Sears 24-channel galvanometer type, the natural frequency of the galvanometers was 500 c/s. The record was produced on 10-inch wide photographic paper. The maximum paper speed was 15 ins/sec.

It was necessary to know the time at which seismic events occur so that they could be correlated with mining activity, rockbursts and earth tremors. A digital clock was designed for this purpose. The clock produced a sequence of ten binary coded pulses repeated three times a second. The first pulse was a marker pulse and was slightly bigger than the others, the remaining nine pulses divided the day into $2^9$ parts, i.e., approximately 2.8 minutes. The clock therefore gave the time to the nearest 1.4 minutes.

/ FIGURE 4. ....

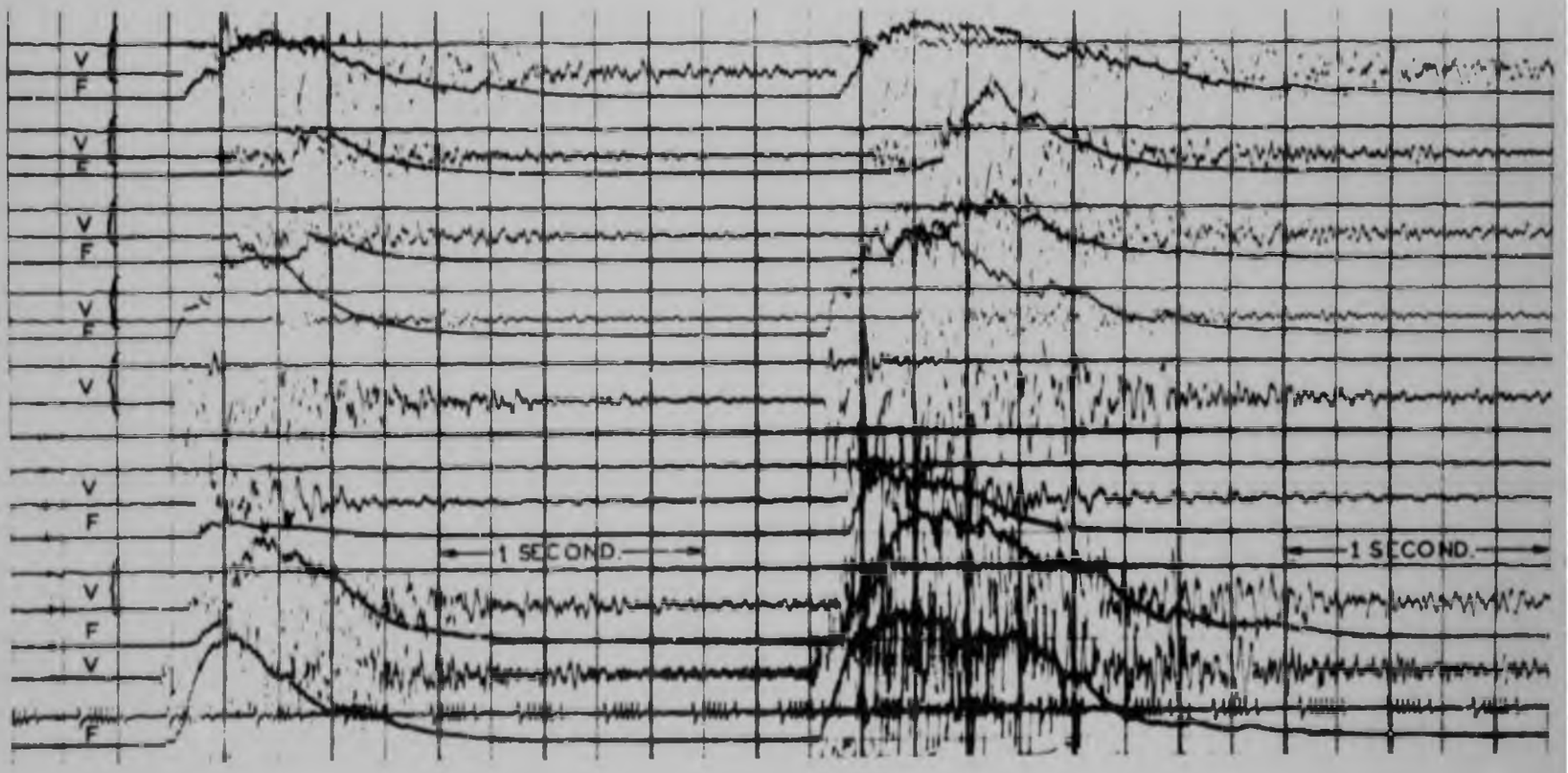


FIGURE 4 RECORD OF TWO SEISMIC EVENTS SEPARATED BY 2¼ SECONDS. TRACES MARKED V ARE PARTICLE VELOCITY, AND TRACES MARKED F ARE ENERGY FLUX. THE PULSED TRACE REPRESENTS THE TIME IN CODE.

In Figure 4, the second trace from the bottom is the time trace and the code indicates that the time is 11.03 a.m. The spacing between the pulses was 25 milliseconds, so that the clock also served as a frequency reference in order to check that the speed of the record deck, the replay deck and the oscillograph remained constant. The time code also served as a position reference along the length of the tape; for example, if it was desired to re-examine a seismic event for further processing, it was an easy matter to find the event by looking for the time at which it occurred.

The heads on the record deck were aligned relative to the heads on the replay deck such that when a pulse was simultaneously applied to all channels on the record deck, the stagger between signals on a time base was less than one millisecond on the photographic record. Each channel of the entire recording system was calibrated for amplitude and frequency response and sense of first motion. Standard signals from a low impedance signal generator were applied in parallel with each seismometer in the mine, so that the entire system was calibrated. To calibrate for sense of first motion, positive pulses were applied to the positive terminals of the seismometers and the direction of motion of the oscillograph trace was observed. Figure 5 shows the overall frequency response of the system, including the frequency response of the seismometers. The bandwidth was narrower than intended; however, it was adequate for energy determinations and spectral analysis, since most of the energy is carried in the 20 to 100 c/s range.

/ FIGURE 5. .....

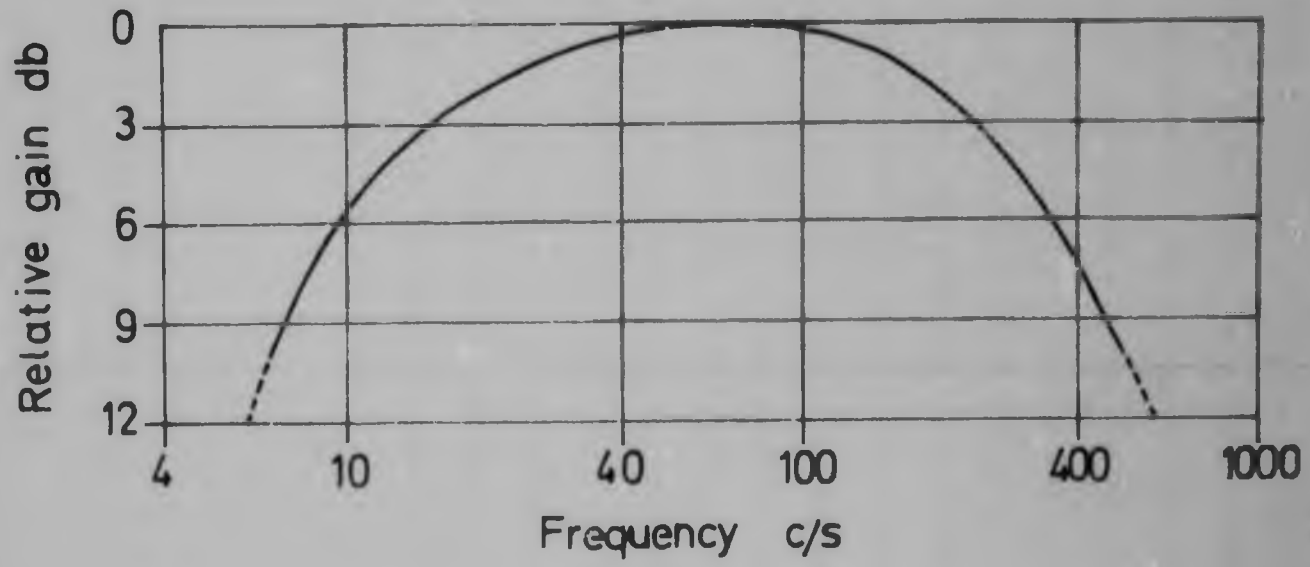


FIGURE 5 THE FREQUENCY RESPONSE OF THE ENTIRE RECORDING SYSTEM, INCLUDING THE FREQUENCY RESPONSE OF THE SEISMOMETER.

An elaborate trigger system was built into the replay system. The purpose of the trigger was to set the oscillograph in motion whenever an event occurred, so that the event could be recorded automatically. It was intended that the trigger should select only events that could be located, therefore a trigger was produced only when there was a signal present on four or more channels and on condition that these signals occurred within 1/8 second of each other. (1/8 second was the replay travel time of a P wave between the most widely spaced seismometers). The trigger operated satisfactorily in selecting seismic events recorded on the magnetic tape; however, it was rejected because numerous false triggers resulted at blasting time in the mine and from transients probably caused by the stopping and starting of electric locomotives underground. Monitoring by ear was found to be superior; seismic events were readily distinguishable from other signals and with a little experience it was possible to estimate the magnitude of the event.

It was also found that playing the tape back in 6 hours or 4 times recording speed, resulted in a build-up of unplayed tapes. The replay speed was changed to 8 times the recording speed for monitoring purposes, and when a seismic event occurred, the speed was switched back to 4 times for making the photographic record.

/ DATA PROCESSING. ....

DATA PROCESSING

The location of Seismic Events

The method of locating seismic events has been described by Cook[9]. The method makes use of a device known as the "locator", Figure 6. The locator is an analogue computer and is a spatial scale model of the seismometers in the mine. The tips of the vertical rods represent to scale the positions of the seismometers. Strings pass up each rod and run over pulleys so that they hang down in front of a scale on the wall. The scale is calibrated in feet and each division represents 200 feet. A string can be pulled out from each seismometer position and the length that is pulled out can be measured by the motion of an indicator attached to the string, as it moves over the scale on the wall.

/ FIGURE 6. ....

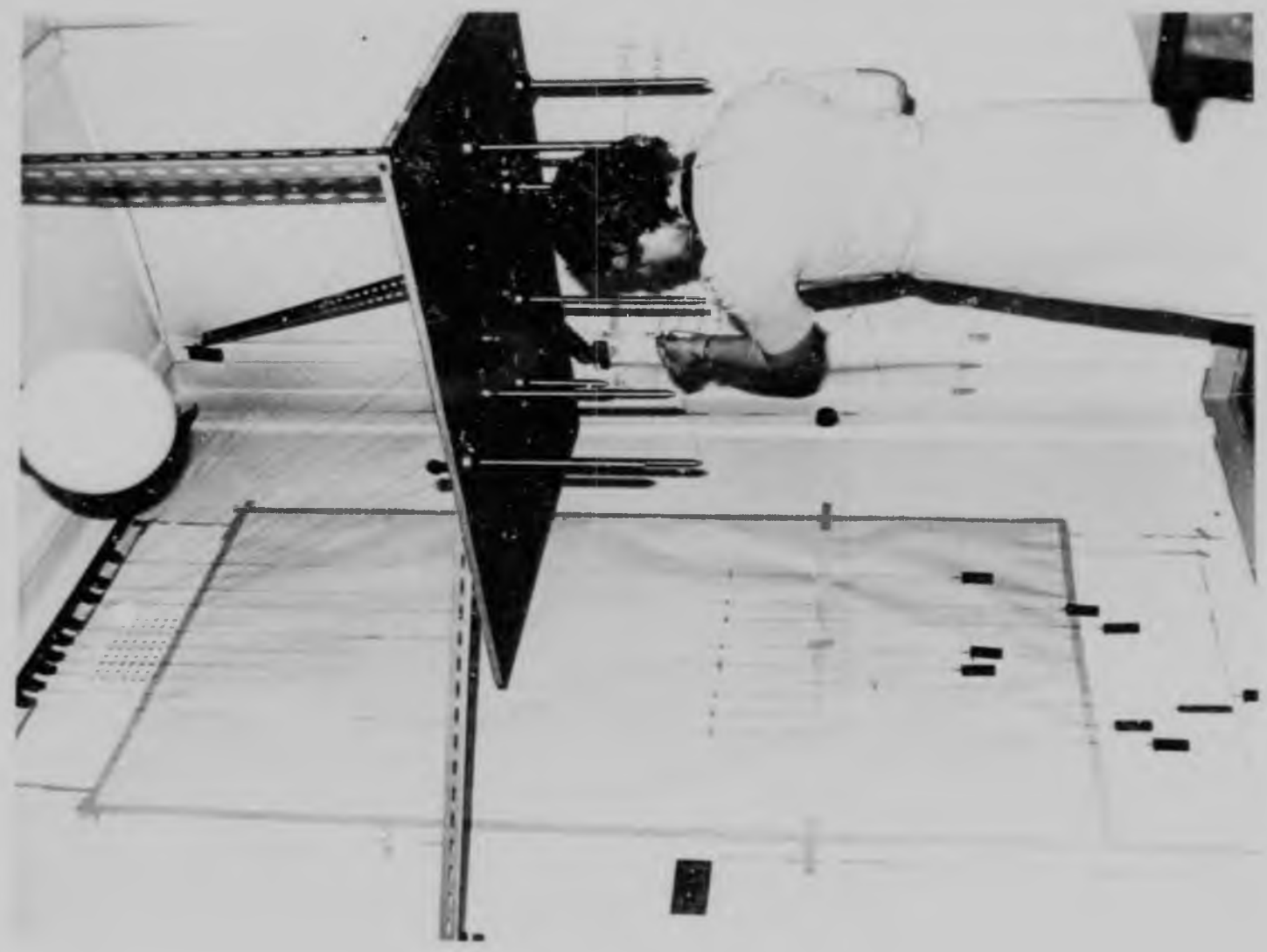

To carry out a location for a seismic event, the differences in times of arrival (delay times) of P waves at each seismometer are determined from the photographic record. These delay times are converted into differences in distances of the seismic event from the seismometers, by multiplying the delay times by the P wave velocity. The indicators are then adjusted to correspond to the differences in distances for each seismometer. The focus of the event can then be found by joining all the strings together and manipulating the common point such that all the indicators form a horizontal straight line. The position of the common point represents the position of the focus and the position where all the indicators line up represents the time of origin of the seismic event to a suitable scale. The location so obtained is called the first location.

In practice the velocity of the P waves varies along different paths on account of the non-uniformity of the geological strata and on account of the fractured rock close to the excavation. Ideally the velocity of propagation should be determined for each path to a seismometer, i.e., for each seismically active area in the mine. The P wave velocity was determined for three regions in the mine corresponding to each of the three tetrahedral seismometer arrays. Two 20 lb. explosive charges were fired in each shaft pillar and a 100 lb. charge was fired in a stope centrally situated in the mine. A seismometer was placed close to the charge and connected to the tape-recorder so that the time of origin could be determined. The Table below shows the velocities obtained.

/ Table. .....

| Seismometer | 3 Shaft Blast α ft/sec. | 2 Shaft Blast α ft/sec. | Stope Blast α ft/sec. |
|---|---|---|---|
| 1 | - | 18,700 | - |
| 2 | - | 18,700 | 19,000 |
| 3 | 18,900 | 18,400 | 19,000 |
| 4 | - | - | - |
| 5 | - | 18,300 | 17,400 |
| 6 | 19,000 | - | 18,800 |
| 7 | - | - | 19,800 |
| 8 | 19,250 | - | 19,700 |
| 9 | - | - | 18,000 |

The low value obtained for seismometer 5 in the case of the stope blast arose because this seismometer was close to the blast and the P wave therefore traversed a high proportion of fractured rock. The 20 lb. charge was found to be rather small; in the case of the 2 shaft blast the first motion at seismometers 3 and 5 was not perfectly clear and these measurements are subject to some doubt. Seismometers 1 to 6 determine the plan position of an event close to the reef plane. Remarkably consistent results were obtained on the locator when a value of 19,000 ft/sec. was used for all these seismometers, and this value was consequently adopted as the P wave velocity in the vicinity of the reef. Seismometers 7, 8 and 9 determine the elevation of seismic events close to the reef plane. The velocity to these seismometers differed by a few percent from 19,000 ft/sec., so that the first location is slightly in error. A second location can be obtained as follows: Since the approximate time of origin of the seismic event has been determined from the first location, the travel time to each seismometer is known. The differences in distance to each seismometer can be obtained more accurately by multiplying each travel time

/ by ....

by the corresponding calibrated velocity. These corrected differences in distance are then applied to the locator to yield the second location and a better approximation to the time of origin, so that a third location can be obtained. In practice there is no advantage in obtaining a third location since the velocities are not sufficiently well known and because there is frequently difficulty in determining the time of arrival of the P wave at each seismometer. Approximately 30 percent of the first motions start in an indecisive manner, with the result that in 10 percent of the cases very little improvement is attained when making a second location. The location obtained is in effect a least squares solution to the focus of the event. This comes about in the following way. Because the system is linear, the least squares solution to the time of origin is the arithmetic average of the positions of the indicators on the locator and since it is very easy to estimate when the indicators form the best horizontal straight line, the solution is effectively a least squares one. After the second location the co-ordinates of the focus were found to be accurate to within ± 100 feet with 90% confidence. For the majority of the seismic events, only the first location was obtained. The seismometers were distributed over a region 10,000 ft. wide, so that this accuracy corresponds to an overall measuring accuracy of ± 1%.

Since the seismometer distribution and the velocity distribution is asymmetrical with respect to the reef plane, an error in the velocity calibration would result in biased locations. A method has been devised which enables the vertical position (elevation) of a seismic event to be determined independently of the velocity calibration. The method is described in Appendix 1, and some examples are shown; there is good agreement between this method and the elevations determined by the velocity calibrations.

/ Energy ....

Energy determination:

For the spherical radiation of seismic energy, the total energy radiated is,

$$E = \int_0^\infty 4\pi \rho C r^2 V^2 \, dt \qquad \ldots\ldots \quad (1)$$

where V = instantaneous particle velocity at a distance r from the focus

C = $\alpha$ or $\beta$

$\alpha$ = P wave velocity

$\beta$ = S wave velocity

$\rho$ = density of medium

All the terms on the right-hand side of (1) are known. The density of quartzite is 167 lbs/ft$^3$, and r is obtained from the locator. The average P wave velocity is 19,000 ft/sec. and the S wave velocity can be calculated from

$$\beta = \alpha \sqrt{\frac{1 - 2\nu}{2(1 - \nu)}} = 0.641 \, \alpha \qquad \ldots\ldots \quad (2)$$

where $\nu$ = Poisson's Ratio

= 0.15 for quartzite.

A seismometer only gives the component of the particle velocity along the axis of the seismometer, so that the angle of incidence of the waves at the seismometer has to be determined from the locator. The angle of polarization of the S wave is not known; however, the energy is determined from vertical and horizontal seismometers, so that the mean value is not seriously in error.

An electronic device was designed to perform the operation $\int_0^T V^2 \, dt$ where T = 1/2 sec. A circuit diagram is shown in Appendix 4. The diodes operate non-linearly and back-to-back so that all odd harmonics cancel; the output is then proportional to the square of the signal. The squaring is very good over the range of signals applied to

/ it. ....

it. Because the integration time is short, the integrator behaves more like a demodulator or a low pass filter and th. output of the device corresponds to the envelope of the energy flux. Eight devices were constructed and connected to the outputs of the replay deck corresponding to seismometers 1 to 8. The surface seismometer was not used for energy determinations since the amplitude of vibration near a free surface is greater than in the solid rock far from a free surface. The outputs of the eight squaring devices were applied to the remaining 8 channels of the 24-channel oscillograph. The whole system was calibrated by applying signals of known amplitude at the seismometer terminals and measuring the outputs of each squaring device on the photographic record.

Figure 4 shows two events of magnitude $10^4$ ft.-lbs. and $5 \times 10^4$ ft.-lbs. that occurred within $2\frac{1}{2}$ seconds of one another. The traces marked F are those of the energy flux and those marked V are the particle velocity; those in pairs are the low sensitivity and the high sensitivity channels of a seismometer. Most of the energy is carried in the S wave.

The energy was carefully determined for about 50 seismic events covering the full magnitude range. These events were then regarded as standards and all other events were compared with these to estimate the magnitude, which was then estimated to the nearest order of magnitude. A simple rule of thumb became apparent; the magnitude was ten times greater if the duration of the wave train was about twice as long. It was found that the energy determined by the different seismometers differed by as much as a factor of 5 for most events. This variation was anticipated since it was not expected that the radiation would be spherical. The mean of the eight values, however, gave a good quantitative estimate of the energy released seismically.

/ Mechanism....

Mechanism studies:

There are two complementary techniques which have been used with some success in studying earthquake mechanisms, namely, First Motion Analysis and Spectral Analysis.

First Motion analysis. This technique is based on the fact that the sense of motion at a distant point is related to the motion at the focus of a seismic source. Theoretically it is possible to determine the complete initial motion and therefore the mechanism at the focus, by determining the first motion at a large number of points around the focus. The theory of first motion has been given authoritatively by Knopoff and Gilbert[32] in which they deal with all possible mechanisms. The main conclusions of this theory are given the section immediately preceding the section on first motion results.

The method of first motions is to determine whether the first motion at each seismometer is either compression or rarefaction and then to fit the first motions of a large number of seismometers to one of the first motion patterns produced by different mechanisms. Only P wave first motions could be examined in this study, since the S wave first motion was obscured by the coda of the P wave.

A central projection is used to represent the three-dimensional distribution of seismometers on paper. This projection is obtained as follows: the plane of the paper (projection plane) is horizontal and at unit distance above the focus of the seismic event. The normal line from the focus to the plane intersects the plane at O. A straight line from the focus to the seismometer is drawn to intersect the plane in P, this line makes an angle Ø with the normal from the focus to the plane. P is the projection of the seismometer and O is the projection of the focus on the plane.

/ The ....

The distance OP is given by

$$OP = \tan \phi$$

The projection is best suited to an array of seismometers in one half-space only. In the seismometer layout at Harmony, some seismometers lie in the half-space above the foci of the seismic events. In the case of the seismometers in the lower half-space, $\phi$ is slightly greater than $90^\circ$, i.e., $\phi = 90^\circ + \delta$ where $\delta$ is small. These seismometers have been plotted in the central projection as though $\phi = 90^\circ - \delta$ and the projected point has been marked -ve to indicate that the seismometer lies in the lower half-space.

The main reason for choosing this projection is that a plane passing through the focus projects as a **straight line.** The direction of the line corresponds to the strike direction of the plane, and the distance of the line from O gives the angle of dip of the plane. In the radiation pattern for shear movements, regions of compression and rarefaction are divided by two planes which pass through the focus and intersect at right angles. If $\phi_1$ and $\phi_2$ are the angles of dip of the two planes, then the angle $\theta$ between the two straight lines which form the projections of the two planes is given by

$$\cos \theta = \tan \phi_1 \tan \phi_2 \qquad \ldots\ldots \quad (3)$$

This relationship is derived in Appendix 2. Now $\cos \theta < 1$, therefore at least one of $\tan \phi_1$ and $\tan \phi_2$ is less than one. This implies that at least one projection line must pass O at a distance less than unit distance. This condition is of importance in establishing or rejecting the shear mechanism as a mechanism for seismic events in mines. The shear mechanism has been found to be the most common type of earthquake mechanism.

/ Spectral .....

Spectral analysis. This technique is used to determine the extent of rupture and is in its infancy; it has only been used successfully in a few cases for earthquakes (Ben-Menahem and Toksöz).[16] In these cases the analysis was done by means of surface waves. The theory for body waves has been examined by Hirasawa and Stauder[17] for some ideal geometrical configurations and no practical solutions have been reported.

This method is based on the fact that a seismic source occupies a finite space and the changes at the source take place in finite time. Hirasawa and Stauder[17] have shown that "the finiteness of the source affects only the Fourier spectra of P and S waves, and has no effect either on the distribution of compression-rarefaction of the P wave, or on the polarization angle of the S wave". In other words, the source finiteness affects the wave-shape of the P and S waves, while the first motion pattern is determined by the type of mechanism (e.g., shear or tensile rupture). In the case of a unilaterally propagating rectangular rupture surface, the effect of the source finiteness on the spectra of the P and S waves is expressed by

$$\exp.^{-i\omega(X + Y)} \quad \frac{\sin \omega X}{\omega X} \quad \frac{\sin \omega Y}{\omega Y}$$

where $\omega$ = angular frequency of the Fourier component

X and Y represent the geometry of the source in relation to the seismometer in terms of the velocity of propagation of the rupture and the velocities of the P and S waves.

The main feature is that there are particular frequencies $\omega = \frac{m\pi}{X}$ , $\omega = \frac{n\pi}{Y}$ at which the spectra have zero amplitude and a phase change by $\pi$ radians, where m and n are integers.

/ The method ....

The method of spectral analysis therefore reduces to determining the Fourier transform of the P and S waves and examining the spectrum for minima in amplitude and changes of $\pi$ in phase which will enable X and Y to be calculated. X and Y in turn give the dimensions of the rectangular rupture and its velocity of propagation in relation to the seismometer. X and Y have to be determined at a number of seismometers in order to determine the absolute dimensions of the source. In addition, the fault plane has to be determined by means of first motions.

A transient spectrograph with the trade name "Missilyzer" was used to determine the amplitude component of the Fourier transform of the waves; the spectrograph does not give the phase component of the Fourier transform. This device has two modes of operation, (a) it produces a three-dimensional graph or "missilgram" in which time is the abscissa, frequency the ordinate and the intensity of the graph represents amplitude, (b) it produces a "section" or graph of amplitude versus frequency at any particular instant in time. The "Missilyzer" and some spectra of standard waves are shown in Appendix 3. Only P waves can be analyzed in t' is study since the coda of the P waves interfere with the S waves.

The great virtue of this method is that the minima, or zeros, in amplitude occur repeatedly and in the case of an ideal source, at regular intervals of frequency $\Delta\omega$, so that a number of values $\Delta\omega$ can be obtained. Note that in the case of the ideal rectangular rupture there are two families of minima yielding $\Delta\omega_X$ and $\Delta\omega_Y$, which have to be distinguished. A further great virtue of this method is that the positions of the zeros or minima in the amplitude spectrum of a P wave are unaffected by the medium through which the P wave has passed or by the recording equipment, provided that harmonic distortion does not occur. Linear attenuation, dispersion

/ and ....

and scattering of the waves can only change relative amplitudes and phases of the spectral components, and can have no effect on components that are missing from the spectrum.

Serious difficulties arise in this method with deviations from the ideal rectangular unilateral rupture propagating at constant velocity. If the velocity of propagation varies slightly, the Fourier spectrum becomes continuous with indistinct minima in the places of the zeros, if an abrupt change occurs in the velocity, the spectrum is completely altered. If the rupture has finite thickness, e.g., a propagating failure of a volume of rock, a third family of minima is introduced into the spectrum. Hirasawa and Stauder[17] have shown that when the ideal rupture propagates bilaterally, zeros no longer appear in the spectrum except in the case of perfectly symmetrical propagation. Consequently spectral analysis can be of value only when the geometry of the seismic source is very simple.

GEOLOGICAL ENVIRONMENT

The seismic network covers the entire Harmony Gold Mine and portion of the neighbouring Virginia Gold Mine. At these mines, the Witwatersrand system rocks, Upper Division, form a shallow basin dipping at approximately $7^{o}$ to the West. The Basal Reef is mined and is approximately 5000 feet below surface. Figures 7 and 8 show, respectively, a generalized vertical section from surface to reef, and a section giving greater detail in the vicinity of the reef. There are three features to which frequent reference is made; they are the Harmony Sill, the Upper Shale Marker and the Khaki Shale. The Harmony Sill is intrusive dolerite interspersed with quartz veins. Its contacts with the quartzite are liable to be weak. The Upper Shale Marker is a band of weak rock. The Khaki Shale varies widely throughout the mine.

Figure 9 shows the distribution in plan, the area with the coarse hatching represents the Khaki Shale. The shale is sometimes three feet thick and varies in its separation from the Basal reef. Where it has been eroded away, a definite bedding plane exists. The stoping width is dictated by the conditions in the hangingwall. When the Khaki Shale is three or more feet from the reef, it is possible to maintain the stoping width at about 42 inches; however, when the shale is closer, the hangingwall is more difficult to control so that the stoping width becomes approximately 60 inches.

/ FIGURES 7 and 8

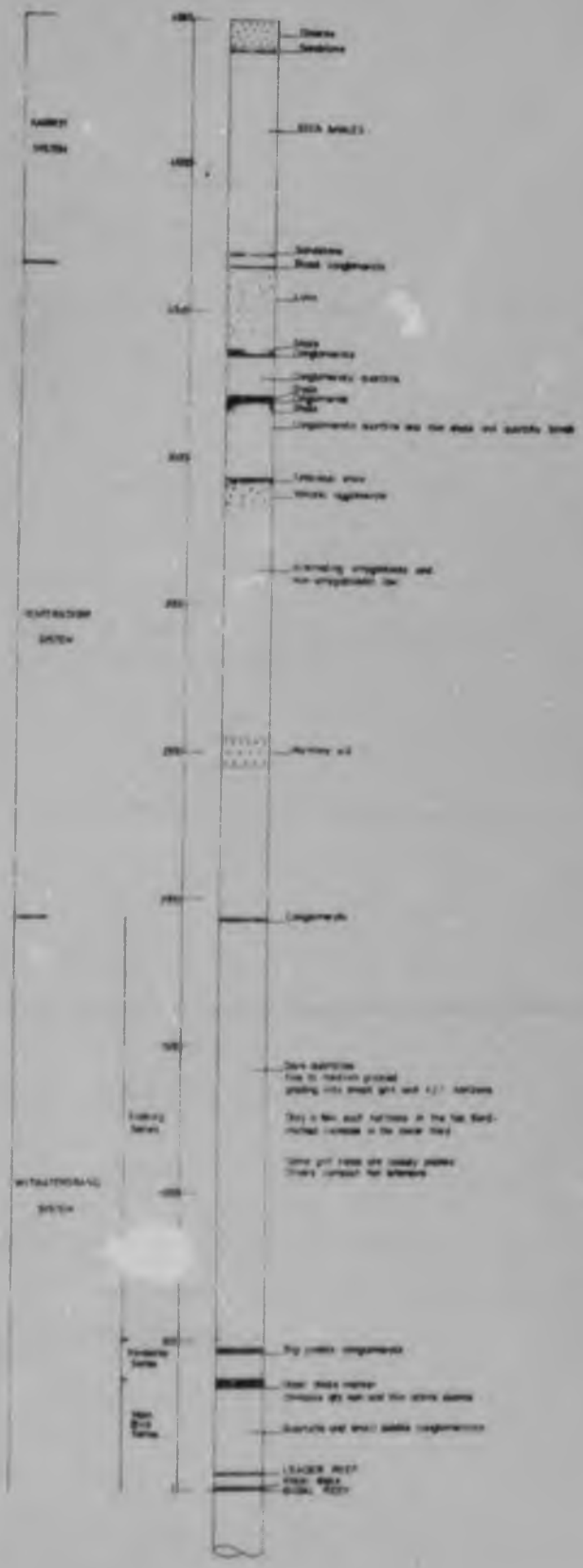

FIGURE 7 A GENERALISED GEOLOGICAL SECTION ON HARMONY FROM SURFACE TO THE REEF PLANE.

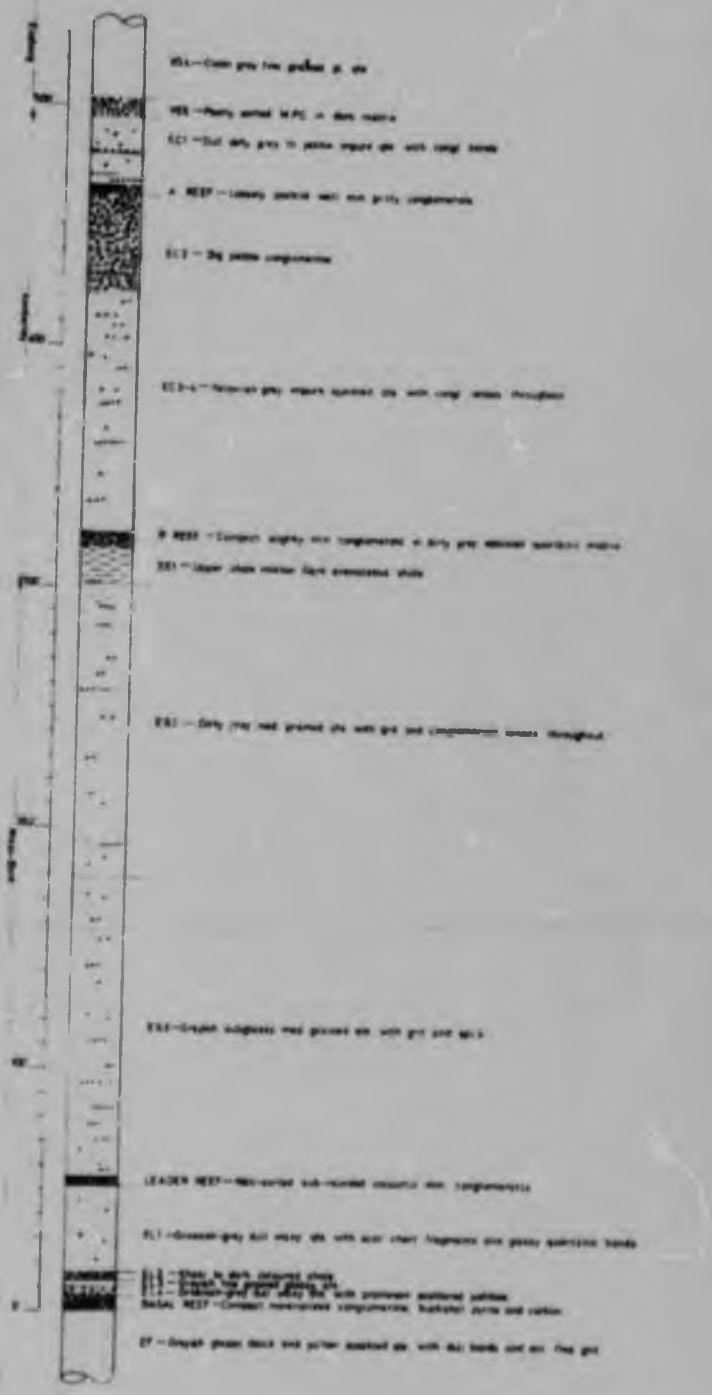

FIGURE 8 PART OF A GENERALISED GEOLOGICAL SECTION SHOWING DETAILS NEAR THE REEF PLANE.

FIGURE 9 PLAN SHOWING THE DISTRIBUTION OF THE KHAKI SHALE AND THE INTERSECTION OF THE SILL IN VIRGINIA WITH THE REEF. THE KHAKI SHALE IS REPRESENTED BY THE COARSE HATCHING.

Rockfalls often occur in the stopes, in which case, all the rock up to the top contact of the Khaki Shale falls down. The exposed rock above the Khaki Shale always appears sound and has widely spaced fracture planes. Rockbursts occur infrequently and usually result in damage which takes a few days to clear.

The rock in the footwall is quartzite for a great depth. In the Virginia area, Figure 9, there is a shallow dipping sill which intersects the reef. This sill appears to be a tongue from a larger and deeper sill, the position of which is not well known. The only footwall damage that is ever observed occurs at this sill.

When mining takes place in stopes with a small [illegible]n, the hangingwall is relatively easy to control and rockfalls are infrequent. On the other hand, in remnants, hangingwall control is difficult and rockfalls and rockbursts occur frequently in spite of increased support.

DISCUSSION AND RESULTS

Magnitude of Seismic Events

The seismic network commenced continuous recording on the 11th August, 1964. In the first year of recording, 3100 seismic events were located. These ranged in magnitude from $10^3$ ft.-lbs. to $10^8$ ft.-lbs. More than half of the events of magnitude $10^3$ ft.-lbs. could be located, while a high proportion of magnitude $10^4$ ft.-lbs. and all of magnitude $10^5$ ft.-lbs. and greater were located. During this year, only on three days were no records obtained, and on these days no tremors or damage were reported. It is thought, therefore, that all events of $10^5$ ft.-lbs. and more have been recorded and located. The Table below shows the number of events of different sizes located during the first year of recording.

| Magnitude ft.-lbs. | $10^3$ | $10^4$ | $10^5$ | $10^6$ | $10^7$ | $10^8$ |
|---|---|---|---|---|---|---|
| Number of Events | 1768 | 897 | 292 | 119 | 11 | 2 |

Figure 10 shows the total energy radiated by different sized events during the year. The total for events of magnitude $10^3$ ft.-lbs. is somewhat higher than shown in Figure 10, since only about half of these events were located.

/ FIGURE 10

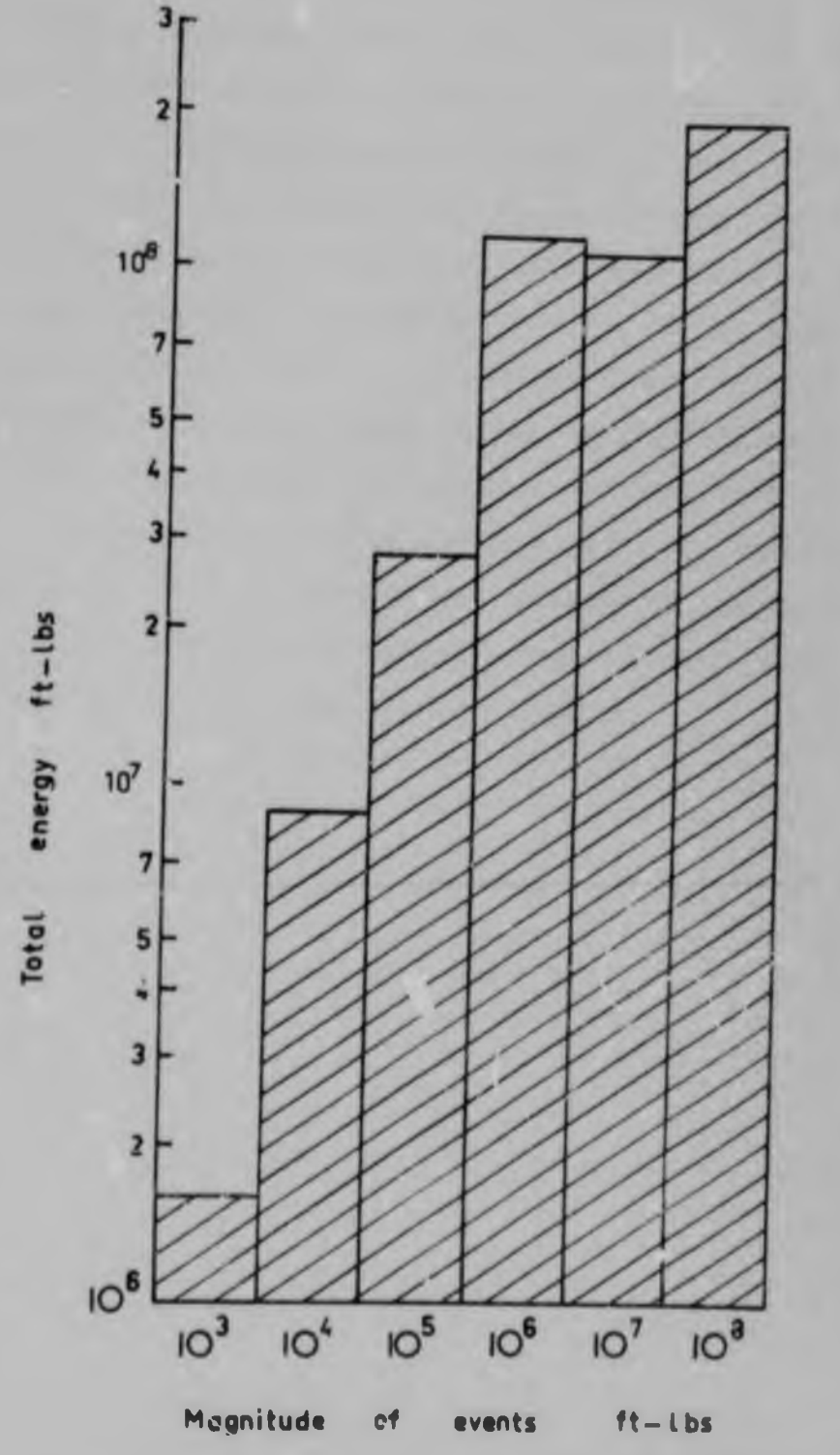


FIGURE 10 THE DISTRIBUTION OF THE TOTAL ENERGY RADIATED BY SEISMIC EVENTS OF DIFFERENT SIZES OVER A PERIOD OF ONE YEAR.

Plan Location of Events

Seismic events rarely occurred in workings surrounded by extensive solid reef, but occurred most frequently above active faces in remnant areas. When an island or peninsula abutment reached a width of 500 feet, there were definite signs of an increase in seismic activity, and the seismicity increased rapidly as the abutment became narrower. These effects can be seen in Figures 11 to 15, each of which shows the events occurring in a six-week period. The figures, drawn on a grid of 2000 feet, are arranged sequentially, and show two face positions, representing the beginning and end of a three-month period. The seismic events plotted in each figure occurred either during the first or second half of each period. Only the events that occurred during the first five months of the year are shown, since the pattern for the remaining part of the year was very similar.

/ SCALE: FIGURES 11-15

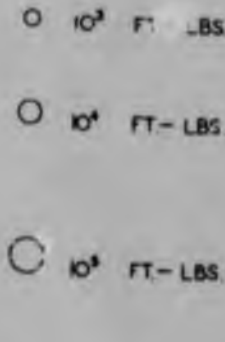


SCALE SHOWING MAGNITUDES OF THE SEISMIC EVENTS PLOTTED IN FIGURES 11 TO 15

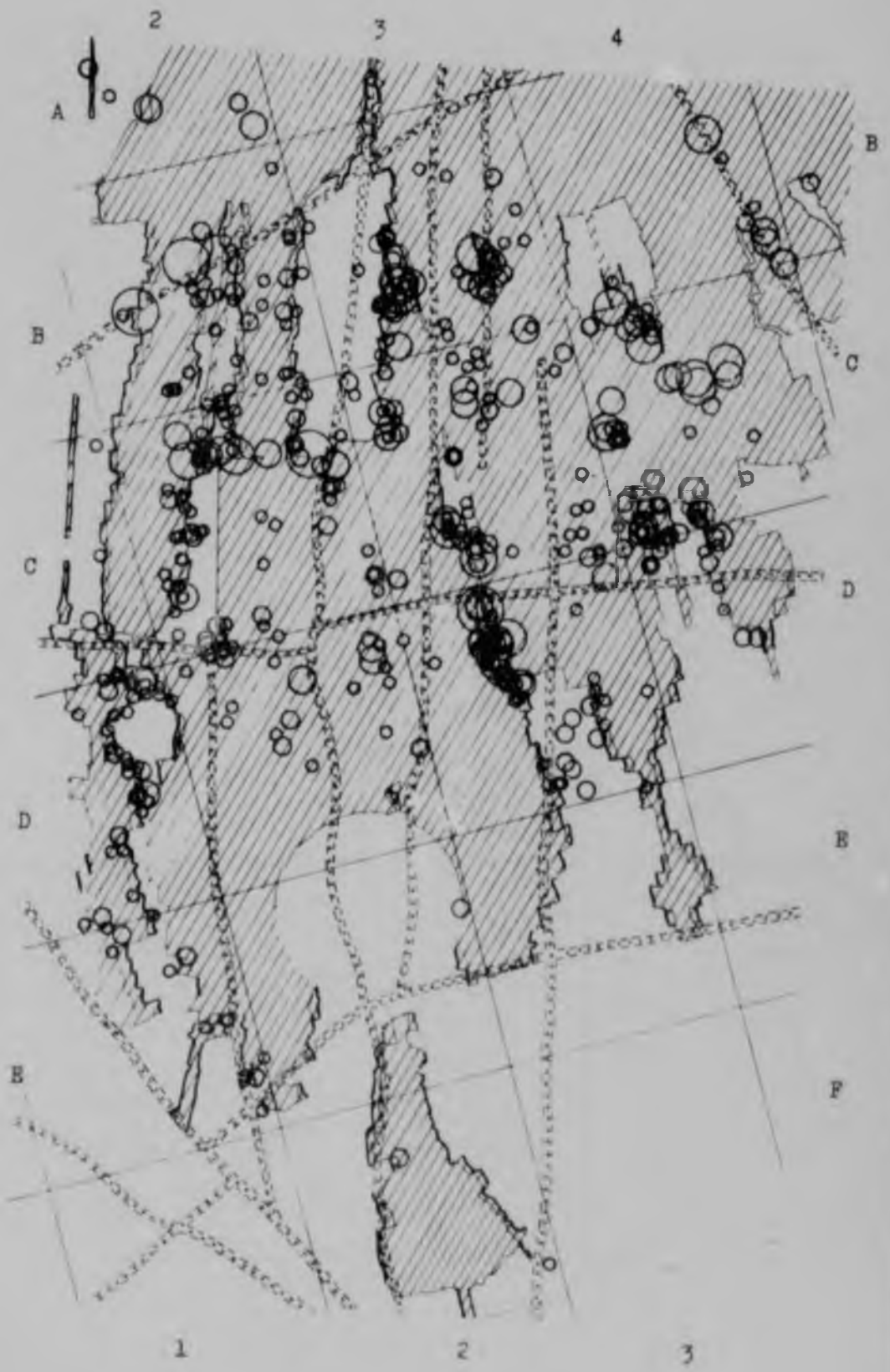


FIGURE 11 PLAN POSITION OF SEISMIC EVENTS

11th AUGUST TO 30th SEPTEMBER, 1964

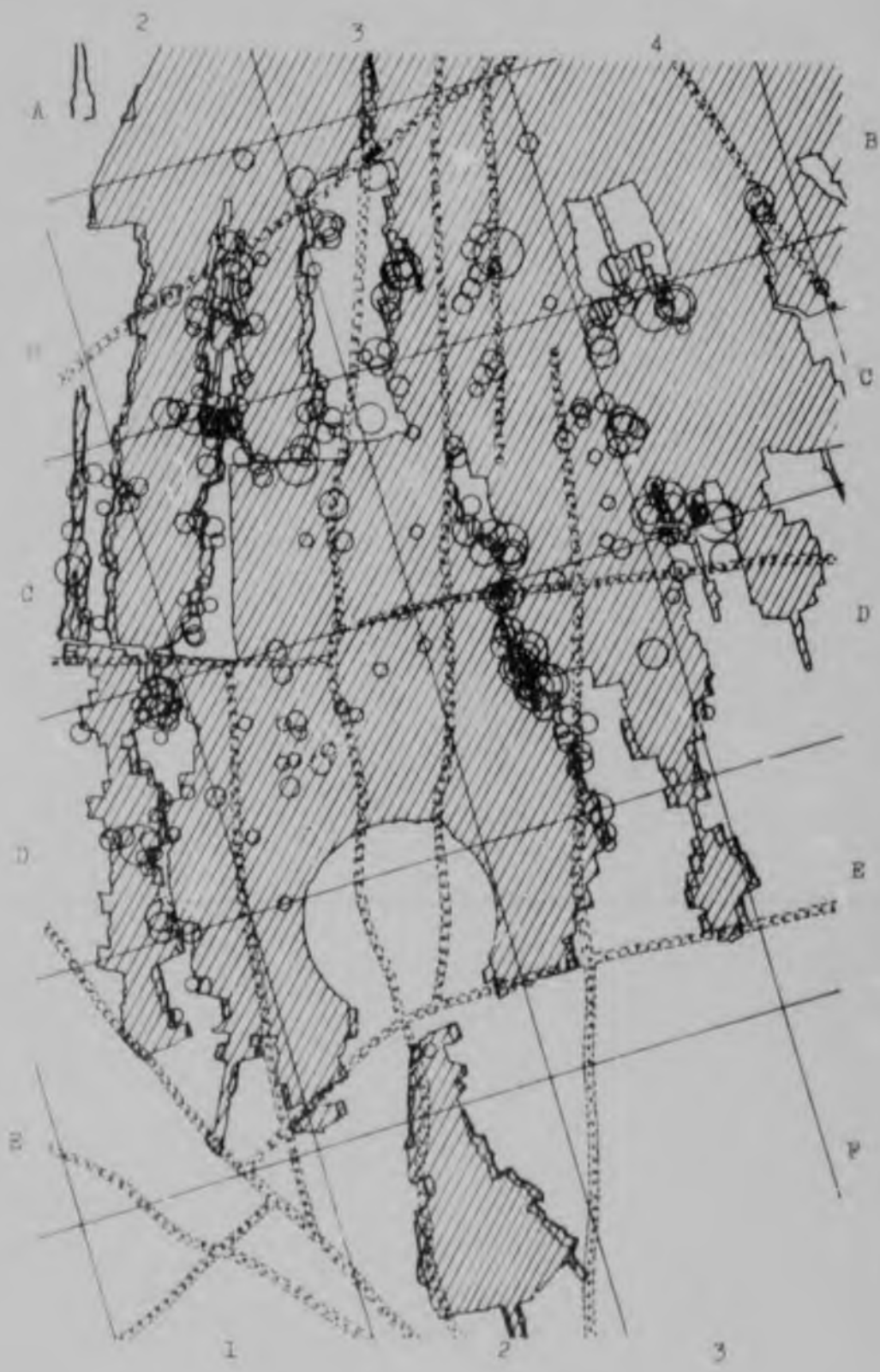


FIGURE 15 PLAN POSITION OF SEISMIC EVENTS

1st OCTOBER to 15th NOVEMBER, 1964


FIGURE 13 PLAN POSITION OF SEISMIC EVENTS
16th NOVEMBER to 31st DECEMBER, 1964

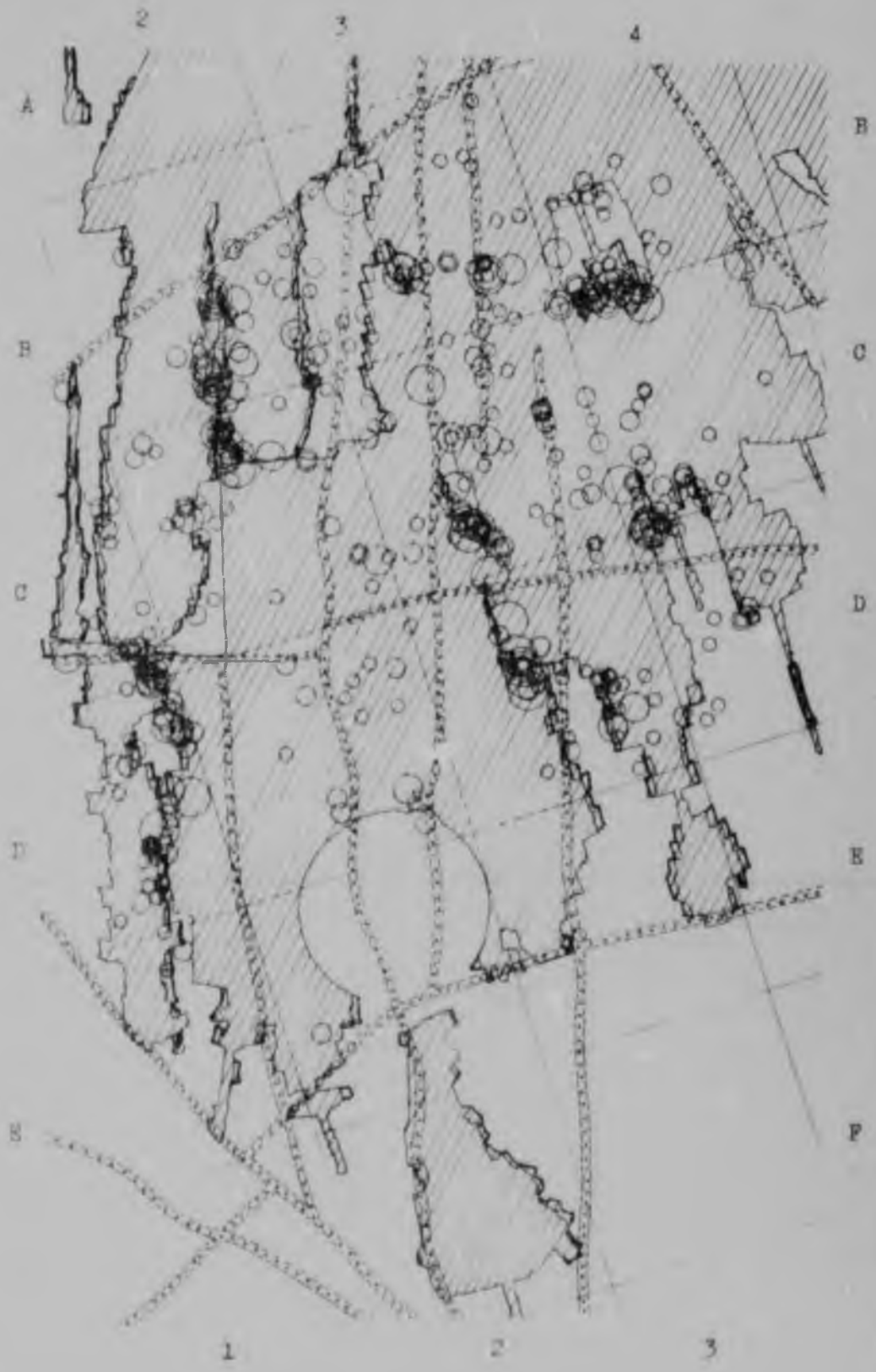


FIGURE 14 PLAN POSITION OF SEISMIC EVENTS

1st JANUARY to 14th FEBRUARY, 1965

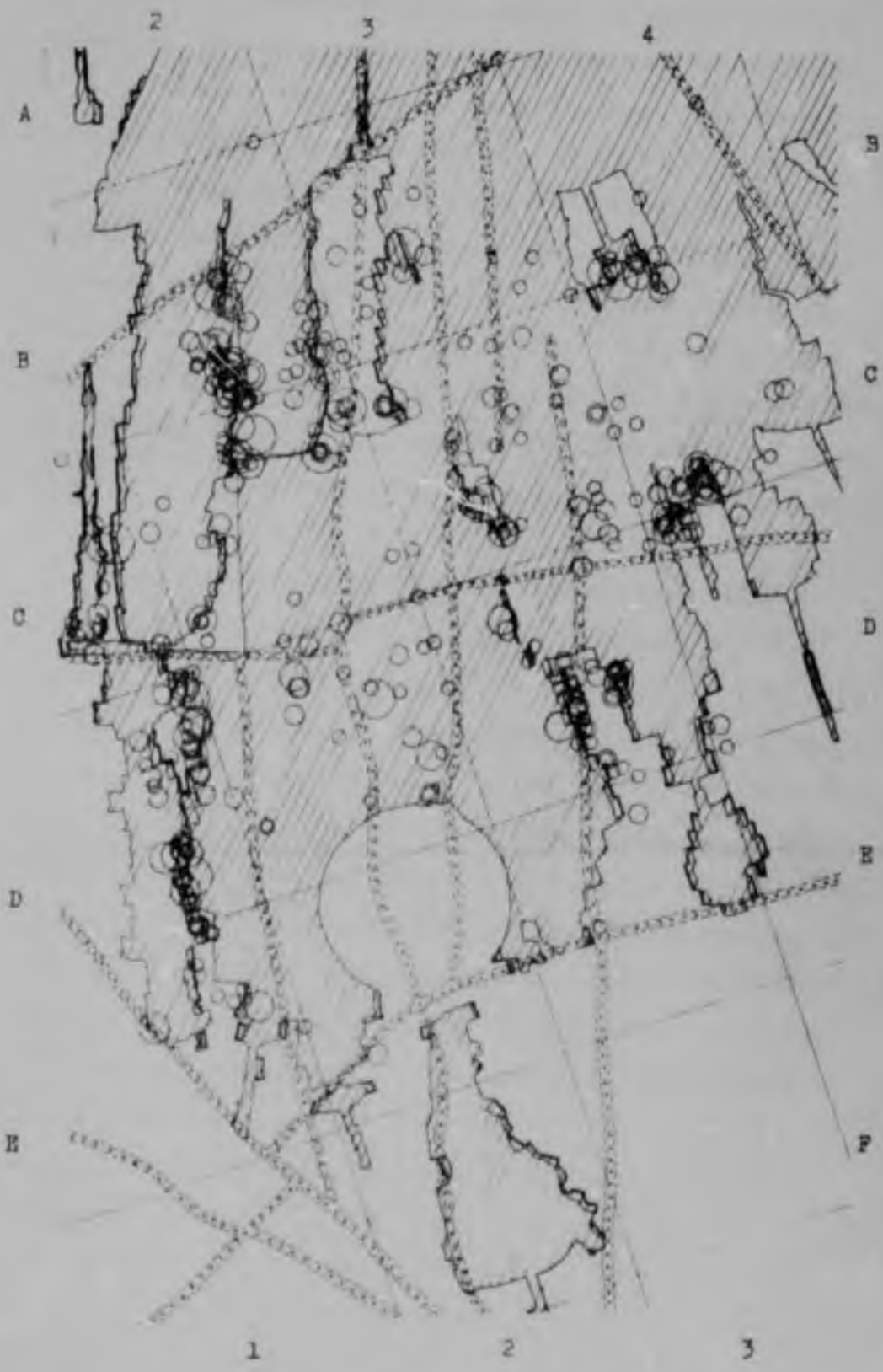


FIGURE 15 PLAN POSITION OF SEISMIC EVENTS

15th FEBRUARY to 31st MARCH, 1965

A great number of events have occurred in the remnant in D3. In the region P2, even though the ground was very irregular, due to numerous small faults, none of which had a throw of more than 10 feet, very few events occurred.

By comparing Figures 11 to 15, the change in seismicity as the remnant in D3 is mined away can be seen. This should be compared with D1, where the events became more frequent and increased in magnitude as mining progressed. The events that occurred in D2 and other worked-out areas were probably associated withrecompression. Stonewalls and other forms of waste filling were sometimes used, and these could be expected to undergo movement when the load on them became high.

Dykes played a major role in producing the largest events. All the events of magnitude $10^7$ ft.-lbs. and $10^8$ ft.-lbs. were located within 200 feet of a dyke; most were located right on a dyke Twenty five percent of the events of magnitude $10^6$ ft.-lbs. were located within 200 feet of a dyke and ten percent of the total were, within the limits of error, on a dyke. A number of small dykes have not been charted, so that this association could be even closer. The dyke in B4, Figure 11, was partially mined out in 1962, and was still the source of some seismic events in 1964.

On comparing Figure 9 with Figures 11 to 15, there is no obvious difference in seismic activity between the regions where the Khaki Shale is present and where it is absent.

Elevation of Seismic Events

The vertical distribution of a representative sample of events is shown in Figure 16. All the events used for drawing this histogram were located twice, using the corrected velocities. There are two distinct sets of events, one group between 2,400 and 2,800 feet above the reef plane and the other between 0 and 300 feet above the reef plane. There is a major geological discontinuity associated with each of these groups. The Harmony Sill lies in the upper group, and the lower group lie between the reef and the Upper Shale Marker. (Figures 7 and 8).

The vertical distribution of events in Figure 16 does not depend on the magnitude of the seismic events. The sizes of the events near the Harmony Sill ranged from $10^3$ ft.-lbs. to $10^6$ ft.-lbs.

The Harmony Sill is not parallel with the reef; in some places it is 2,800 feet above the reef and at the Ventilation Shaft only 1,800 feet, consequently there is a spread in the elevation of the events in the histogram. The events at the Sill did not occur above the entire mining excavation; they were confined to a small strip-like region which is parallel with the Iron Curtain Dyke.

/ FIGURE 16

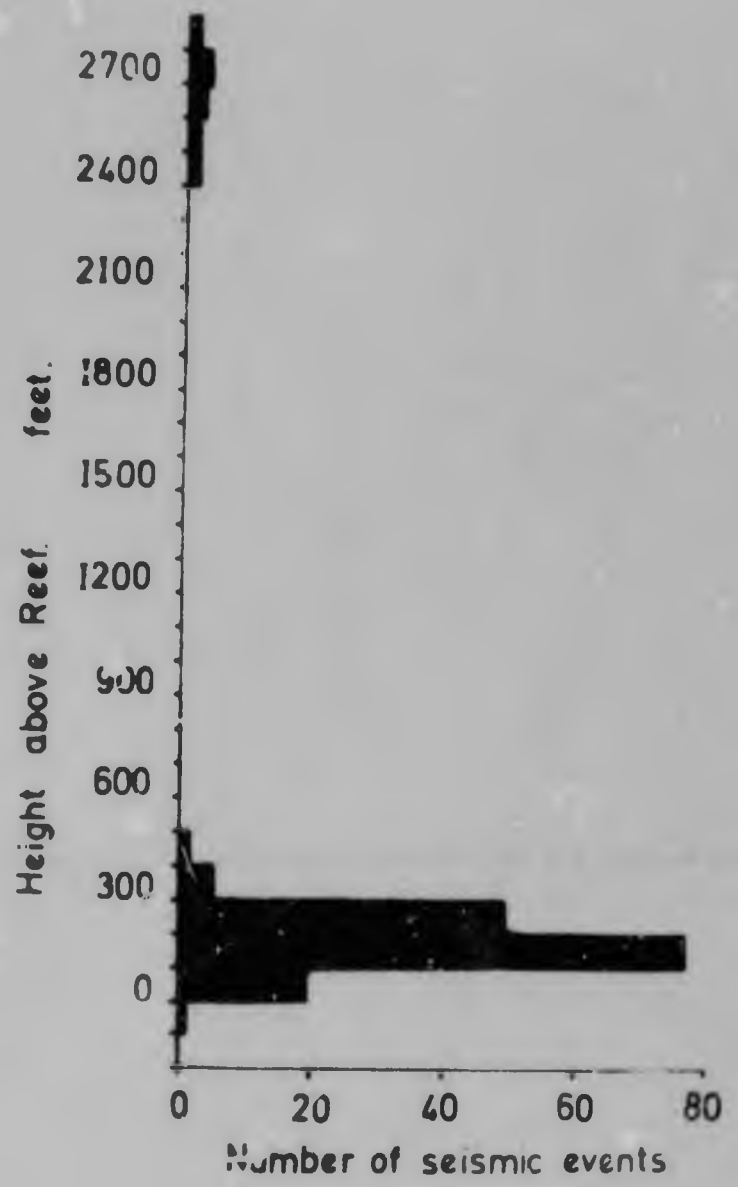


FIGURE 16 THE VERTICAL DISTRIBUTION OF THE SEISMIC EVENTS RELATIVE TO THE REEF PLANE.

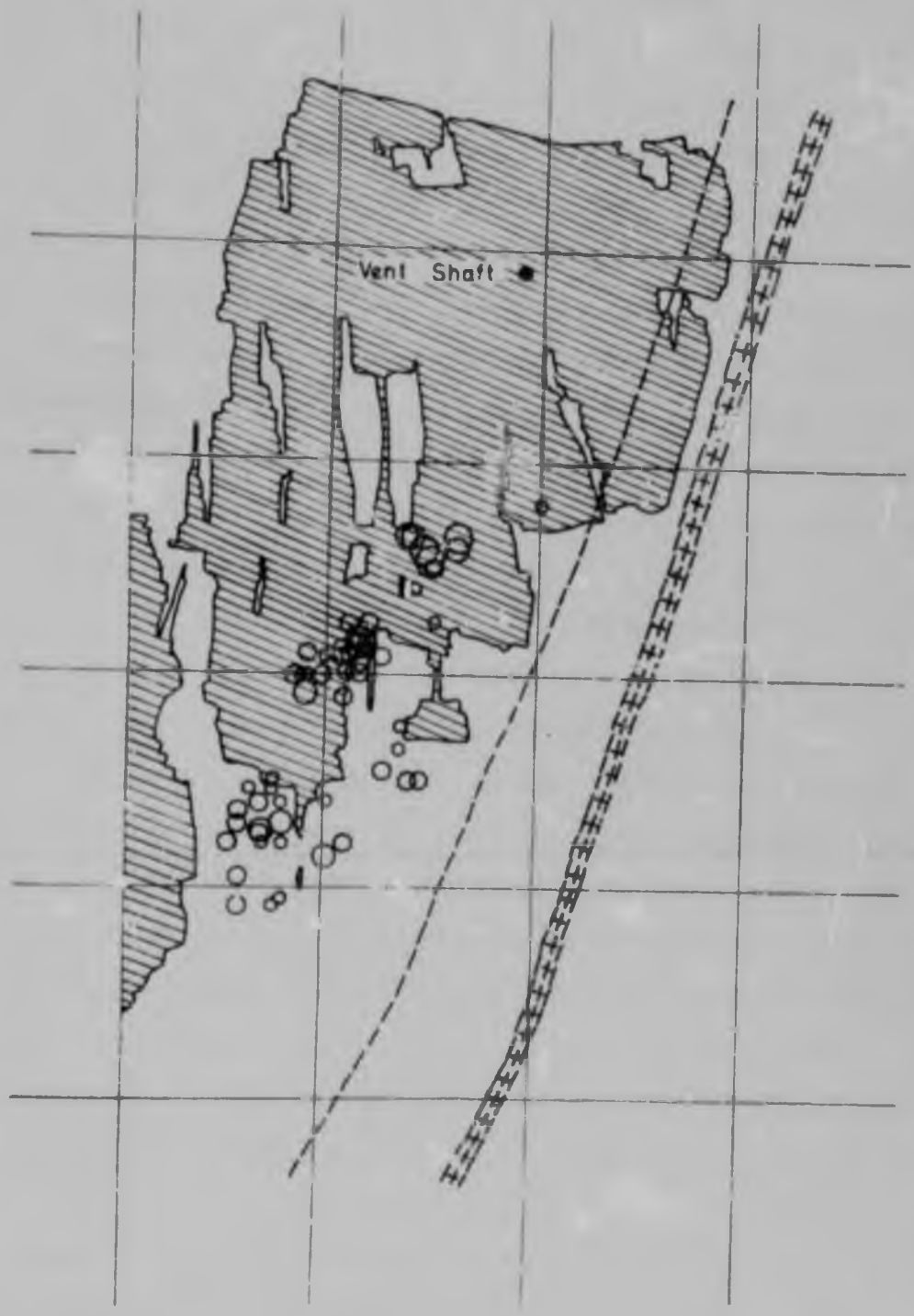


FIGURE 17 PLAN ON A GRID OF 2000 FEET SHOWING THE POSITIONS OF THE SEISMIC EVENTS THAT OCCURRED NEAR THE HARMONY SILL OVER THE PERIOD 11 AUGUST, 1964 TO 11 JANUARY, 1965.

Figure 17 shows the plan distribution of these events. The possibility that these events might lie on the intersection of the Iron Curtain Dyke and the Harmony Sill was investigated. The position of the dyke at the elevation of the sill is not known; however, the dyke dips at 65° at the reef plane, and assuming this dip to remain unchanged, the intersection of the dyke and sill would bees shown in Figure 17. No conclusions can be drawn from this result. The strip on which the upper group of events lie can be extrapolated to pass through the Ventilation Shaft. Measurements of vertical movements in the Ventilation Shaft reported by Ortlepp(20) showed considerable differential movement in the vicinity of the Harmony Sill. This movement was accompanied by cracks in the shaft lining and by the inflow of water, and is examined in greater detail in the following discussion.

The Upper Shale Marker is at an average height of 300 feet above the reef plane and it therefore appears that this weak band of rock forms a boundary for the lower group of seismic events. There is a disturbing feature about this distribution; notice that if this distribution were shifted downwards by 100 feet (the 90% confidence limit), the peak in the distribution would coincide with the reef plane. To resolve this doubt, the alternative method of determining the elevation described in Appendix 1, was employed to determine the elevations of the seismic events. As can be seen in Appendix 1, this method agrees with the elevations obtained by using the velocity calibrations, and it must be accepted that this asymmetrical distribution is real. It is not unreasonable that an asymmetrical distribution should arise, since the geological environment is asymmetrical and the hangingwall tends to be weaker than the footwall.

/ Seismic ....

Seismic events must be associated with the violent failure of rock, thus a knowledge of the distribution of the seismic events would reveal the fracture zone. The only mode of large scale fracturing which may not be detected seismically is strata separation. Since the bonding between well defined strata may be weak, strata separation can occur at low tensile stress levels, resulting in a low seismic yield. Therefore, the type of fracture dome which is made up of strata separated into huge beams may not be detected; however, should these beams fail, enormous amounts of seismic energy would be released. The type of fracture dome envisaged by Denkhaus[2] would result in large amounts of seismic energy being released, since the rock is required to fail at high shear and tensile stress levels.

The distribution of seismic events shown in Figure 16 indicates that the fracture zone is confined to a narrow region 300 feet high, between the excavation and the Upper Shale Marker. This zone extends horizontally with the faces, as these advance. Fracture may, however, occur at the Harmony Sill. Although it is not certain that strata separation does not occur between the Upper Shale Marker and the Harmony Sill, it is most unlikely that vertical fracturing occurs here.

Since the seismic observations are not in agreement with the accepted theories on the state of the rock mass, the only evidence that has ever been used to verify dome theory in a deep mine is re-examined here. This information was kindly made available by Rand Mines, Limited, and consists of vertical strain measurements made in the Ventilation Shaft at Harmony. It must be emphasized that these measurements were originally reported by Barcza and von Willich[3] who made no attempt to interpret them in terms of dome theory; however, in a subsequent paper by Denkhaus, Hill and Roux[4] they were regarded as conclusive evidence of the fracture dome.

/ Strain....

Strain Measurements

The Ventilation Shaft at the Harmony Mine is unique in South Africa in that no pillar was left for the support of the shaft. Mining operations commenced at the foot of the shaft and extended almost symmetrically about it for the first 5 years of the life of the mine. It was anticipated that movements in the shaft would yield some information on the behaviour of the strata. To measure these movements, 40 pegs 3 feet long were installed in a vertical row at the side of the shaft, and measurements of the distance between the pegs were made at regular intervals. Figure 18 is a vertical section through the Ventilation Shaft showing the position of the pegs in relation to thegeological structure.

/ FIGURE 18

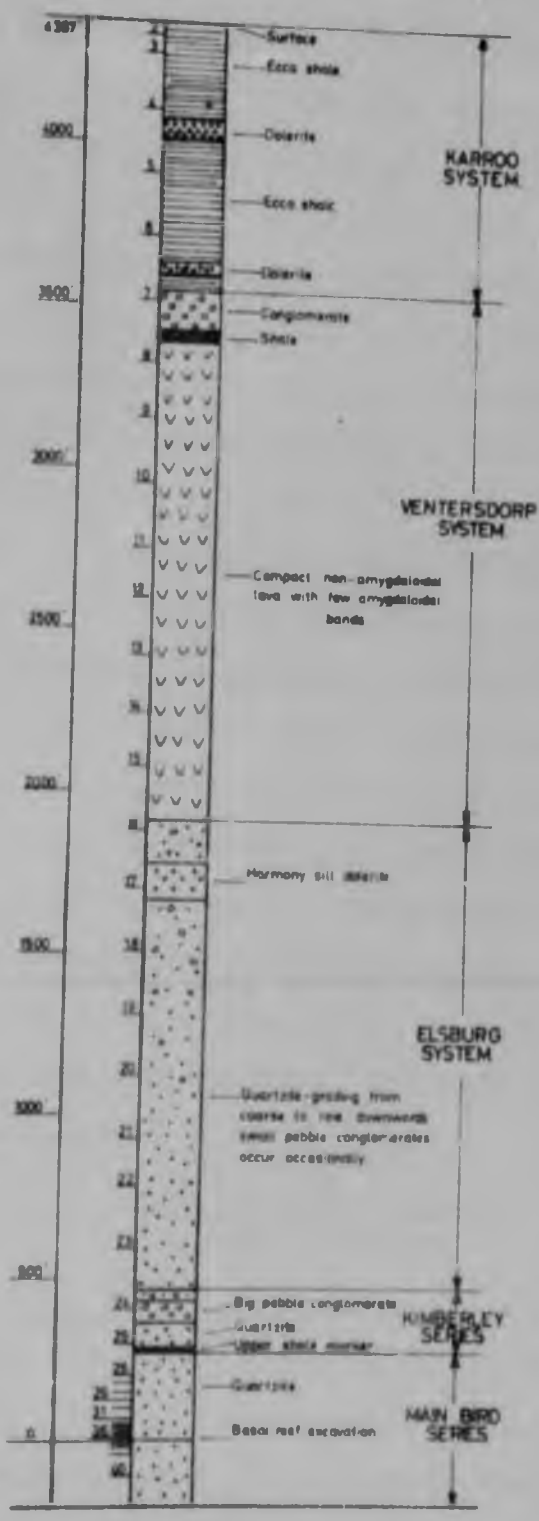


FIGURE 18 A VERTICAL SECTION THROUGH THE VENTILATION SHAFT SHOWING THE POSITIONS OF THE REGS IN RELATION TO THE GEOLOGICAL STRUCTURE.

The shaft was lined with a 9-inch layer of unreinforced concrete. The concrete contained calcium chloride, consequently severe shrinkage occurred and the concrete was of low mechanical strength. A detailed record of the development of cracks in the lining and the inflow of water was kept. It was found that cracks and water inflow became noticeable at successively higher levels as mining progressed. This observation is to be expected because, even in the case of a continuous elastic model, elastic relaxation would stretch the shaft at progressively higher levels as the excavation enlarged, and so allow fissures to open and cause shrinkage cracks in the lining to become obvious.

It is assumed that the vertical component of the virgin rock stress at any point is equal to the weight of the superincumbent rock at that point. Before strata separation or horizontal fracturing can occur, the vertical virgin stress must be removed from the rock and a large vertical strain must occur by elastic relaxation. The modulus for relaxation in the vertical direction is approximately equal to the Young's modulus. Since the tensile strength in the vertical direction is assumed to be zero the criterion for strata separation or horizontal fracturing is

$$\text{Vertical Strain} > \frac{\text{Vertical Virgin Stress}}{\text{Young's Modulus}}$$

Ortlepp and Nicoll[11] made measurements of the movements in the quartzite below the excavation at the Harmony Mine. They found that their measurements agreed reasonably well with the movements predicted by elastic theory, when a value of approximately $10 \times 10^6$ p.s.i. was used for the Young's Modulus. This value will be adopted for the Young's Modulus in the hangingwall. A typical value for the density of quartzite is 170 lbs/ft.$^3$.

/ FIGURE 19

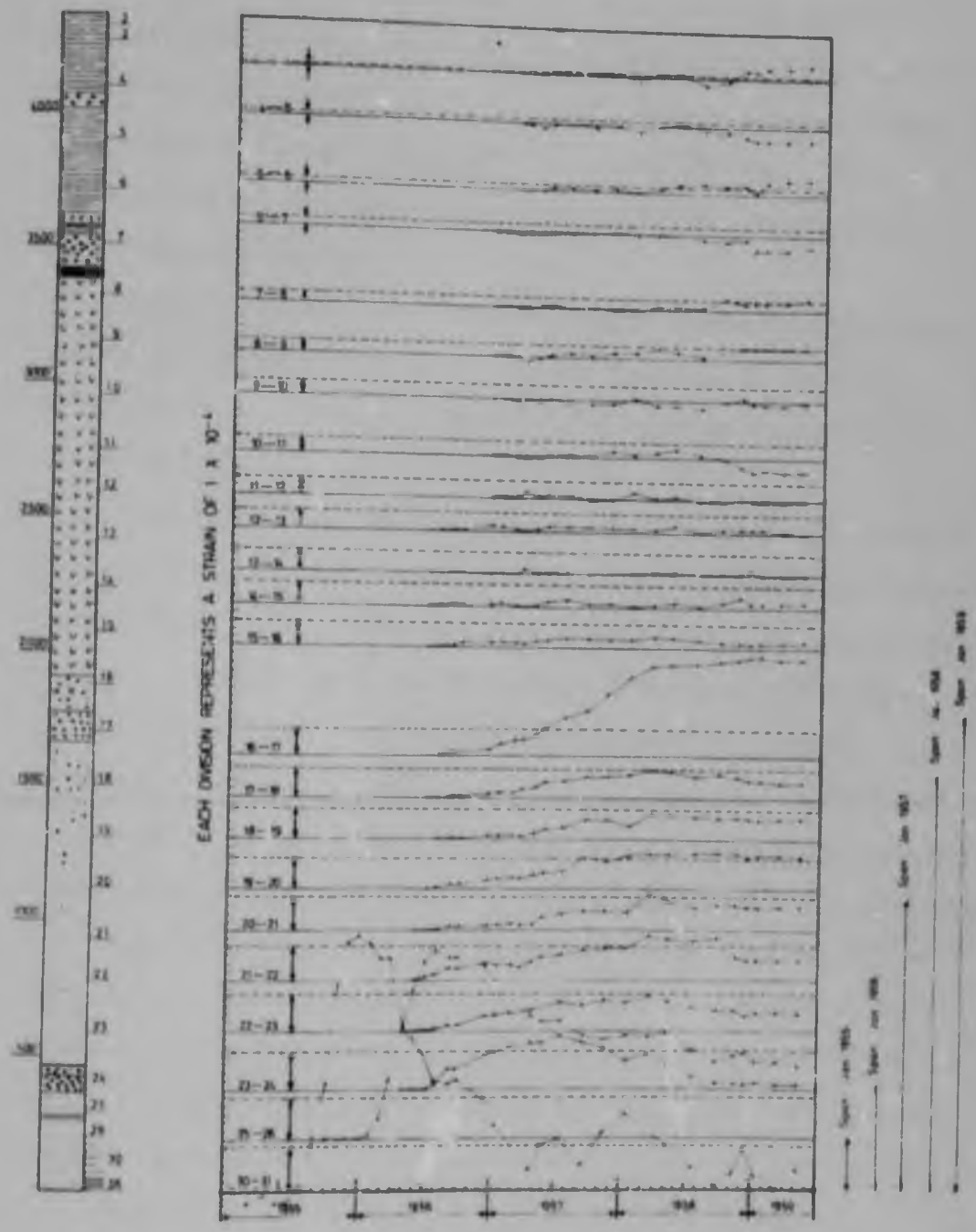


FIGURE 19 THE VARIATION OF STRAIN WITH TIME, AT DIFFERENT LEVELS IN THE VENTILATION SHAFT. THE BROKEN LINES REPRESENT THE ELASTIC STRAIN DUE TO RELAXATION.

Figure 19 shows the strain at various levels in the shaft plotted against time, and the maximum strain due to elastic relaxation is shown as the dotted line. Mining operations commenced in September, 1954 and measurements were made at regular intervals until May, 1959. No measurements were made again until 1962, at which stage a number of pegs had suffered damage. Ortlepp(20) showed that by 1963 recompression had occurred and the shaft had almost regained its original length.

Pegs 36 to 24: The vertical strain between these pegs was so great that bed separation and fracture must have occurred in this region. Most of the seismic events also occurred here.

Pegs 24 to 23: The maximum strain was 40 percent higher than the maximum relaxation strain. A large crack was observed in the shaft lining between these pegs at a point corresponding to the contact between the Kimberley Series and the Elsburg Series. This indicates that strata separation probably occurred at this contact.

Pegs 23 to 22. The strain was at all times less than the relaxation strain, therefore no strata separation occurred here.

Pegs 22 to 21. The maximum strain was 30 percent more than the relaxation strain. A large quantity of water was observed to flow into the shaft near peg 21; however, the shaft lining was in good condition and had only a few small cracks. Strata separation may have occurred between these pegs.

Pegs 21 to 20. The strain exceeded the relaxation strain at one point only and for the most part it was considerably less. The shaft lining was in excellent condition and no water was observed to flow into the shaft. The rock was probably unfractured in this region.

Pegs 20 to 19. The strain was 15 percent higher than that for relaxation and a large quantity of water was observed

/ to ....

to flow into the shaft. The geological record of the shaft showed no obvious discontinuity here; however, a borehole drilled only 300 feet away from the shaft showed a very narrow intrusive sill at this level. The strata may have separated at this discontinuity, but the separation would have been less than 1/4 inch.

Pegs 19 to 17. The strain here was less than that for relaxation and the shaft lining was observed to be in good condition, therefore no bed separation occurred here.

Pegs 17 to 16. The maximum strain was four times that due to elastic relaxation. There was a very large crack in the shaft at a point corresponding to the upper contact of the Harmony Sill. The small group of seismic events occurred at this Sill. Strata separation must have occurred here.

Pegs 16 to 8. The strain was at all times less than the relaxation strain, which indicates that this rock was probably solid.

Pegs 8 to surface. Earlier than September, 1958, the strain was small; after September, 1958, alternating regions of high compression and tension were observed. Such a situation is physically most improbable and this apparently anomalous behaviour was probably due to damage to some pegs. It is assumed that no strata separation occurs above peg 16.

The results of the seismic and strain measurements are summarized in Figure 20. Both sets of observations show that the highly fractured region extends only to a height of about 300 feet above the excavation, and that fracture or separation occurs at the Harmony Sill.

/ FIGURE 20

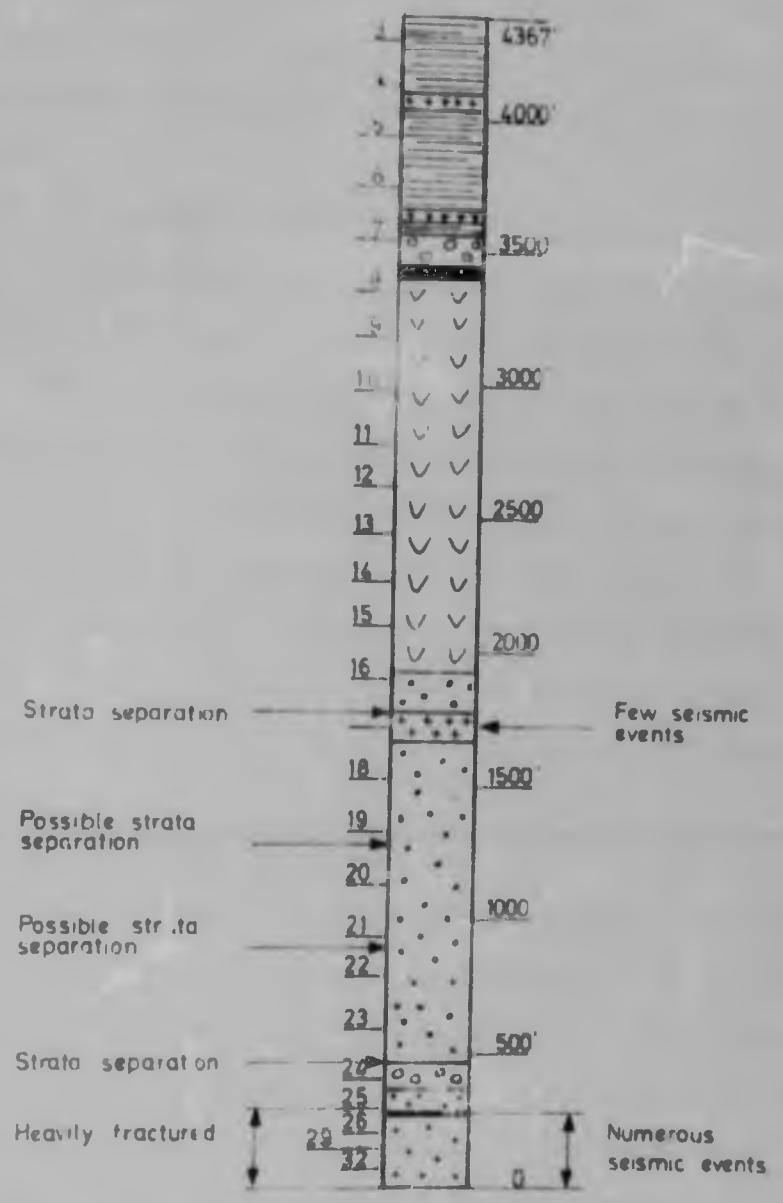


FIGURE 20 A COMPARISON RELATIVE TO THE GEOLOGICAL STRUCTURE OF THE CONCLUSIONS FROM THE STRAIN MEASUREMENTS AND THE SEISMIC OBSERVATIONS.

The strain measurements show that the rock between the the Kimberley Series and the Harmony Sill may have separated into three slabs. This conclusion is based on the modulus of relaxation being $10 \times 10^6$ p.s.i.; as this could be lower, it could be argued that no strata separation occurred. In any event, if strata separation has occurred, these slabs are probably unbroken since no seismic activity was observed in this region.

Strata separation at the Harmony Sill occurred at a surprisingly early stage. The strain exceeded the relaxation strain in May, 1957 when the span of the excavation was only 1500 feet. On the basis of a continuous elastic medium the stress change induced by the excavation at this distance should be much smaller than the normal virgin stress, so that strata separation would not be expected. Also, the fairly large energy releases detected seismically at this sill are difficult to explain. Therefore it appears that the fracture mechanism at the sill is not simply one of strata separation.

It can be concluded therefore that both the seismic observations and the strain measurements indicated that most of the fracturing was limited to a zone extending to a height of approximately 300 feet above the excavation. The height of this zone was not related to the horizontal extent of the surrounding excavation, and it extended laterally as the faces advanced. The rock mass did not exhibit gross inelastic behaviour except in a restricted region at the Harmony Sill where unexplained movements occurred.

/ The Kate....

The Rate of Energy Release.

The detailed mechanism of rockbursts and other forms of damage due to rock failure is still unknown. Studies of the energy changes which necessarily occur when an excavation is made underground seem to provide the best understanding of the phenomena leading to rock failure and damage (Cook[18]). It is common knowledge that the damage and rockburst hazard increases with depth and is greatest at remnants and in regions mined in an irregular manner. The observations above have qualitatively shown that seismicity is also related to the configuration of the excavation. The rate at which energy is released as an excavation is enlarged provides an objective parameter to describe mining geometry in terms which are significant to rock failure. In the following discussion, it is shown empirically that the rate of energy release per unit area increase in the size of an excavation is closely related to seismicity and incidence of damage in the mines.

The rate of energy release was determined by means of an electrical resistance analogue described by Cook and Schümann.[19] The value of the energy release rate obtained from the analogue refers to elastic rock behaviour; any deviation from elastic behaviour would result in a higher energy release rate. In the preceding section it was shown that the rock mass does not exhibit gross inelastic behaviour.

The most realistic method of assessing damage is to determine the inconvenience it causes. The mine keeps a record of the daily activities in each stope. It is therefore possible to determine the days spent in clearing working places after rockbursts and rockfalls. The number of days delay arising from this cause per unit area mined is, therefore, used to assess the damage, or inconvenience, to the mine caused by rock failures. It is also possible to determine

/ the ....

the number of labourers employed in each working place, so that additional difficulties of maintaining satisfactory strata control can be estimated from the additional number of man-shifts per unit area mined.

Four portions of the mine were chosen for making a comparison. They were all close together so that geological differences were at a minimum, and the average stoping width was 42 inches in all regions. The four regions are shown in relation to the whole mine in Figure 21. Two face positions are shown in the Figure, representing a year's mining. Region 1 contains a remnant in which a great deal of damage and seismic activity occurred and for which the average energy release rate was high. This remnant was not regarded by the mine management as exceptionally difficult; however, the mining conditions were far more difficult than in the other three regions. Region 2 contains a longwall face with a large span, but not large enough for complete closure to have occurred at the centre. Mining conditions were good and the average energy release rate was moderate. Regions 3 and 4 contain longwall faces with a short span, consequently the average energy release rate was low. The mining conditions were excellent.

Figure 22 shows a plan view of the seismic events that occurred in the four regions during the year's mining.

Figure 23 shows the same plan view with damage centres occurring over the same year; the diameters of the circles represent the extent of the damage measured in days delay. Only damage and seismic events that occurred in the four regions are shown.

Average values for all the variables in each of the four regions were determined.

/ FIGURE 21

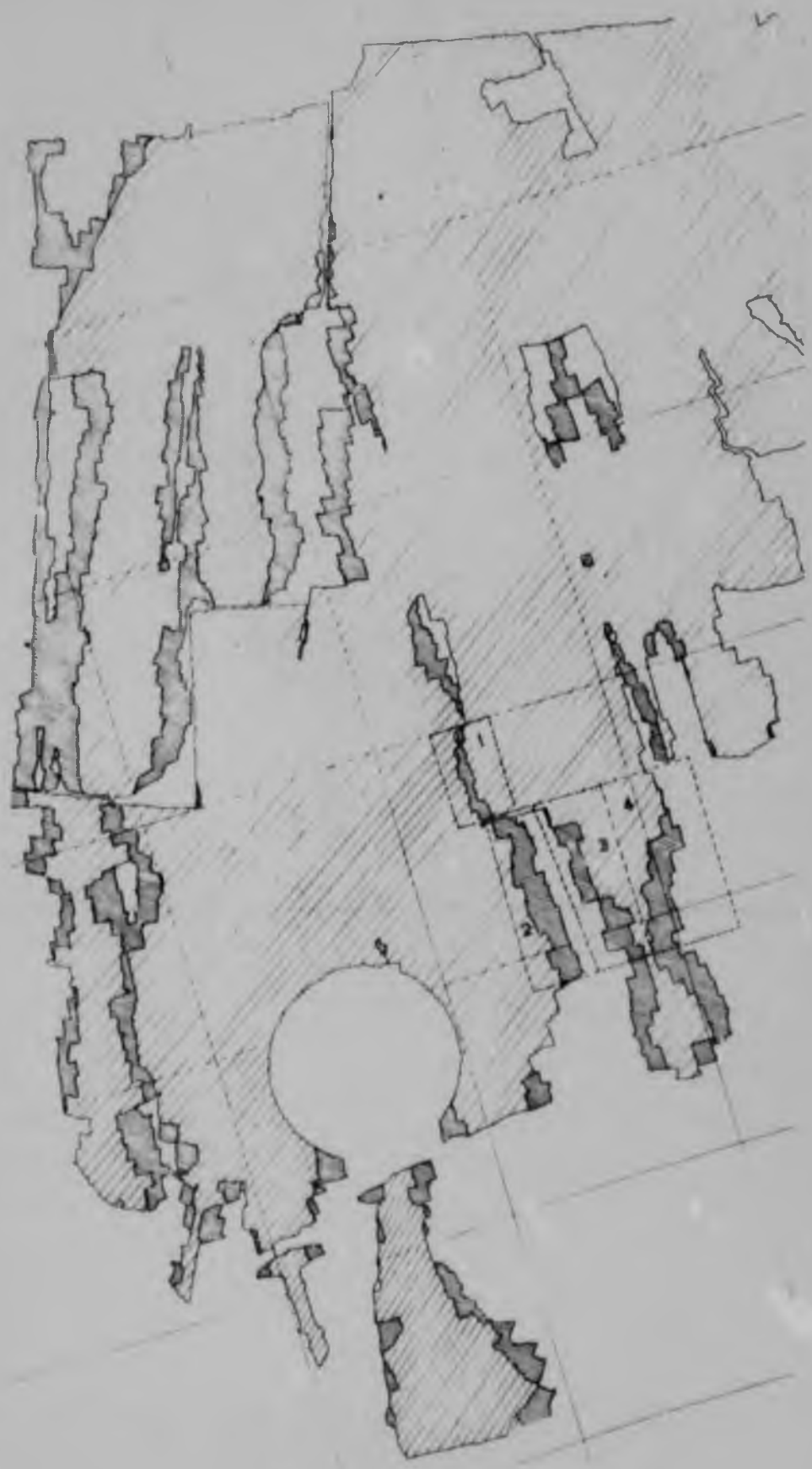

FIGURE 21 PLAN SHOWING THE FOUR REGIONS SELECTED FOR COMPARING THE RATE OF ENERGY RELEASE WITH DAMAGE, LABOUR REQUIREMENTS AND SEISMICITY.

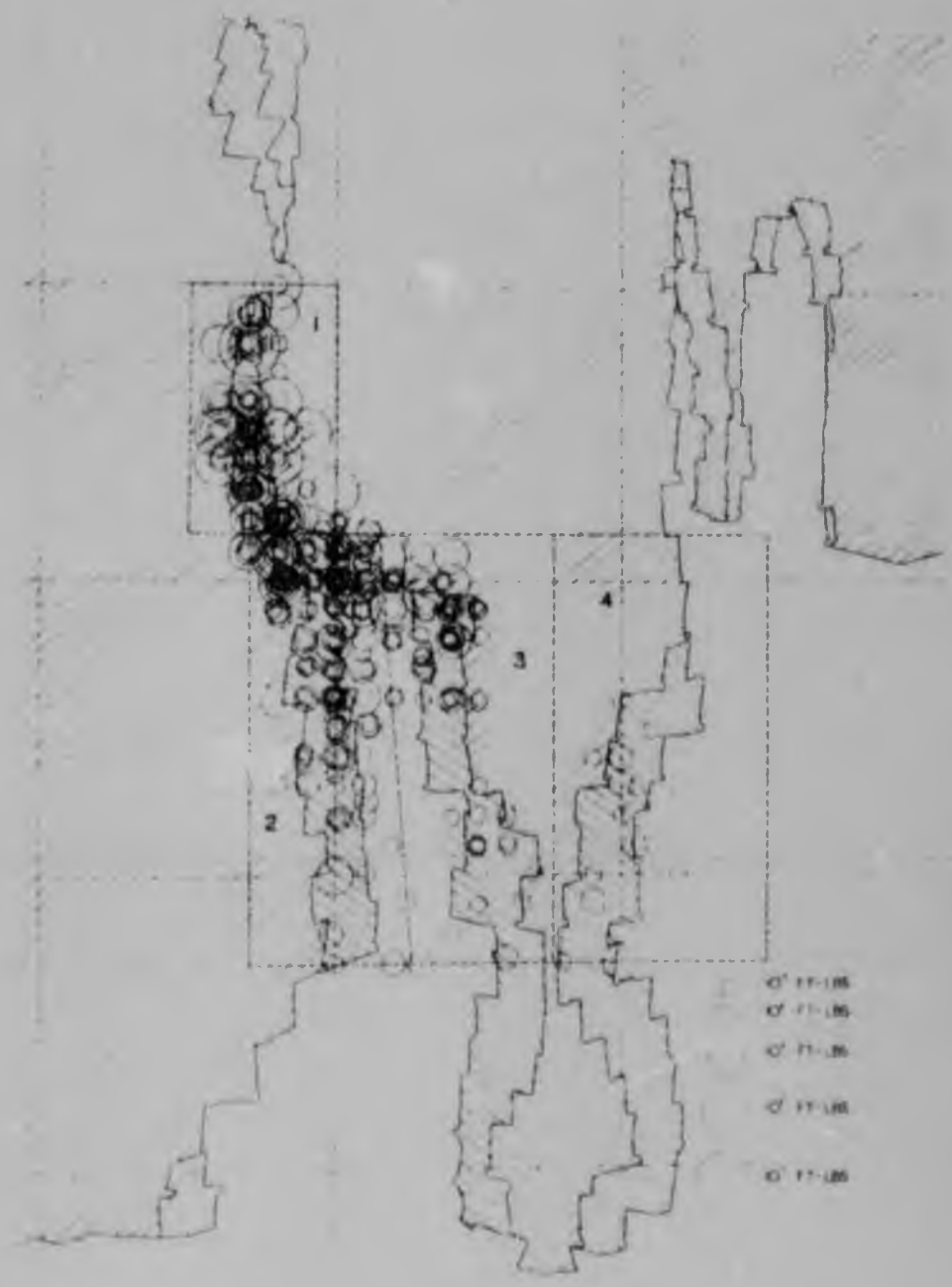


FIGURE 22 PLAN ON A GRID OF 1000 FEET SHOWING THE POSITIONS OF THE SEISMIC EVENTS THAT OCCURRED IN THE FOUR REGIONS SELECTED FOR COMPARISON WITH THE RATE OF ENERGY RELEASE.

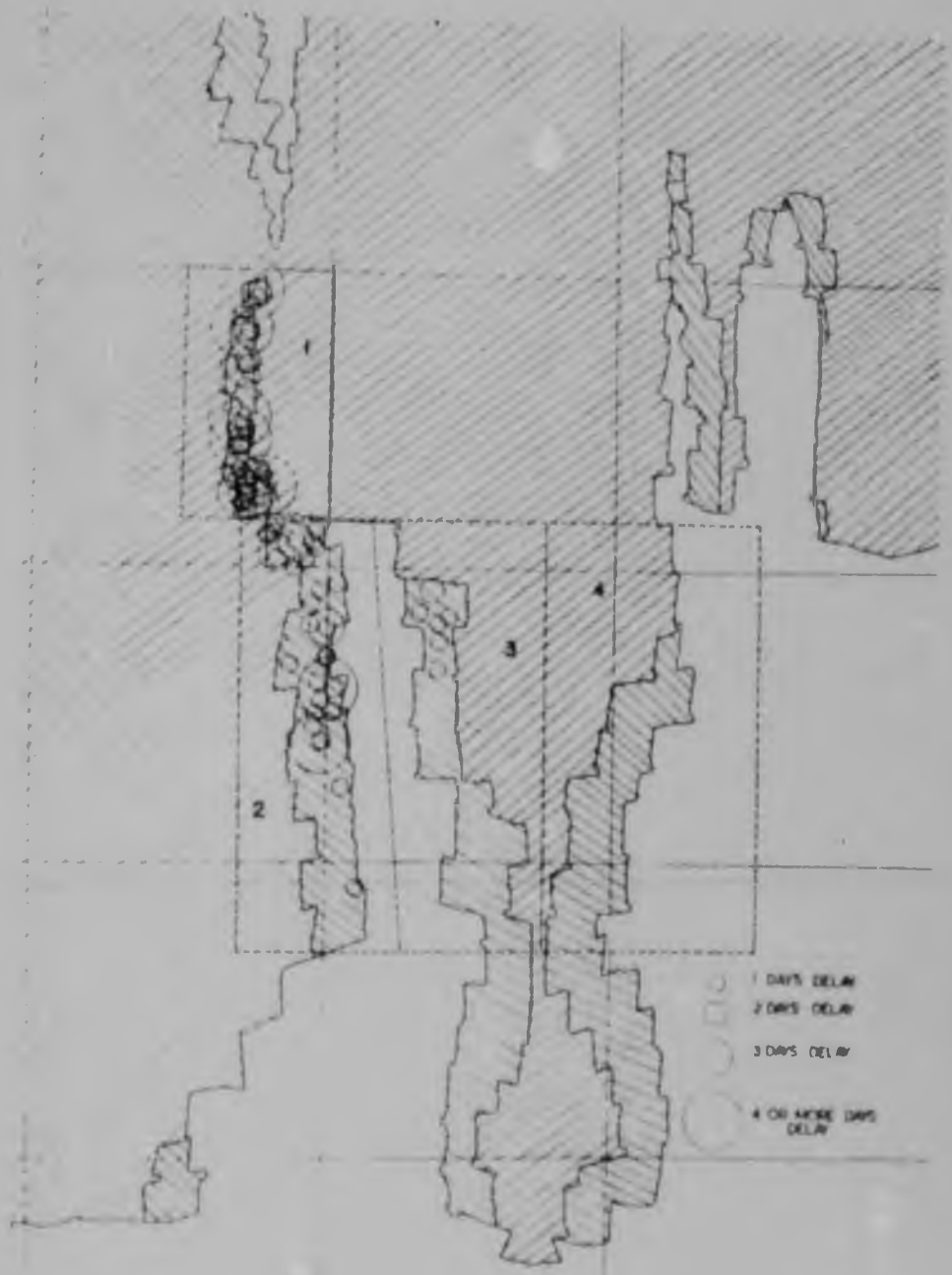


FIGURE 13 PLAN ON A GRID OF 1000 FEET SHOWING THE CENTRES OF DAMAGE THAT OCCURRED IN THE FOUR REGIONS SELECTED FOR COMPARISON WITH THE RATE OF ENERGY RELEASE.

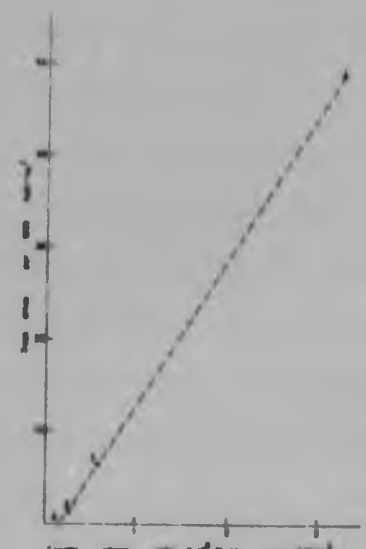

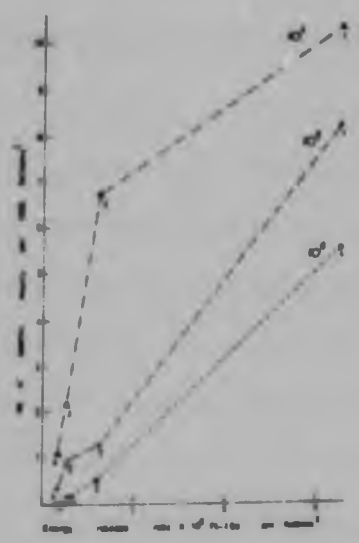

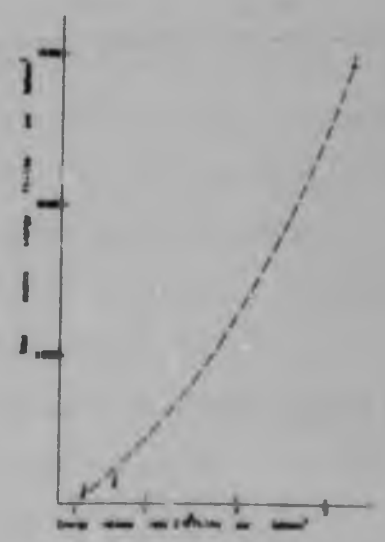

FIGURES

Fig.24 DAMAGE MEASURED IN DAYS DELAY PER 1000 FATHOMS$^2$ PLOTTED AGAINST THE ENERGY RELEASE RATE.

Fig.25 THE LABOUR REQUIREMENTS MEASURED IN MAN-SHIFTS PER FATHOM PLOTTED AGAINST THE ENERGY RELEASE RATE.

Fig.26 THE NUMBER OF SEISMIC EVENTS OF DIFFERENT SIZES PER 1000 FATHOMS$^2$ PLOTTED AGAINST THE ENERGY RELEASE RATE.

Fig.27 THE TOTAL SEISMIC ENERGY PLOTTED AGAINST THE ENERGY RELEASE RATE.

Figures 24 to 27 show damage, labour, seismicity and total seismic energy respectively, plotted against the energy release rate. The incidence of damage is almost linearly dependent on the energy release rate; it is also dependent on other factors, such as geological conditions and the type of support used in the stopes. Thus, in a particular mine where standard support methods are practised, the energy release rate will serve as a reliable parameter for predicting damage. At Harmony it can be said that when the energy release rate is less than $10^8$ ft.-lbs. per square fathom, mining conditions will be good. The simplest mining geometry would consist of two longwall faces advancing away from each other into virgin ground; eventually the stope span becomes so large that closure takes place at the centre of the stope and the energy release rate reaches a maximum value. The maximum energy release rate is $0.95 \times 10^8$ ft.-lbs./fathom$^2$ for a 42 inch stoping width at a depth of 5000 feet, which fallswithin the criterion for good mining conditions.

The labour required to mine the remnant in region 1 is twice that required to mine an equivalent area in the regions, which means that the cost of mining is approx-ely double. Furthermore the hazard per unit area mined is an order of magnitude higher, since twice as many men are exposed to five times as much damage. More isolated remnants in the mine, in which the energy release rate was still higher, have resulted in far worse mining conditions, and it is doubtful whether it was worthwhile mining those remnants.

There were only two seismic events of magnitude $10^7$ ft.-lbs., and both occurred in region 1. The total seismic energy radiated by the largest events exceeds the total seismic energy radiated by all the smaller events for any region. Figure 10 shows this phenomenon for the whole mine; in a remnant, however, it was far more pronounced than this.

/ Consequently ....

Consequently Figure 27 was almost completely controlled by the largest seismic events in each region. Under remnant conditions, the total seismic energy was less than $10^{-4}$ of the energy released. This implies that the vast majority of the energy released is dissipated in a stable manner and that the mechanism of unstable or violent energy release is obscured.

From Figure 26 it is interesting to note that the ratio of the small events to the large events decreased when the energy release rate was high or when extremely large events occurred. This behaviour is contrary to that of earthquakes where the ratio of small earthquakes to large earthquakes is approximately a constant for different regions.

/ Temporal Behaviour....

Temporal Behaviour of Seismic Events

The Harmony and Virginia Mines use a centralized blasting system, with the result that all charges in the stopes in each mine are fired in a matter of 10 to 30 minutes. At Virginia the blasting time is usually 3.00 p.m. to 3.30 p.m., and at Harmony it is usually 4.30 p.m. to 5.30 p.m. On Saturdays blasting is approximately one hour earlier. Figure 28 shows the diurnal distribution of (a) all the seismic events near the reef plane at Harmony, (b) all the seismic events at Virginia and (c) all the seismic events at the Harmony Sill that occurred during the first year of recording. The events at the Harmony Sill occurred randomly, but the events at the reef plane were strongly influenced by blasting. The peak in the Virginia distribution was earlier and narrower than the peak in the Harmony distribution, corresponding to earlier and a narrower spread in blasting times.

At Virginia, 50 percent of all the events occurred between 2.00 p.m. and 5.00 p.m., and at Harmony less than 40 percent of all the events occurred between 3.00 p.m. and 7.00 p.m.; this implies that the majority of seismic events were not triggered by blasting. It was thought that events of a particular size might be more sensitive to blasting than others and the diurnal distribution for each magnitude was determined, Figure 29. Only the distributions for Harmony are shown, since those for Virginia were similar. There is no obvious difference between these distributions and again 40 percent to 50 percent of the events occurred between 2.00 p.m. and 5.00 p.m., in the case of Virginia, and 3.00 p.m. and 7.00 p.m. in the case of Harmony. The large amount of seismic activity that occurred without external stimulus testifies to the time dependent behaviour of rock fracturing.

/ FIGURE 27

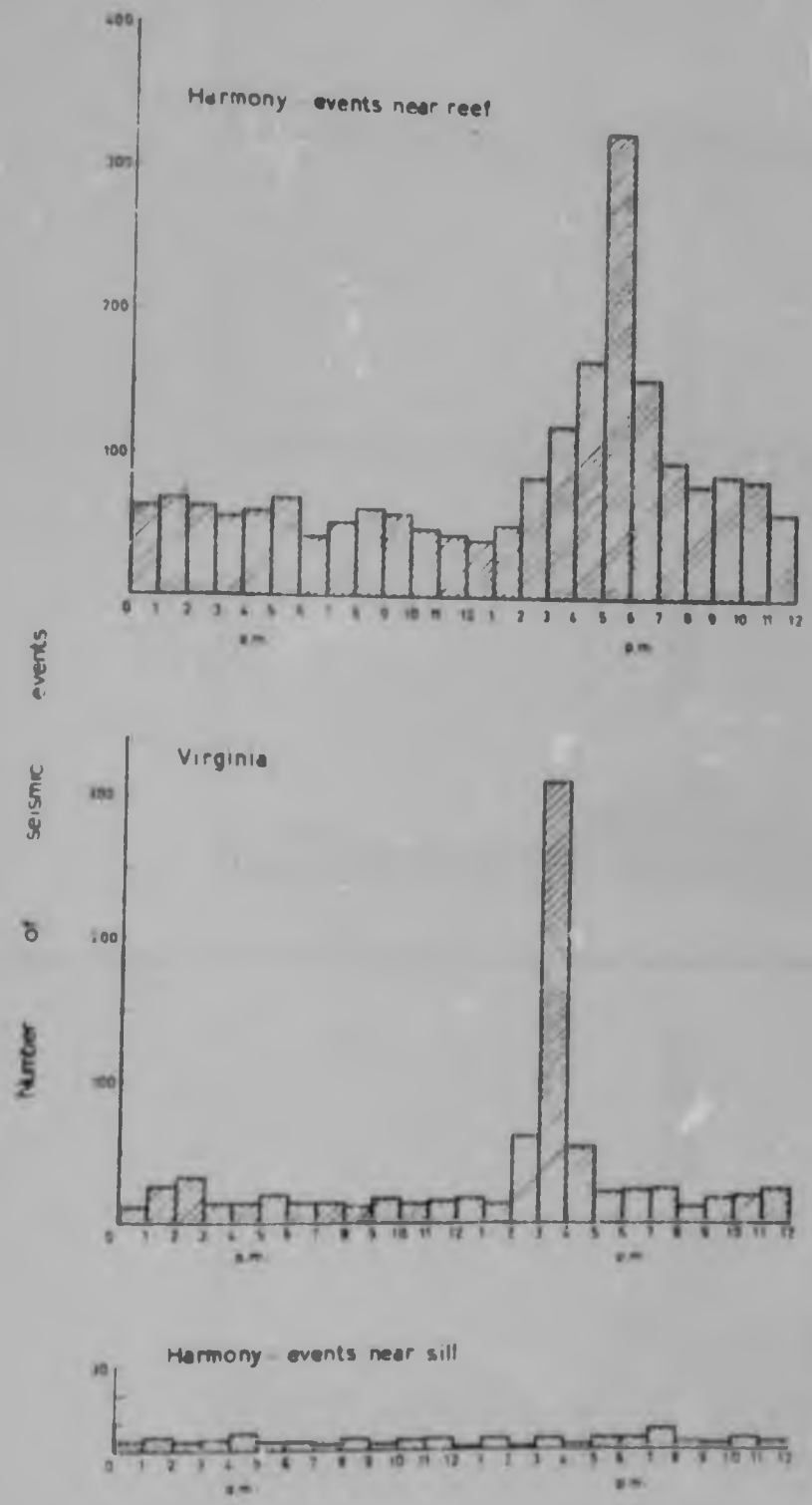


FIGURE 28 THE DIURNAL DISTRIBUTION OF ALL THE SEISMIC EVENTS THAT OCCURRED DURING ONE YEAR NEAR THE REEF AT HARMONY, NEAR THE REEF AT VIRGINIA, AND NEAR THE HARMONY SILL.

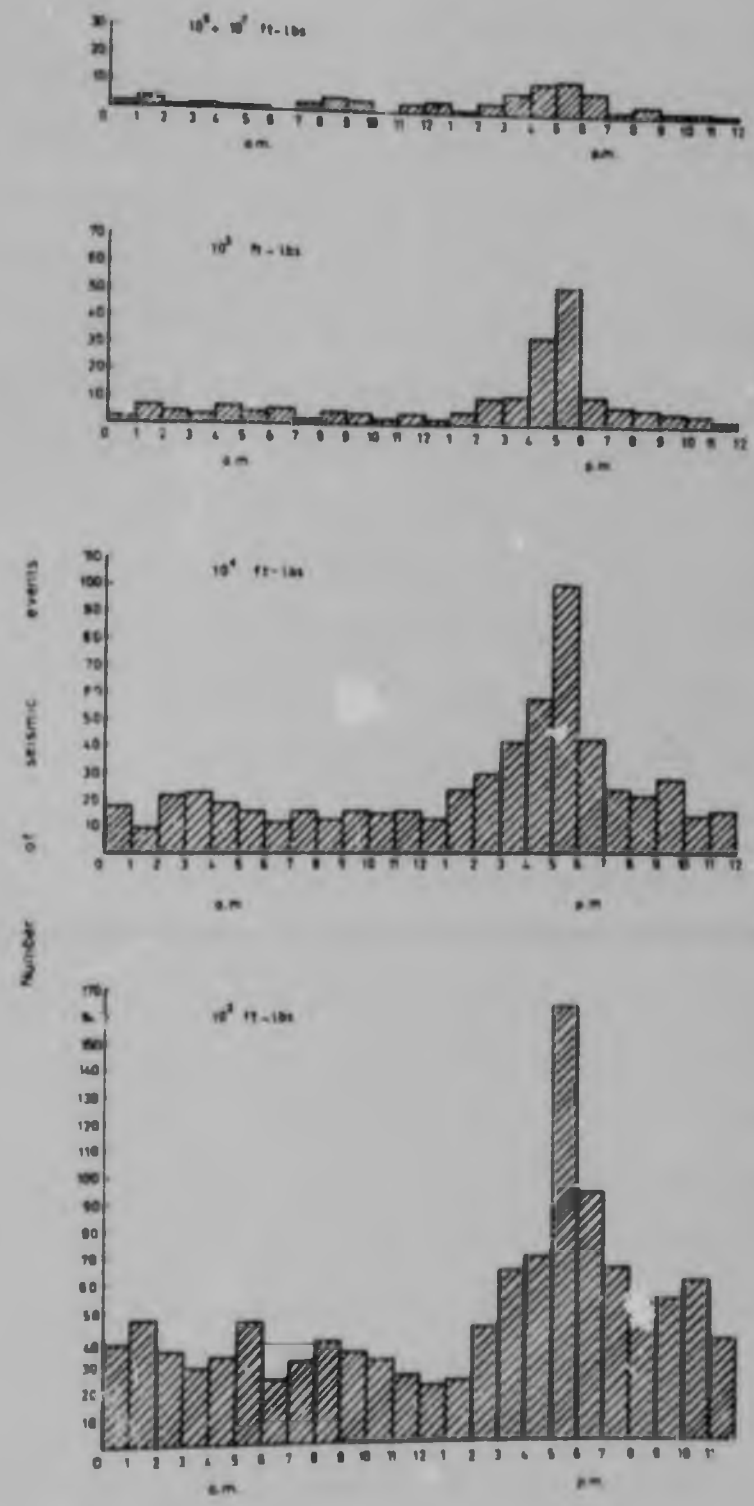


FIGURE 29 THE DIURNAL DISTRIBUTION OF SEISMIC EVENTS OF DIFFERENT SIZES THAT OCCURRED DURING ONE YEAR NEAR THE REEF IN HARMONY.

It is also interesting to see how the seismicity varies throughout the week, and it is more informative if this can be compared with the activity in the mine. The best method of estimating the mining activity is by means of the number of holes drilled and blasted in the stopes. It has been suggested that since the miners record the number of holes drilled themselves, they might report dishonestly on Mondays and Saturdays. The Harmony Mine management is confident that the reporting is honest; however, as a check on the human factor, the total number of stoping holes drilled was compared with the total amount of compressed air used during the working shift. Figure 30 shows the daily distribution of the total number of stoping holes drilled and of the total amount of compressed air used between 7.00 a.m. and 3.00 p.m. The compressed air is also used for purposes other than rock drilling; however, since there are no serious discrepancies between the two distributions, it can be concluded that the reported holes drilled reflects the true situation. The slightly smaller amount of compressed air used on Saturdays shown in Figure 30 is not necessarily indicative of less drilling, since drilling can start before 7.00 a.m. on Saturdays. Figure 31 shows the daily distribution of (a) all the seismic events near the reef at Harmony, (b) all the seismic events at Virginia and (c) all the seismic events at the Harmony Sill. Breaking these distributions down into distributions for different sized events yields patterns similar to those in Figure 31. The events near the reef have a distinct minimum on Sundays and a weak maximum in the middle of the week. The large number of events on Sundays again indicates time dependent behaviour in rock fracturing.

/ FIGURE 29 ....

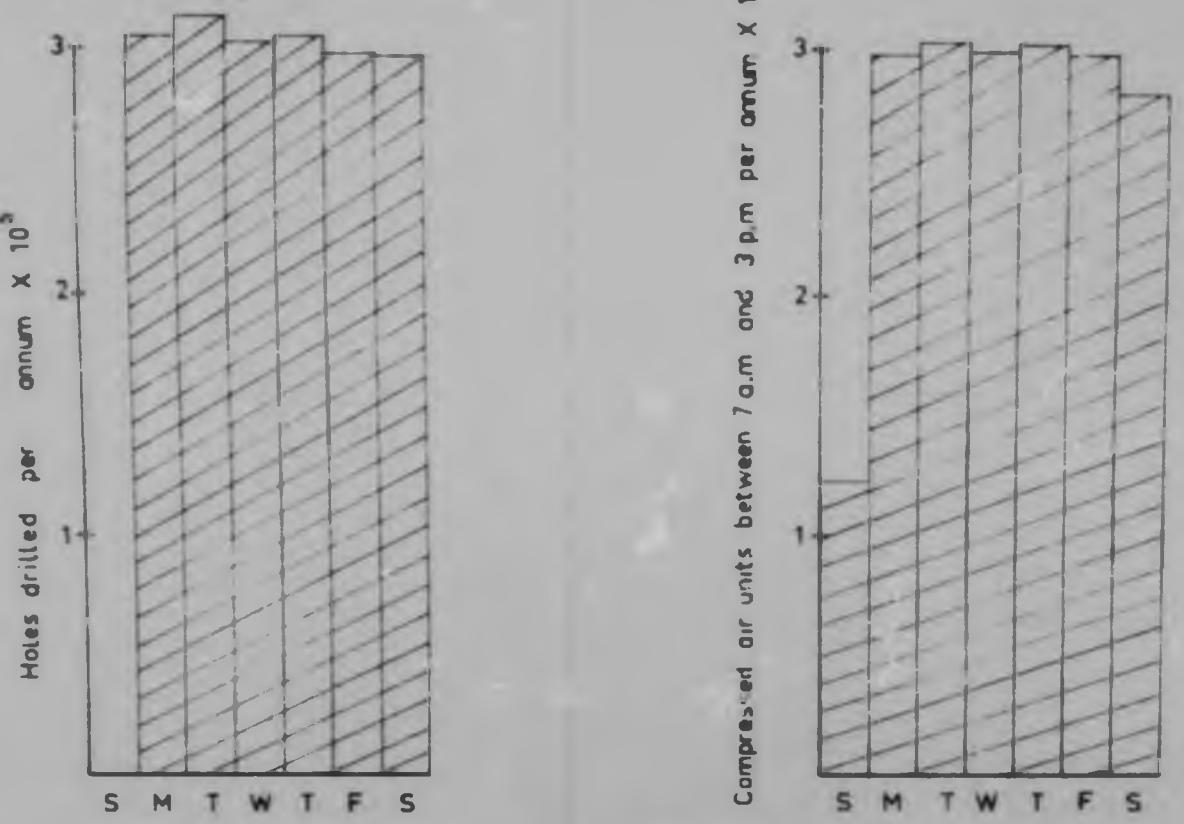


FIGURE 30 THE DAILY DISTRIBUTION OF THE TOTAL NUMBER OF STOPING HOLES DRILLED, AND OF THE TOTAL NUMBER OF UNITS OF COMPRESSED AIR USED BETWEEN 7.00 A.M. AND 3.00 P.M., DURING ONE YEAR.

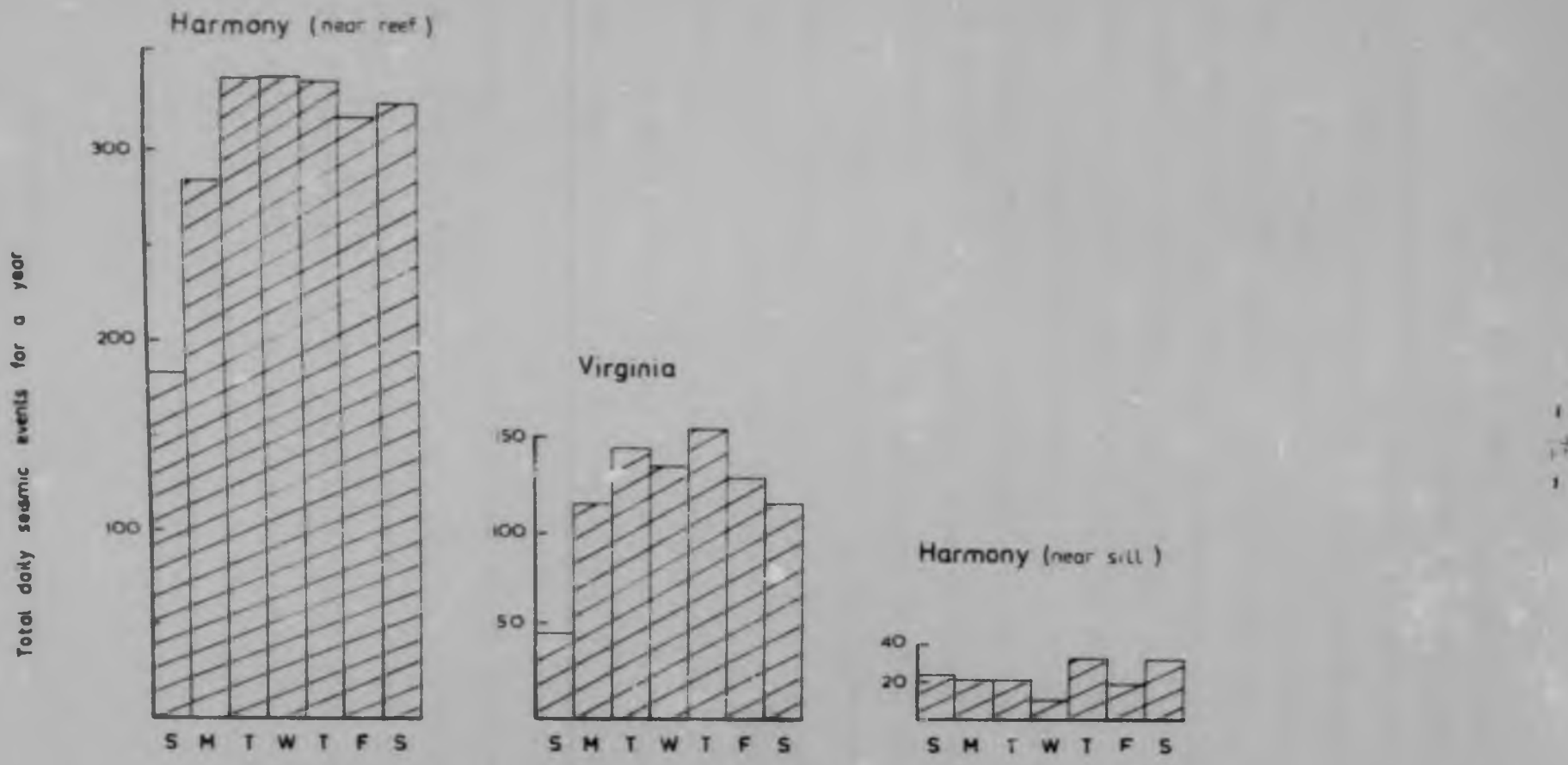


FIGURE 11 THE DAILY DISTRIBUTION OF SEISMIC EVENTS THAT OCCURRED AT HARMONY NEAR THE REEF, AT VIRGINIA NEAR THE REEF, AND NEAR THE HARMONY SILL.

Figure 32 shows the variation with time of the total number of stoping holes drilled each week, the total number of events near the reef at Harmony in each week, and the total number of events near the Harmony Sill in each week.

A fire broke out in the mine on the 29th October, 1964 and brought mining operations to a standstill over a large portion of the mine. The reduction in mining activity, caused a marked decrease in the seismic activity near the reef; at other times, however, the seismic activity has fluctuated widely while the mining activity has remained appreciably constant. The events at the Harmony Sill are quite independent of the mining rate, although the peaks in activity roughly correspond with the peaks in the seismic activity near the reef. Figure 33 shows the activity of the different sized events; there appears to be no interdependence between them. There were no obvious seasonal variations and no connection with earth tides could be found. Seismic events at the Harmony Sill frequently occur in swarms with the events separated by a few seconds to a few hours. The events near the reef plane show a very much less marked tendency to swarming. Events of magnitude $10^7$ and $10^8$ ft.-lbs. are usually preceded and followed by a period of low seismic activity in their immediate neighbourhood. Events of magnitude $10^6$ ft.-lbs. are sometimes accompanied by two or three small events. This type of behaviour hints that the mechanism of the events at the Sill is different from the mechanism of the events in the reef plane.

/ FIGURE 32

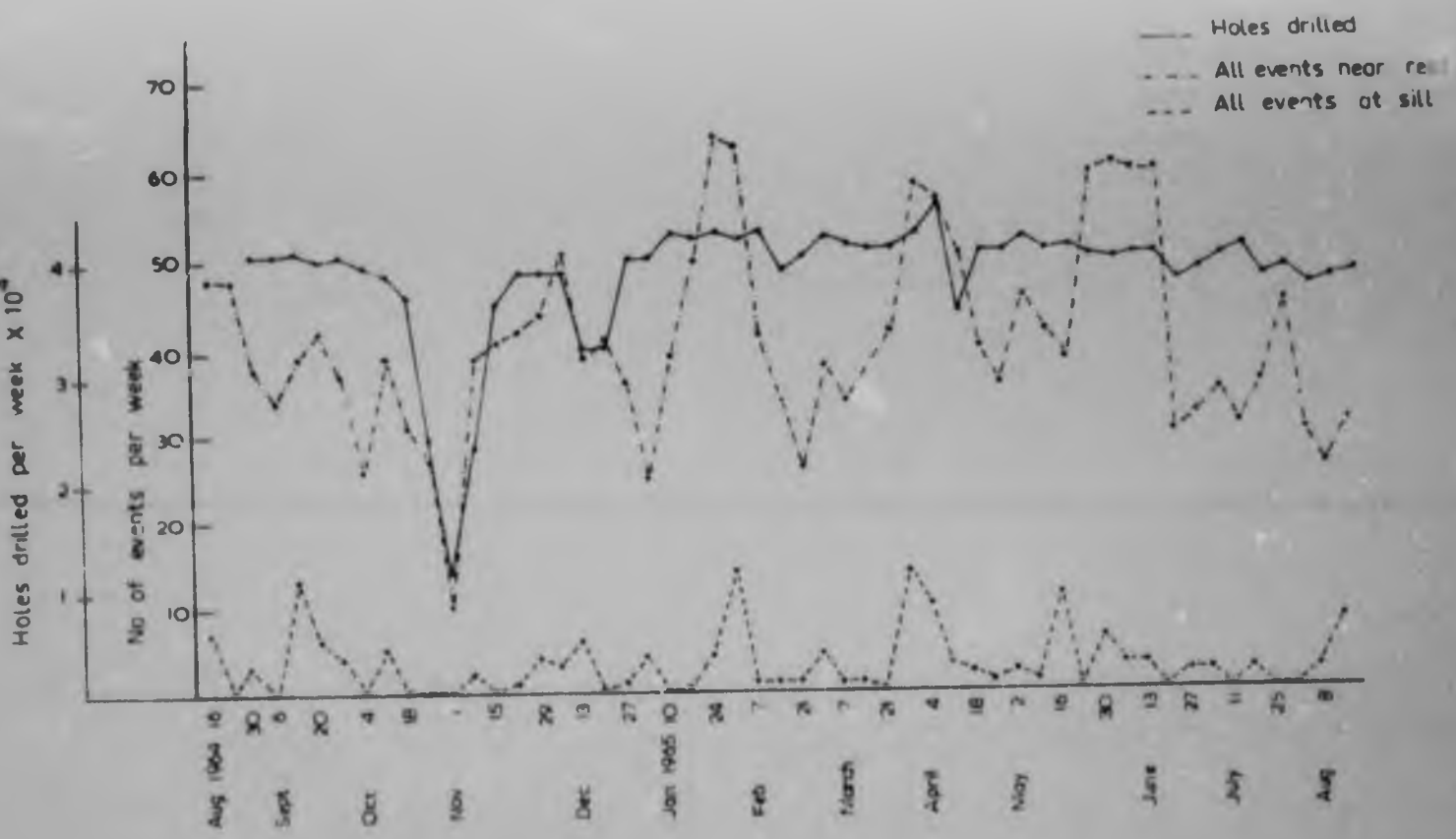


FIGURE 72 THE VARIATION WITH TIME OF THE TOTAL NUMBER OF HOLES DRILLED PER WEEK, THE TOTAL NUMBER OF SEISMIC EVENTS THAT OCCURRED NEAR THE REEF AT HARMONY, AND THE TOTAL NUMBER OF SEISMIC EVENTS THAT OCCURRED NEAR THE HARMONY SILL.

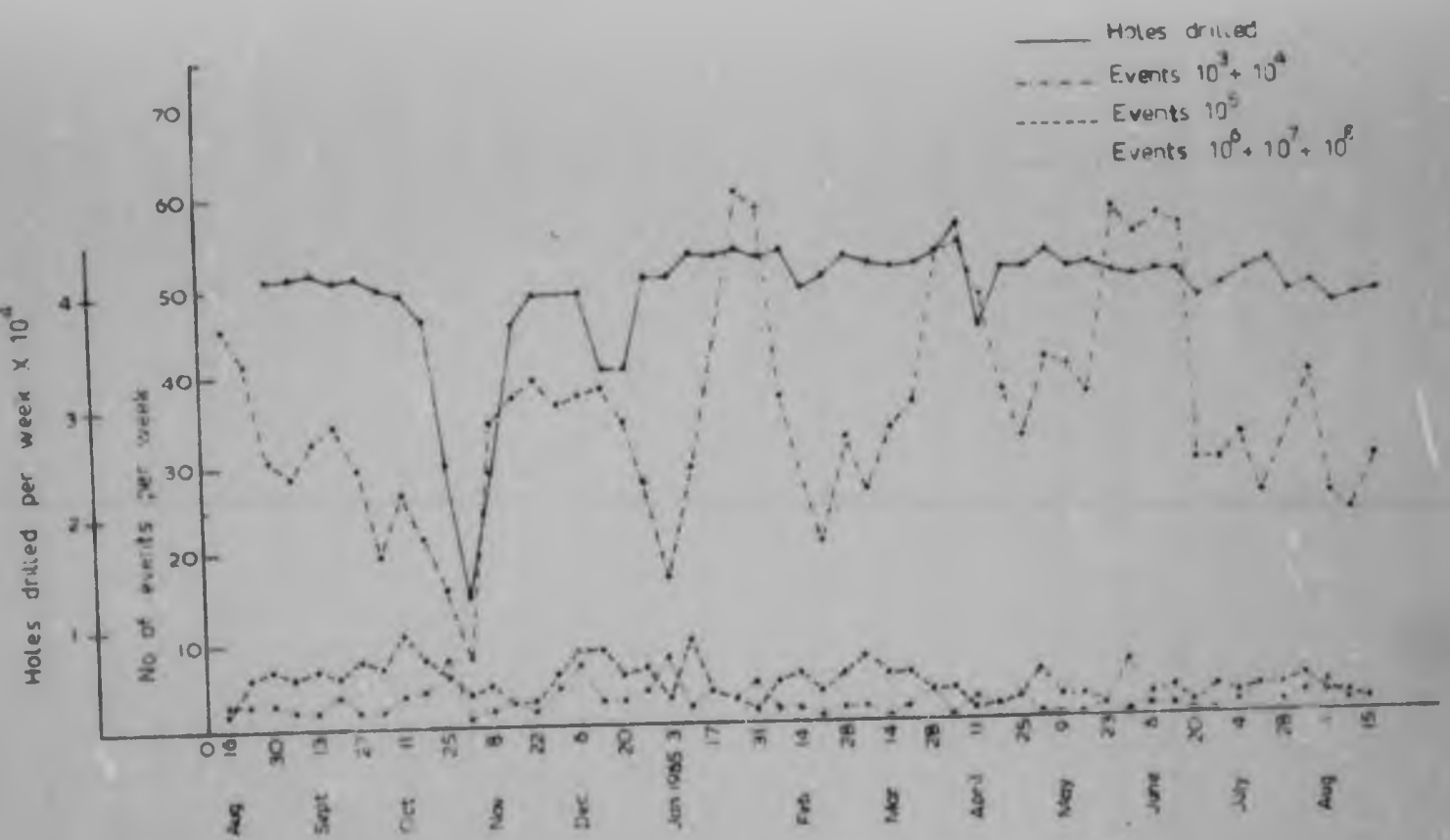


FIGURE 33 THE VARIATION WITH TIME OF THE TOTAL NUMBER OF STOPING HOLES DRILLED PER WEEK AND OF THE TOTAL NUMBER OF SEISMIC EVENTS OF DIFFERENT SIZES PER WEEK.

Tremors and Damage

The Harmony Mine keeps a record of tremors. The observations were made by four or five persons who made a note of the time whenever they felt a tremor. This record obviously cannot be complete, and tremors originating in neighbouring mines could also have been recorded. By comparing the time at which a tremor occurred with the times of the seismic events, it was possible to identify the source of the tremor and its magnitude. Of the reported tremors, 80 percent corresponded with seismic events, the remainder probably originated in neighbouring mines. Table I shows the percentage of different sized events noticed as tremors.

The Mine also keeps a record of "Rockburst Reports". The damage that was reported was primarily in the nature of rockfalls which affected an area ranging from 300 square feet to 8000 square feet in extent. Minor damage was not reported. In some cases, rockfalls were accompanied by damage to the face, and in 20 percent of the cases no rockfall was reported, but the damage was described as "face bumped". 92 percent of the reported incidents occurred in declared remnant areas, while the remaining incidents occurred on corner abutments.

Seismic events can be associated with damage by comparing the plan position of the events with the known position of the damage. In a number of cases the time at which the damage occurred was also known. Since the time at which the seismic events occurred is known, the time at which the damage occurred can be determined in those cases for which the time was not known.

/ TABLE I

TABLE 1

| Magnitude ft.-lbs. | $10^3$ | $10^4$ | $10^5$ | $10^6$ | $10^7$ | $10^8$ |
|---|---|---|---|---|---|---|
| Total Number of Events Harmony + Virginia | 535 | 441 | 152 | 62 | 6 | 2 |
| % Associated with Tremors | 0 | 4.6 | 21 | 42 | 50 | 100 |
| % Associated with Minor Damage. Harmony + Virginia | 18.8 | 18.2 | 15.4 | 75 | 100 | - |
| Total Number of Events: Harmony | 364 | 313 | 118 | 51 | 4 | - |
| % Associated with Reported Damage: Harmony | 0 | 1.3 | 5.1 | 22 | 0 | - |

The data in this Table is for the period 11th August, 1964 to 11th January, 1965, except for the minor damage which covers a 12 day period only.

---

TABLE II

| Correlation | Total | Good | Doubtful | Very Doubtful | None |
|---|---|---|---|---|---|
| Number of Incidents | 660 | 264 | 35 | 40 | 321 |
| Number of Incidents as % of Total | 100% | 40% | 5% | 6% | 49% |

---

/ Official ....

Official "Rockburst reports" submitted between the 11th August, 1964 and 11th January, 1965 were compared with seismic events. (Very few reports were submitted after 11th January). 81 percent of the reported incidents of damage could be positively identified with seismic events, the remaining incidents were all small.

A more intensive experiment was conducted to determine the relationship between seismic events and minor damage. The seismic events were located within 36 hours of their occurrence. The co-ordinates of the foci of the events were immediately relayed to the mine, whereupon an observer would be sent to the nearest point to the focus of each event to see whether there had been any damage. This experiment was carried out for 12 days during which time 100 events were located and no official "Rockburst reports" were submitted. The nature of the damage observed was small rockfalls, broken sticks and scaling. Table I shows the percentage of different sized events causing damage; minor damage, i.e., damage that is not reported, and the officially "Reported damage" are shown separately.

/ FIGURE 34

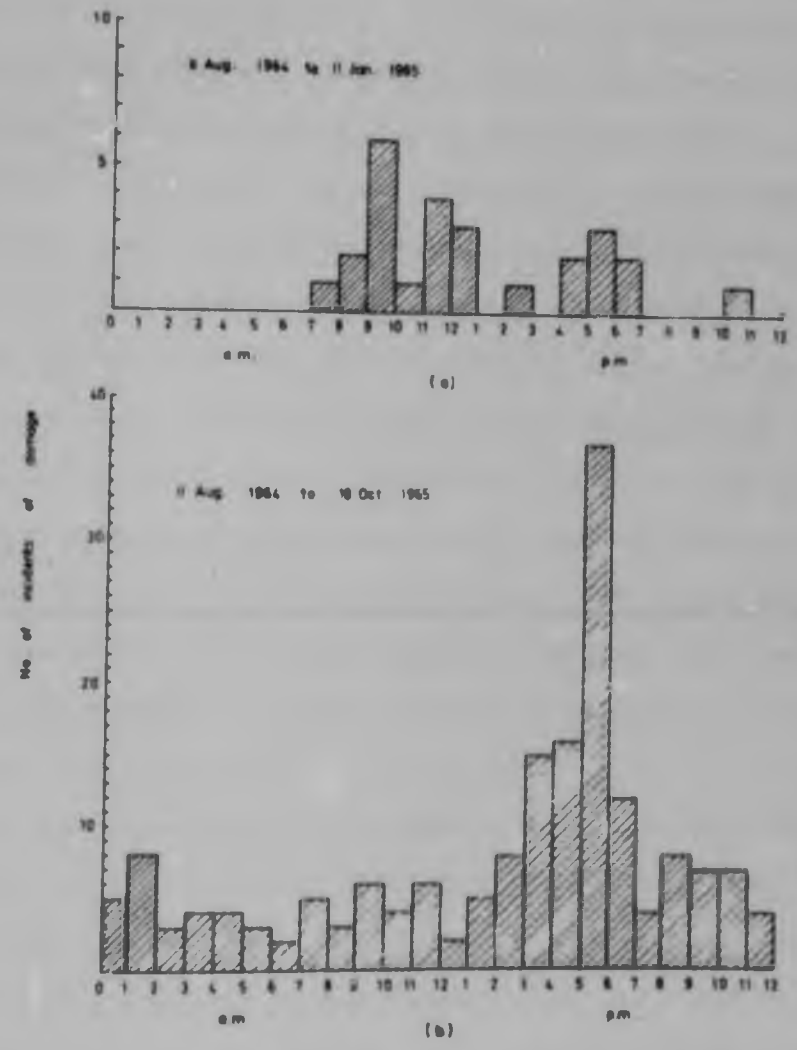


FIGURE 34

a) THE DIURNAL DISTRIBUTION OF OFFICIALLY REPORTED DAMAGE.

b) THE DIURNAL DISTRIBUTION OF SEISMIC EVENTS THAT COINCIDED WITH DAMAGE WHICH PREVENTED NORMAL MINING OPERATIONS IN THE STOPES.

Figure 34a shows the diurnal distribution of officially reported damage from 11th August, 1964 to 11th January, 1965. This distribution shows a surprising amount of damage during the working shift, namely between 7 a.m. and 2 p.m. The Mine Management feels that this distribution arises from biased reporting, since on psychological grounds, a rockfall occurring during the working shift is more likely to be reported than one occurring in off-shift periods. In addition the "rockburst reporting" is not complete, consequently an alternative method for assessing damage was adopted. The daily activities in each stope are recorded, and it is thus possible to determine the days on which the normal mining operations were obstructed by rockfalls or rockbursts. The number of days on which normal mining operations were prevented in a stope is a measure of the severity of the damage.

At Harmony the mining cycle takes the following form: On one day a stope face is drilled and blasted, and on the next day it is cleaned by means of scrapers. No night shift work was carried on in the stopes under consideration. According to this method of assessing damage, only rockbursts or rockfalls which prevented drilling and blasting and scraping are considered damaging.

In order to identify a seismic event with an incident of damage, two conditions have to be fulfilled; they have to be coincident in time and in space. The exact time at which damage occurred is not known, since the records only give the days on which a stope was inactive. If a rockfall occurred after the working shift had left the stope at about 2.00 p.m., it would only be noticed on the next day, which would then be recorded as the first inactive day. However, if the rockfall occurred during the working shift, that day on which the rockfall occurred would be recorded as the first inactive day. Thus, to form a time correlation, the

/ seismic .....

seismic event must have occurred between 2.00 p.m. on the day before the first inactive day and 2.00 p.m. on the first inactive day. When Monday was the first inactive day, the seismic event must have occurred between 2.00 p.m. on Saturday and 2.00 p.m. on Monday. There are a few situations which do not fit this time coincidence condition; for example if a rockfall occurred in an advance track cutting (a.t.c.) during the working shift, it would not prevent drilling and blasting on the one stope face adjoining it, but it would prevent cleaning in the other stope. Thus it was possible for one rockfall to cause inactivity on different days in adjoining stopes. Also a rockfall could be followed by a second rockfall and a seismic event a day or more later, and the seismic event would thus not be identified with any damage.

The accuracy of location of the seismic events is approximately 100 feet. The accuracy with which the co-ordinates of the centre of the damage can be determined is also about 100 feet, since a stope face can have a length of 300 feet and a rockfall at one end in an a.t.c., say, could cause a stoppage. It is feasible that the focal mechanism of a seismic event could extend over a distance of 100 feet, and it is also feasiblethat a violent event could cause a rockfall at a distance of 200 or 300 feet away. Hence it has been considered reasonable to choose the condition that the seismic event should be less than 500 feet away from the centre of damage.

It was decided to make correlations on three bases in order that exceptional cases and misunderstandings in the reporting of the first inactive day may be included:

/ i) Good ....

i) Good correlation. The seismic event must occur between 2.00 p.m. on the day before and 2.00 p.m. on the first inactive day and must be less than 500 feet from the centre of damage.

ii) Doubtful correlation. The seismic event must occur between 2.00 p.m. two days before and 2.00 p.m. one day before the first inactive day, and must be less than 500 feet from the centre of damage.

iii) Very Doubtful correlation. The seismic event must lie within 700 feet of the damage and must occur between 2.00 p.m. three days before the first inactive day and 2.00 p.m. one day after the first inactive day.

iv) No correlation. No seismic event can be found which fulfils any of the conditions in categories (i), (ii) or (iii).

When more than one seismic event fulfilled these conditions, the larger event was selected unless the smaller event was much closer to the centre of damage.

The Harmony Mine Management made their records from the 11th August, 1964 to 18th October, 1965 available for examination. In the records a distinction was made between damage due to rockfalls and damage due to rockbursts. Table II shows the number of incidents of damage falling into the different correlation categories, for which a seismic event can be found. Only 11 percent of the incidents lie in the doubtful categories and since only a small fraction of these incidents can be expected to be directly related to seismic events, they were grouped with the 'no correlation' category in the following analysis. Thus it can be concluded that at least half the damage is not accompanied by seismic activity of sufficient intensity to be located by the seismic recording network.

/ TABLE III ....

TABLE III

| Magnitude of seismic event, ft-lbs. | | $10^7$ | $10^6$ | $10^5$ | $10^4$ | $10^3$ | No correlation |
|---|---|---|---|---|---|---|---|
| Delay of more than 3 days | Rockburst | 2 | 11 | 0 | 4 | 3 | 15 |
| | Rockfall | 1 | 3 | 1 | 0 | 0 | 12 |
| Delay of 2 or 3 days | Rockburst | - | 6 | 1 | 6 | 6 | 11 |
| | Rockfall | - | 12 | 2 | 3 | 3 | 29 |
| Delay of 1 day | Rockburst | - | 23 | 4 | 23 | 26 | 76 |
| | Rockfall | - | 14 | 19 | 42 | 49 | 253 |
| Number of events coinciding with damage | | 2 | 36 | 21 | 52 | 69 | |
| Total number of events | | 4 | 91 | 217 | 715 | 1542 | |
| Seismic events coinciding with damage, as a percentage of total number of events | | 50% | 40% | 9.6% | 7.3% | 4.5% | |

Table III shows the number of incidents of damage recorded as rockfalls and the number of incidents recorded as rockbursts which correlate with seismic events of different size. The damage has been subdivided into three groups representing the severity of the damage. There were 660 incidents of damage of which 80 percent delayed mining operations for one day only. Amongst the smallest incidents, only 38 percent coincided with seismic events, while amongst the larger incidents about 48 percent coincided with seismic events. Rockbursts have been defined by Cook et. al.(21) as "damage to underground workings caused by uncontrolled disruption of rock associated with a violent release of energy additional to that derived from falling rock fragments". Because about half of the incidents of damage reported as rockbursts are not accompanied by seismic events, it must be concluded that at least half of them are not proper rockbursts. Damage reported as rockbursts shows a slightly greater tendency to be accompanied by seismic events than damage reported as rockfalls, particularly in the case of severe damage. Thus even though a great deal of damage has been incorrectly classified, some cases do show rockburst characteristics. Table III also shows the number of seismic events that coincided with damage; this number is shown as a percentage of the total number of seismic events of each size that occurred over the same period as the damage. There are fewer seismic events than incidents of damage since often a seismic event can be identified with damage in more than one stope. In fact more seismic events must have been associated with damage than that given in Table III, since this analysis considered damage near stope faces only.

The fact that few seismic events cause damage within a short while of their occurrence, implies that the seismic events must occur at a relatively large distance either

/ ahead ....

ahead of the face or above the face. This conclusion lends credence to the vertical distribution of seismic events in Figure 16. The vertical distribution of the events of magnitude $10^6$ ft.-lbs. which coincide with damage is shown in Table IV.

TABLE IV

| Height of events above excavation - ft. | +300 | +200 | +100 | 0 | -100 |
|---|---|---|---|---|---|
| Number of events of magnitude $10^6$ ft.-lbs. | 3 | 6 | 11 | 11 | 4 |

TABLE V

| Distance between event and damage - ft. | 0-100 | 100-200 | 200-300 | 300-400 | 400-500 |
|---|---|---|---|---|---|
| Number of incidents | 51 | 66 | 59 | 58 | 30 |

These events lie closer to the reef plan than those in the general vertical distribution of Figure 16. Table V shows the distribution of the distances between the foci of seismic events and the centres of damage which coincide with them; since so many distances lie between 300 feet and 500 feet, it means that a number of events which coincided with damage were really unrelated to the damage, particularly in the case of small seismic events.

/ Figure ....

Figure 34b shows the diurnal distribution of the seismic events which coincide with damage. This distribution is similar to that of Figure 28 and different from that of Figure 34a, and confirms that the official "rockburst reports" were biased towards frightening instances of damage.

The main conclusion from this section is that most of the damage occurs unaccompanied by seismic events or the violent release of energy. This implies that the non-violent damage is due to the collapse of rock that has already been fractured. The only preventative measure against this damage is to reduce the degree of fracturing around theexcavation and the only remedial measure is to improve the support in the stopes. At Harmony, nine-pointer packs at 8 ft. 8 in. centres consisting of 2 ft. 8 in. chocks have been used in normal stopes. However, at present, they are now using the same nine-pointer pack, but with concrete bricks replacing every alternate row of timber; this pack forms a more rigid support (Petersen and Botha[22]). The hangingwall conditions have improved noticeably with the new support, and it is anticipated that there will be fewer rockfalls in the future. The degree of fracturing is dependent on the stress concentrations ahead of the face, and therefore also also on the rate of energy release, thus by controlli the the rate of energy release, the extent of fracturing be c be controlled. It has already been shown that damage is d is directly related to the rate of energy release.

/ Mechanism of ....

Mechanism of Seismic Events

It has been shown that only a minute fraction of the energy released appears in a violent form, therefore there must be a large scale mechanism for dissipating the bulk of the energy stably. The viscosity of hard rock is far too high to dissipate any appreciable amount of energy in the time scales common in mining, consequently the only way in which energy can be dissipated is by developing or causing movement on fracture surfaces. Most plastic behaviour in hard rock can be attributed to the growth of numerous small cracks (Griffith cracks), while true plastic behaviour is negligible. In producing fracture surfaces, energy can be dissipated in three forms, namely, kinetic energy, frictional energy and surface energy which includes plastic deformation at crack tips.

At this stage it is worthwhile to review some of the most recent work on rock fracture. In a comprehensive analysis, Hoek[10] has shown that the Griffith's Crack Theory, modified for closed cracks under compression, satisfactorily predicts the onset of crack growth under static loading conditions. The onset of crack growth is expressed by

$$\tau - \mu\sigma_n = -2\sigma_t = \tfrac{1}{2}\sigma_c \left(\sqrt{1+\mu^2} - \mu\right) \quad \ldots\ldots \quad (5)$$

where $\tau$ = shear stress parallel to crack surfaces

$\sigma_n$ = stress normal to cracks surfaces

$\mu$ = coefficient of friction between crack surfaces

$\sigma_t$ = tensile strength of rock

$\sigma_c$ = uniaxial compressive strength of rock.

/ Equation ....

Equation (5) is dependent on the orientation of the cracks and the cracks most likely to fail have an orientation given by

$$\tan 2\theta = {}^{1}/_{\mu} \qquad \ldots\ldots \quad (6)$$

where $\theta$ = the angle between the crack surfaces and the maximum principal stress.

Griffith's theory predicts that rock fails under stress conditions inversely proportional to the square root of the crack length. Brace[23] has shown that the tensile strength of several types of rock is predicted by the Griffith's theory when the crack length is taken as the maximum grain diameter, and in the case of limestone, the tensile strength is inversely proportional to the square root of the maximum grain diameter. Equation (5) therefore can be written in the form

$$c = \frac{a}{(\tau - \mu\sigma_n)^2} \qquad \ldots\ldots \quad (7)$$

where $2c$ = crack length

$a$ = constant

Brace and Bombolakis[24] and Hoek and Bieniawski[25] have shown that under compression, cracks do not grow along their own length, but grow in a direction such that they tend to become parallel with the direction of the maximum principal stress. Cook and Fairhurst[26] have used this phenomenon to explain the failure mode resulting in the formation of slabs parallel to free surfaces. They have also shown that this stable or non-violent failure mode is dependent on the method of loading of the rock.

/ In analysing....

In analysing the energy changes associated with the extension of Griffith's cracks, Cook[15] has shown that the rate at which energy is supplied to the rock by the loading system determines whether the rock fails violently or non-violently. He also shows that under certain conditions, the rock can fail spontaneously. Since this work is highly pertinent to the rockburst problem it has been examined in greater detail, and extended slightly.

The strain energy stored around an infinitely long slit-like crack of width 2c, and in a plane strain, tensile stress field, per 2c length of crack is given by

$$W_{s1} = \pi \frac{(1 - \nu)}{G} \sigma^2 c^3 \qquad \ldots\ldots \text{(Orowan[27])}$$

where $\nu$ = Poisson's Ratio

$G$ = Modulus of rigidity

$\sigma$ = tensile stress in a direction normal to crack surfaces.

The energy stored around a penny-shaped crack of diameter 2c in a tensile stress field is given by

$$W_{s2} = \frac{4}{3} \frac{(1 - \nu)}{G} \sigma^2 c^3 \qquad \ldots\ldots \text{(Sack[28])}$$

The energy stored around a slit-like crack in a plane strain compressive stress field per 2c length of crack is given by

$$W_{s3} = \frac{\pi}{2} \frac{(1 - \nu)}{G} \tau^2 c^3 \qquad \ldots\ldots \text{(Starr[29])}$$

where $\tau$ = shear stress parallel with the crack surfaces.

/ The energy .....

The energy stored around the slit-like cracks is $3\pi/4$ times the energy stored around a penny-shaped crack in a tensile stress field. This ratio will be almost the same in compressive stress fields, differing only by a fraction of Poisson's Ratio, which is itself much less than unity. Therefore, it is assumed that the energy stored around a penny-shaped crack in a compressive stress field is given by

$$W_s = \frac{2}{3} \frac{(1 - \nu)}{G} \tau^2 c^3 \qquad \ldots\ldots \quad (8)$$

Following an argument identical with that given by Cook[15], the energy stored when there is friction between the crack surfaces is

$$W_s = \frac{2}{3} \frac{(1 - \nu)}{G} (\tau - \mu\sigma_n)^2 c^3 \qquad \ldots\ldots \quad (9)$$

where $\mu$ = coefficient of friction,

$\sigma_n$ = stress normal to crack surfaces

and the energy dissipated in friction as the crack surfaces move relative to each other as the rock is loaded from zero is

$$W_F = \frac{2}{3} \frac{(1 - \nu)}{G} (\tau - \mu\sigma_n) \mu\sigma_n c^3 \qquad \ldots\ldots \quad (10)$$

If there are n cracks per unit volume, and if the interaction of cracks is ignored, the total energy stored around cracks and dissipated in them as the rock is loaded, is

$$(W_S + W_F)\, n = \frac{2}{3} \frac{(1 - \nu)}{G} nc^3 (\tau - \mu\sigma_n)\tau \qquad \ldots\ldots \quad (11)$$

The energy stored in an elastic material without cracks under plane strain conditions is

$$W_E = \frac{1}{4} \frac{(1 - \nu)}{G} \left\{k^2 - 2k \frac{\nu}{1-\nu} + 1\right\} \sigma_1^2 \qquad \ldots\ldots \text{ (Jaeger[30])}$$

where $\sigma_1$ = maximum principal stress

$$k = \frac{\text{minimum principal stress}}{\text{maximum principal stress}} = \frac{\sigma_3}{\sigma_1}$$

/ Thus....

Thus the total energy per unit volume supplied to a material containing Griffith's cracks is

$$W = \frac{(1-\nu)}{4G}\,\sigma_1^2\left\{k^2 - 2k\,\frac{\nu}{1-\nu} + 1 + \frac{8}{3}\,nc^3\,(\tau - \mu\sigma_n)\,\frac{\tau}{\sigma_1^2}\right\}$$

$$= {}^1/_2\sigma_1\,\epsilon_1 + {}^1/_2\sigma_3\,\epsilon_3$$

$$= {}^1/_2\sigma_1\,(\epsilon_1 + k\epsilon_3)$$

where $\epsilon_1$ and $\epsilon_3$ are the principal strains in the material containing cracks.

Now

$$\tau = {}^1/_2\sigma_1\,(1-k)\,\text{Sin}\,2\theta$$

$$\sigma_n = {}^1/_2\sigma_1\,(1+k) - {}^1/_2\sigma_1\,(1-k)\,\text{Cos}\,2\theta$$

and $\tau - \mu\sigma_n$ is a maximum when $\tan 2\theta = \frac{1}{\mu}$

Thus the equation for W can be rewritten in the form

$$\epsilon_1 + k\epsilon_3 = \sigma_1\,\frac{(1-\nu)}{2G}\left[k^2 - 2k\,\frac{\nu}{1-\nu} + 1 + \right.$$

$$\left. + \frac{2}{3}\,nc^3\left\{(1-k)^2 - (1-k^2)\,\frac{\mu}{\sqrt{1+\mu^2}}\right\}\right] \qquad \ldots\ldots (12)$$

Equation (12) is only valid for

$$\frac{\mu - \sqrt{1+\mu^2}}{\mu + \sqrt{1+\mu^2}} < k < \frac{\sqrt{1+\mu^2} - \mu}{\sqrt{1+\mu^2} + \mu}$$

since slip can only occur on the crack surfaces when $\tau - \mu\sigma_n > 0$, and since friction can only occur when $\sigma_n > 0$. For k constant, Equation (12) yields a family of straight lines when $\sigma_1$ is plotted against $\epsilon_1 + k\epsilon_3$, as in Figure 35.

/ FIGURE 35

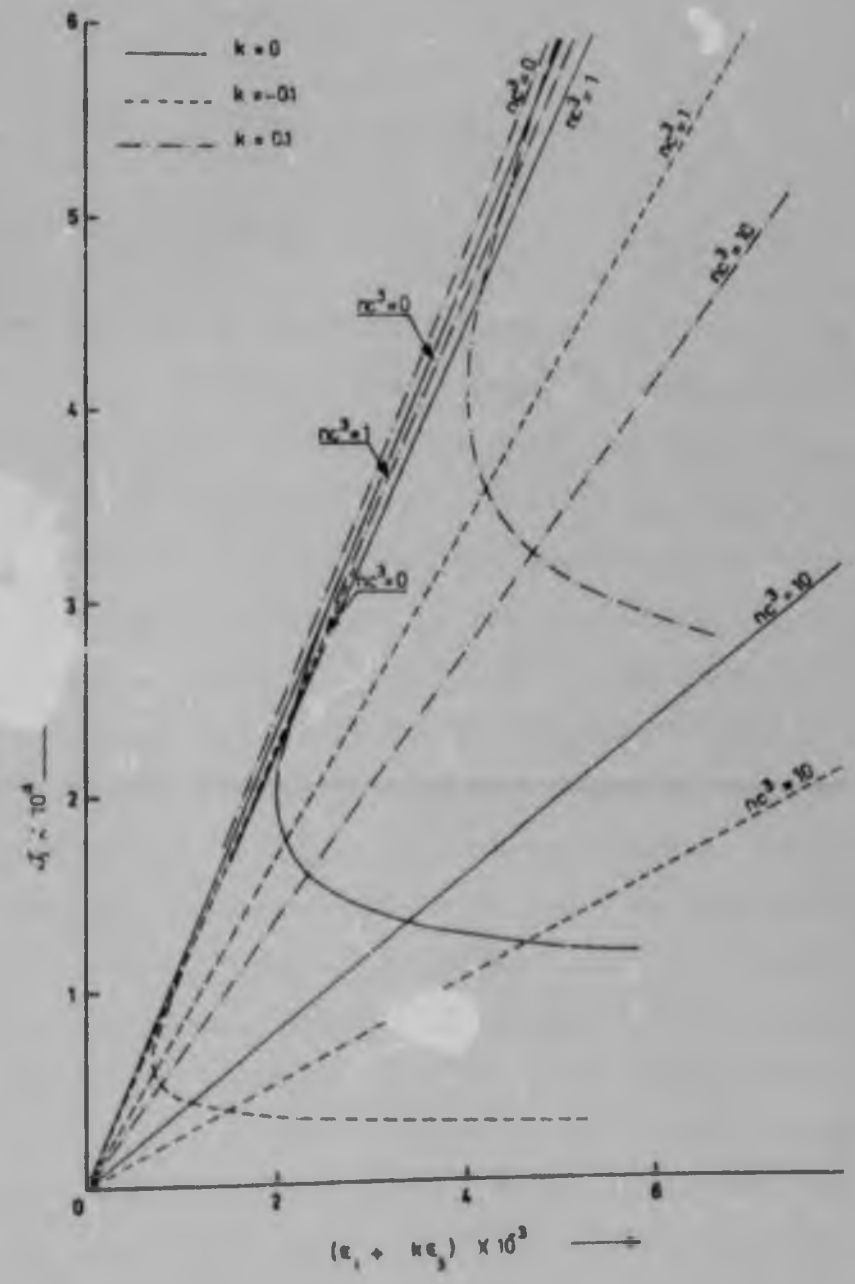


FIGURE 35 GRIFFITH'S LOCI UNDER DIFFERENT LOADING CONDITIONS

The presence of cracks effectively reduces the rigidity of the material.

If the value of c at failure is substituted in equation (12), a family of curves result which represent the onset of crack growth. Substituting (7) in (12) yields

$$\varepsilon_1 + k\varepsilon_3 = \sigma_1 \frac{(1-\nu)}{2G}\left[k^2 - 2k\frac{\nu}{1-\nu} + 1 + \frac{2^7 na^3 (1-k)}{3\sqrt{1+\mu^2}\left\{(1-k)\sqrt{1+\mu^2} - (1+k)\mu\right\}^3 \sigma_1^e}\right]$$

$$= \sigma_1 \frac{(1-\nu)}{2G}\left\{P + \frac{Q}{\sigma_1^e}\right\} \qquad \ldots\ldots \quad (13)$$

The curves defined by equation (13) and shown in Figure 35 have been called Griffith's Loci. Cook[15] has shown that when the slope of the Griffith's Locus is negative, additional energy has to be supplied to the rock by the loading system to cause the cracks to propagate, and violent failure only results if energy is supplied at a rate greater than that which the rock can absorb. Cook[15] has defined brittle failure as failure occurring when the Griffith's locus is positive, since it appears that in this condition rock can fail spontaneously, releasing the redundant strain energy as kinetic energy. The Griffith's locus, however, only describes the onset of crack growth and not changes that take place after crack extension. Hoek and Bieniawski[25] have shown that cracks do not propagate along their own length, but tend to grow in a direction approaching that of the maximum principal stress, consequently (5) does not apply after the cracks have started to grow. The re-orientated cracks are more stable so that non-brittle failure may still occur when the Griffith's Locus is positive.

Even if the details of the above argument are incorrect, in principle a curve such as the Griffith's locus exists. For the purposes of this discussion, it is only necessary

/ to note ....

to note that certain materials containing numerous cracks may exhibit both stable and brittle failure, depending on the loading conditions. The brittle failure of rock represents an interesting possibility for the mechanism of rockbursts. A volume of rock could spontaneously become weaker by brittle failure, so that the surrounding rock would suddenly converge on the failed rock and produce kinetic energy. Also, the stable failure of rock could account for the enormous amounts of energy dissipated stably in mining excavations.

The Griffith's Locus does not necessarily determine when brittle failure occurs; however, it can be used to indicate the more important loading conditions and rock properties which result in brittle failure. From (13), the Griffith's Locus is vertical when

$$\sigma_1^* = 5\,\frac{Q}{P} \qquad \ldots\ldots \quad (14)$$

Substituting (14) in (13) yields

$$\left(\frac{\varepsilon_1 + k\varepsilon_3}{\sigma_1}\right) = \frac{(1-\nu)}{2G}\,\frac{6}{5}\,P \qquad \ldots\ldots \quad (15)$$

and substituting (15) in (12) yields

$$nc' = \frac{3\left(1 - 2k\,\frac{\nu}{1-\nu} + k^2\right)}{10\left(1 - \frac{\mu}{\sqrt{1+\mu^2}}\right)(1-k)\left(1 - k\,\frac{1+\sqrt{1+\mu^2}}{1-\sqrt{1+\mu^2}}\right)} \qquad \ldots\ldots \quad (16)$$

Equation (16) gives the value of $nc'$ when the Griffith's Locus is vertical. Brittle failure can only occur when $nc'$ is less than that given by (16)

/ FIGURE 36


FIGURE 36 GRAPHS SHOWING THE CRITICAL VALUES OF $nC^3$. BRITTLE FAILURE CANNOT OCCUR WHEN $nC^3$ LIES ABOVE THE GRAPHS.

Figure 36 shows the critical values of $nc^3$ for different coefficients of friction and principal stress ratios. As k increases, $nc^3$ has to be larger for stable failure to occur, and since the critical value of $nc^3$ approaches infinity, it is always possible to find a stress field which will result in brittle failure; however, the magnitude of this stress field must also increase. Rock types with a higher value of $\mu$ tend to be more brittle. For dyke material $\mu$ is about 1.5 and for Witwatersrand quartzite $\mu$ is about 1 (Hoek[10]), which could account for the tendency of rockbursts to occur near dykes.

To form some idea of the maximum value of $nc^3$ that can be found in rocks, consider penny-shaped cracks of diameter 2c lying at the grain boundaries of cubic grains of size 2c. Each cube is in contact with six cracks, and each crack is in contact with two cubes; thus there are three cracks per volume of cube and therefore $nc^3 = 3/8$.

This value has been over-estimated since neighbouring cracks would be touching each other and since all cracks would not be active. A more reasonable estimate is therefore $nc^3 = 0.1$. The critical value given by (16) is greater than 0.1; however, this value has also been over-estimated since the Griffith's Locus merely represents the initiation of crack growth. It therefore seems possible that a rock such as quartzite may exhibit both brittle and non-brittle failure, since the critical value of $nc^3$ may be fairly close to 0.1 when allowances are made for changes in the direction of crack propagation.

/ Stable Energy....

Stable Energy Dissipation

It has been indicated that the energy could be dissipated by causing the stable growth of numerous cracks and this possibility is now investigated.

Cook[15] has determined the energy stored around a slit-like crack and the energy dissipated in friction as the crack is allowed to extend in rock under load. Modifying this equation for penny-shaped cracks yields

$$(W_s + W_F)' = \frac{2}{3} \frac{(1 - \nu)}{G} c^3 ( \tau^2 - \mu^2 \sigma_n^2) \quad \ldots\ldots \quad (17)$$

When $k = 0$, the crack can only extend when $\sigma_1$ reaches the uniaxial compressive strength. Thus for $k = 0$ and $\mu = 1$ (17) becomes

$$(W_s + W_F)' = \frac{2}{3} \frac{(1 - \nu)}{G} c^3 \sigma_c^2 ( .207)^2 \quad \ldots\ldots \quad (18)$$

If $k > 0$ $(W_s + W_F)'$ will be less than that given by (18). In addition, energy has to be provided to develop the free surfaces of the crack and this surface energy is

$$W_s = 2\pi \ c^2 \ T$$

where T = free surface energy/unit area

Therefore

$$(W_s + W_F)' = 2800 \ c \text{ to } 280 \ c$$

where $\nu = 0.15$ $G = 5 \times 10^6$ p.s.i.

$T = 6 \times 10^{-4}$ to $6 \times 10^{-3}$ lb.in/in$^2$.

c is in inches.

In Witwatersrand quartzite the maximum grain size, and therefore the effective crack size, varies from $^1/_{100}$ inch to 1 inch. Thus the free surface energy is significant only in the case of very small cracks. In the following discussion on the energy dissipated, it is ignored, since it can result in an error of only a small factor.

/ In ....

In an ideal longwall stope, the maximum amount of energy that can be released for each volume v mined is

$$W_R = \sigma_o \, v \qquad \ldots\ldots \quad (20)$$

where $\sigma_o$ = vertical virgin stress.

For each volume v mined, a volume V of rock must fail to dissipate the released energy. Suppose the rock contains the maximum number of cracks and suppose that these cracks double in size so that the rock becomes almost incompetent, the maximum amount of energy that can be dissipated in the volume V by stable crack growth is

$$(W_s + W_F)' \, nV = (.207)^2 \times \frac{2}{3} \frac{(1 - \nu)}{G} \, n \, (2c)^3 \, \sigma_c^2 \, V$$

This energy must equal $W_R$, so that V represents the minimum volume of rock that could possibly dissipate the energy.

$$\text{Thus } \frac{V}{v} = \frac{3\sigma_o \, G}{0.34 \times 2 \, (1 - \nu) \, \sigma_c^2 \, nc^3} \qquad \ldots\ldots \quad (21)$$

For typical values encountered at Harmony,

$\sigma_o$ = 6000 p.s.i.

G = 5 x $10^4$ p.s.i. $\qquad \nu = 0.15$

$\sigma_c$ = 30,000 p.s.i.

$nc^3_{max} = 0.1$

then V = 1700 v

This is impossible. If the stoping width is 4 feet, then the failed zone would have to extend from 3400 feet above to 3400 feet below the excavation. Therefore the bulk of the energy released is not dissipated by the growth of numerous Griffith's cracks.

The basic mechanism of energy dissipation must be in friction, since stress concentrations around cracks, surface energy, viscous and plastic effects can only account for a small fraction of the energy dissipated.

/ It is ....

It is a common phenomenon that the rock surrounding an excavation is broken into almost parallel slabs which strike in a direction nearly parallel with the face. The slabs are known to move relative to each other and must therefore dissipate energy in friction. The fracture planes which separate the slabs are commonly called shear planes; the mechanism of the development of these fracture planes is not known, but it could be the slabbing mechanism proposed by Cook and Fairhurst[26]. It is not suggested that the fracture zone around the working face and the energy dissipation mechanism is simply one of parallel slabs moving relative to each other, but it is shown that at moderately low stress levels and allowing small movements, the energy released could be dissipated in a comparatively small volume of fractured rock.

Consider a volume of rock, V, which is broken into slabs of average thickness t, and which dissipates the energy released by mining a volume, v. Let the average frictional force across the slab surfaces be $\mu\sigma_n$ and the average relative displacement between slabs be d. Thus the energy dissipated in friction is

$$W_f = \mu\, \sigma_n\, d\, V/t \qquad \ldots\ldots \quad (22)$$

In the case of an ideal longwall stope, the maximum energy released by mining a volume v is given by (20), and for stable energy dissipation $W_R = W_f$, thus

$$\frac{V}{v} = \frac{\sigma_o}{\mu\sigma_n} \times \frac{t}{d} \qquad \ldots\ldots \quad (23)$$

If $\mu = 1$, $\sigma_n = \sigma_o$, $t = 2\frac{1}{2}$ inch, $d = \frac{1}{2}$ inch, and the stoping width is 4 feet, then $V = 5v$ and the fracture zone need only extend 10 feet into the hangingwall and 10 feet into the footwall.

It is concluded that the bulk of the energy released could be dissipated by friction in a small fracture zone around the excavation.

/ Unstable....

Unstable Release of Energy

It is necessary that the fracture zone around the face must advance as the face advances and the extent of this zone must remain sufficiently large so that the released energy can be dissipated stably. If for any reason the fracture zone is prevented from advancing normally, the stress concentrations in the solid rock ahead of the face become higher and the volume of the fractured rock becomes smaller as the face advances. Eventually this fracture zone must grow, and since the stress concentrations in the solid rock are higher, there is a greater tendency for brittle fracture to occur, accompanied by the release of kinetic energy. Geological irregularities can affect the advance of the fracture zone. For example, fracture in a dyke will almost certainly occur at stress levels higher than that in the surrounding quartzite, so that the development of the fracture zone into the dyke will be retarded. In addition, dyke material is often more brittle than quartzite. There is also reason to believe that a dyke has a "stress shielding" behaviour; the virgin stresses in the rock near a dyke can be different from that in the rock at the same depth but far from the dyke, (Barron[31]). The stress field is probably different in the rock on either side of the dyke and different from the stress in the dyke itself. Clearly the development of the fracture zone around an advancing face can be affected to a far greater extent when the face is parallel with the dyke than when it is at right angles to it, in which case the extent of the fracture zone can be different on either side of the dyke. When the face is parallel with the dyke, there is a greater disturbance in the fracture zone when the face advances from the low stress side of the dyke. Mining experience does in fact show that more difficulties are encountered on one side of a dyke than the other.

/ Lesser .....

Lesser geological discontinuities can also affect the development of the fracture zone; different stress fields can occur on either side of a fault or a joint plane, and a reduction in the separation between bedding planes can restrict the fracture zone.

Cook[13] has proposed a mechanism in which the failed and fractured zone around the face advances smoothly, but in a crudely period fashion the extent of the failed zone suddenly increases. The argument for this mechanism is based on the shape and therefore the compressibility of the failed and fractured zone.

In the above two models, the unstable energy release must necessarily occur near the excavation. It is feasible that brittle failure can occur in a volume of rock at some distance removed from the excavation where the stress field could be favourable for such failure to occur. It is also widely believed that rockbursts and earth tremors are caused by shear or tensile fractures.

/ Visual Observations

Visual Observations

As a preliminary means to determine the mechanism of violent events, some visual examinations of haulages were carried out. The degree of slabbing or fracturing around a haulage is an indication of the maximum stress encountered in the life of the haulage. Shear fractures or tensile fractures could be revealed by evidence of recent movement at fracture or joint planes and by the presence of open cracks.

All the footwall haulages at Harmony were developed before extensive stoping took place above them. In haulages below faces with a high energy release rate, the slabbing and fracturing around the haulage was so severe that other features were usually obscured. There was no evidence of open cracks or shear movement which could be assumed to extend far into the surrounding rock.

At Harmony there is only one haulage in the hanging-wall, which fortunately was developed over a fairly large mined-out area. Figure 37 shows the 11 Level haulage, 2 Shaft. This haulage is not parallel with the reef; it intersects the Upper Shale Marker at A and the Basal Reef at B; at C it is about 200 feet above reef and at D it is about 100 feet above reef. It was developed simultaneously from the reef end and the shaft end, with the result that it "holed through" about midway above the worked-out area. Figure 37 shows the extent of the mined-out area when the haulage was almost complete (coarse hatching) and when the examination of the haulage was made. The footwall of the haulage was concrete lined from the shaft to C. The haulage was being used as an airway, so that there was some dust on the walls, but not sufficient to obscure the geological features.

/ FIGURE 37

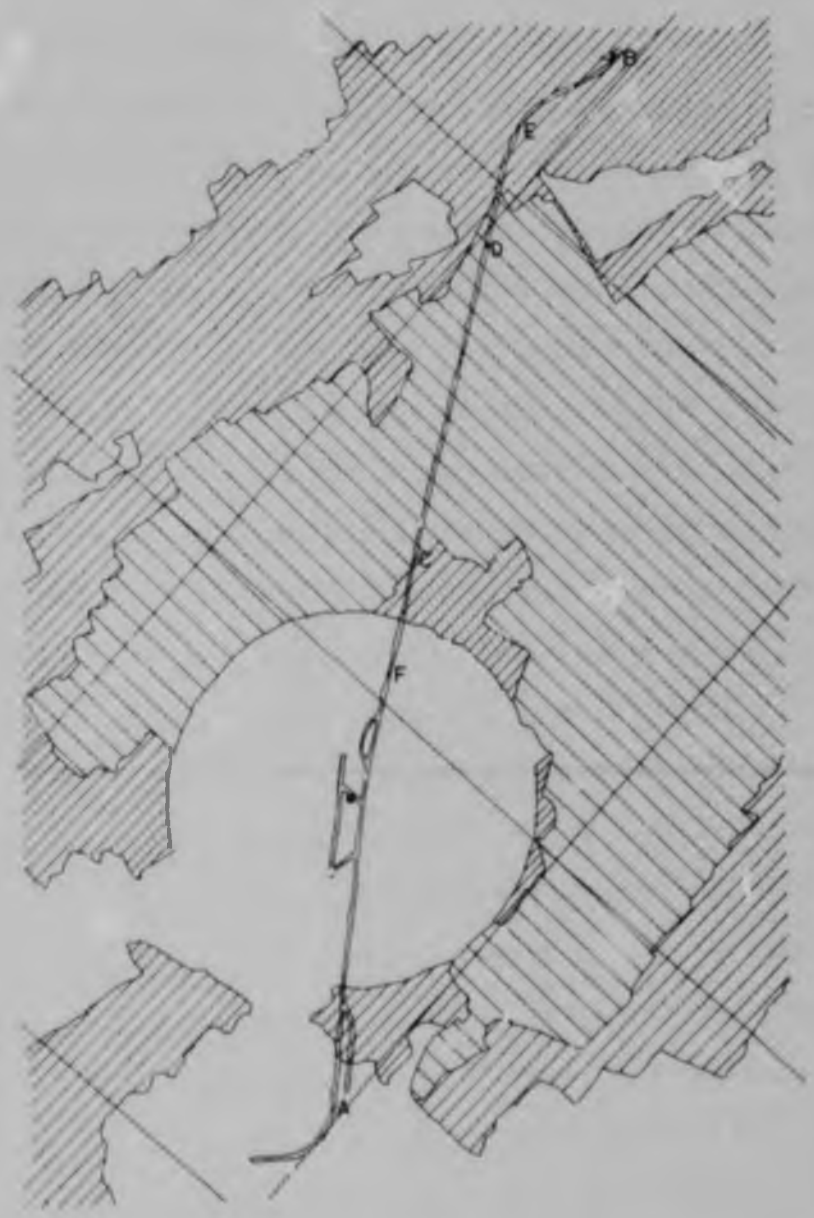


FIGURE 37 PLAN SHOWING THE 11 LEVEL HAULAGE, 2 SHAFT. THE TOTAL HATCHED AREA REPRESENTS THE AREA THAT WAS MINED OUT AT THE TIME THE EXAMINATION WAS MADE. WHILE THE COARSE HATCHING REPRESENTS THE MINED-OUT AREA AT THE TIME THE HAULAGE WAS ALMOST COMPLETED.

From A to the shaft, the haulage was in good condition; however, there was more slabbing than in a haulage in a virgin stress field.

From the shaft to the edge of the shaft pillar the slabbing steadily became worse; near the shaft the sidewalls were laced with cable and a fairly dense pattern of rockbolts had been used, while at the edge of the shaft pillar a number of rockbolts had snapped and it had been necessary to install arch support. The concrete in the footwall had numerous cracks across it, which indicates reduced stresses in the direction of the haulage. This observation must be treated with caution, since calcium chloride was used in the concrete and resulted in severe shrinkage. Between C and F there were some joint planes and faults on which rather indefinite signs of movement were visible. The joint planes appear to have opened up by 2 mm. to 5 mm., and coincide with cracks in the concrete. There were no signs of shear movement.

From the edge of the shaft pillar to C, the conditions in the haulage steadily improved. From C to D the haulage was in remarkably good condition with almost no slabbing of the sidewalls. There were numerous joint planes, small dykes and faults on which no recent movement was visible. The rock appeared to be perfectly solid.

From D to B the slabbing in the haulage got progressively worse and was so severe at E that the cross-section of the haulage was effectively halved. Most features were obscured by slabbing; however, near E, there was a vertical dyke 3 feet wide which quite clearly had openings along its sides. At this point the haulage was about 50 feet above the excavation.

/ The ....

The observations in the hangingwall did not show the existence of extensive shear movements or tensile ruptures, and for the most part, they were consistent with a continuous elastic rock mass.

In going from C to D, a distance of 100 feet normal to the reef plane was effectively traversed. In all this region, there was definitely no sign of bedding plane separation. On the other hand, the strain measurement in the Ventilation Shaft showed that extensive bedding plane separation occurred between the reef and the Upper Shale Marker. No satisfactory explanation has been found for this discrepancy.

/ First Motion....

First Motion Theory

The theory of First Motions from seismic sources has been authoritatively dealt with by Knopoff and Gilbert[32]. They use dynamic dislocation theory to derive the elastodynamic radiation from a seismic source. The seismic source is visualized as a geometrical discontinuity across which there exists a sudden discontinuity in either one component of the strain tensor or one component of the displacement vector. They show that there are eight independent models. If the plane z = 0 forms the geometrical discontinuity, then the eight independent changes which can occur are (i) the sudden application of strain discontinuities in $e_{xx}$, $e_{yy}$, $e_{zz}$, $e_{zx}$ or $e_{zy}$ across the boundary and (ii) the sudden application of displacement discontinuities in $u_x$, $u_y$ or $u_z$, across the boundary. If a discontinuity in the ninth term $e_{xy}$ were suddenly applied across the surface, no motion would be radiated. A seismic source can consist of a linear combination of any of these eight dislocation types; nowever, in physical sources one of these dislocations will predominate.

The main conclusions are given below and have been presented in a form more suited to the present application. Only the results for P waves are given. The plane z = 0 is taken as the geometrical discontinuity and the x direction as the direction of propagation of the strain or displacement discontinuity. The symbol A will be used to represent that part of the amplitude of the radiated wave which is sensitive to the direction of propagation of the wave, i.e., A describes the radiation pattern. The other symbols used are:

/ α ....

$\alpha$ = P-wave velocity

$\beta$ = S-wave velocity

$\lambda$ = Velocity of propagation of the dislocation

$\gamma_x$, $\gamma_y$ and $\gamma_z$ are direction cosines.

All the strain dislocations have a similar first motion radiation pattern which is unaffected by the velocity of propagation. These are shown in Figure 38 and are

$$A_{e_{xx}} = A_{e_{yy}} = A_{e_{zz}} = \gamma_z$$

$$A_{e_{xz}} = \gamma_x \qquad A_{e_{yz}} = \gamma_y$$

The patterns are two-lobed, the first motion in the one lobe represents compression and in the other it represents rarefaction. These dislocations can result from the sudden yielding or failure of the material on one side of the boundary. The displacement discontinuity, $u_y$, also results in a pattern independent of $\lambda$ and is shown in Figure 38. This pattern $A_{u_y} = \gamma_y \gamma_z$ is four-lobed, with alternating lobes of compression and rarefaction. This type of dislocation corresponds to shear movement in a direction at right angles to the direction of propagation.

The displacement discontinuities in $u_x$ and $u_z$ are dependent on $\lambda$ and the radiation patterns are shown in Figures 39 and 40 respectively, for different values of $\lambda$.

/ FIGURE 38

$A_{e_{xx}} \cdot A_{e_{yy}} \cdot A_{e_{zz}} \cdot \gamma_z$

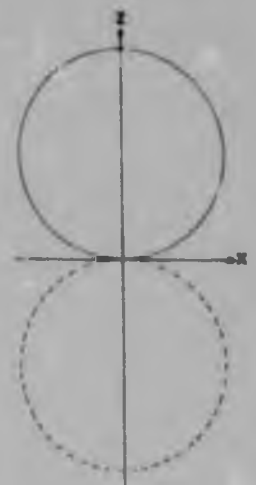


$A_{e_{xz}} \cdot \gamma_x$

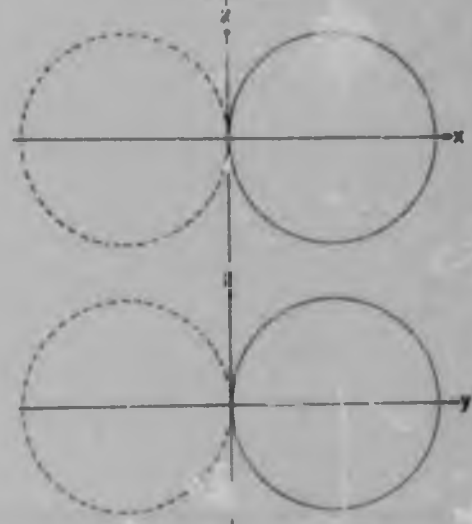


$A_{e_{yz}} \cdot \gamma_y$

$A_{u_y} \cdot \gamma_y \gamma_z$

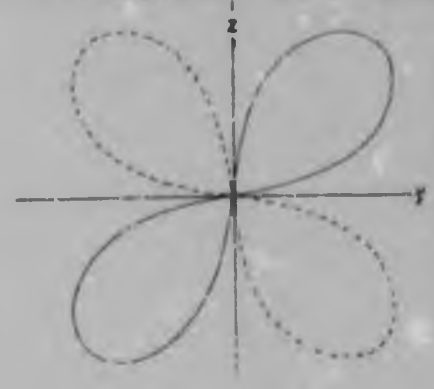


FIGURE 3: FIRST MOTION RADIATION PATTERNS FOR STRAIN DISLOCATIONS, AND A DISPLACEMENT DISLOCATION IN A DIRECTION TRANSVERSE TO THE DIRECTION OF PROPAGATION, X. THE PATTERNS ARE INDEPENDENT OF THE VELOCITY OF PROPAGATION. THE SOLID LINE REPRESENTS COMPRESSION AND THE BROKEN LINE RAREFACTION.

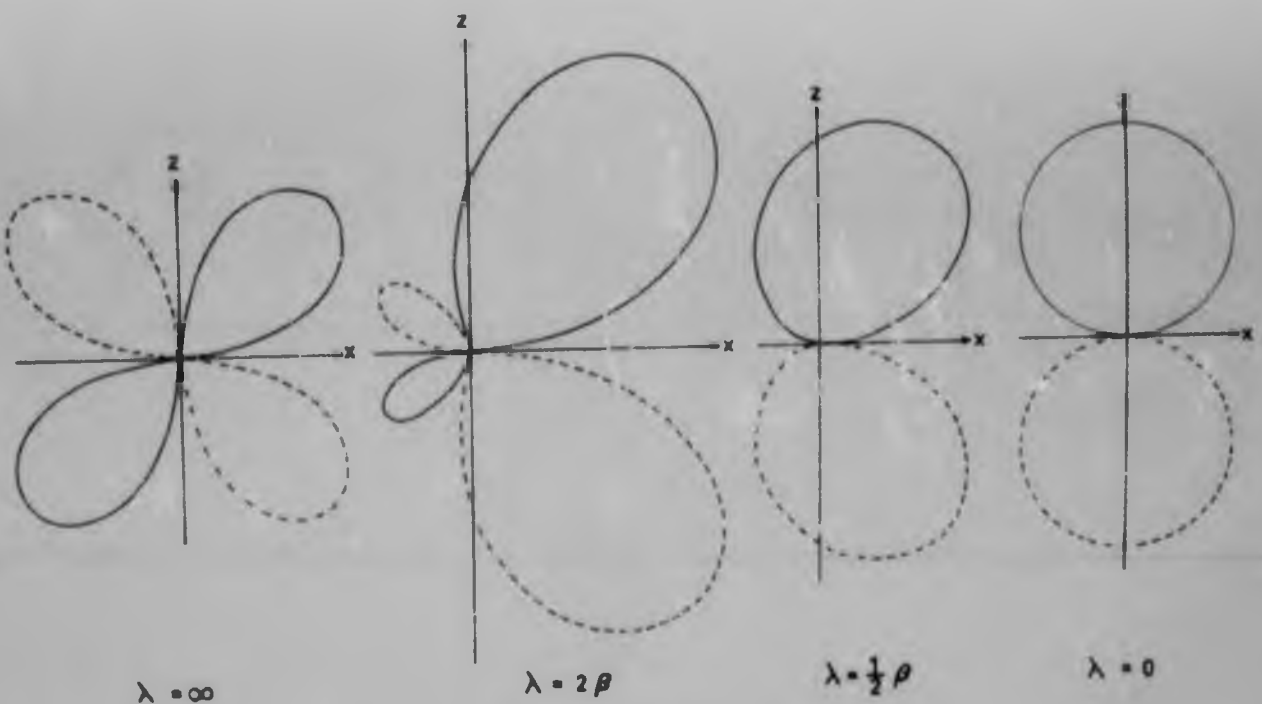


$$A_{U_1} = 2\gamma_x\gamma_z + \alpha\gamma_z$$

PIGURE 39 FIRST MOTION RADIATION PATTERNS FOR A DISPLACEMENT DISLOCATION IN A DIRECTION PARALLEL WITH THE DIRECTION OF PROPAGATION, X. PATTERNS ARE SHOWN FOR DIFFERENT VELOCITIES OF PROPAGATION, λ. THE SOLID LINE REPRESENTS COMPRESSION AND THE BROKEN LINE RAREFACTION.

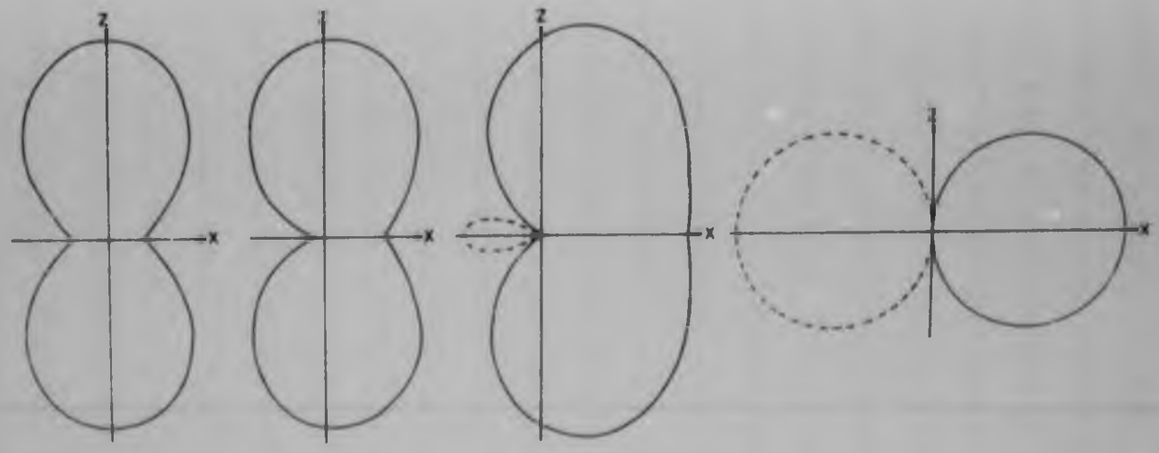


$\lambda = \infty$ $\lambda = 2\beta$ $\lambda = \frac{1}{2}\beta$ $\lambda = 0$

$$A_{U_z} = 1 + \frac{\alpha}{\lambda}\gamma_x + \frac{2\beta}{\alpha^2 - \beta^2}\gamma_z'$$

FIGURE 4U FIRST MOTION RADIATION PATTERNS FOR A DISPLACEMENT DISLOCATION IN A DIRECTION AT RIGHT ANGLES TO THE DIRECTION OF PROPAGATION, X. PATTERNS ARE SHOWN FOR DIFFERENT VELOCITIES OF PROPAGATION. THE SOLID LINE REPRESENTS COMPRESSION AND THE BROKEN LINE RAREFACTION.

$$A_{u_x} = 2\,\gamma_x\,\gamma_z + \frac{\alpha}{\lambda}\,\gamma_z$$

$$A_{u_z} = 1 + \frac{\alpha}{\lambda}\,\gamma_x + \frac{2\beta^2}{\alpha^2 - \beta^2}\,\gamma_z^2$$

In both cases the patterns degenerate to the two lobed pattern when $\lambda = 0$. However, in practice, $\lambda$ has been found to be of the order of $^1/_2\,\beta$ for most materials. Knopoff and Gilbert[32] have shown that if the dislocation extends bilaterally or radially along the boundary surface, the first motion radiation pattern becomes equal to that for $\lambda = \infty$. Now the first motion radiation pattern depends only on the very first changes at the discontinuity surface. In practice, a discontinuity will start at a point and develop approximately radially into a discontinuity surface, thus it is quite likely that dislocations in $u_x$ and $u_z$ result in their respective patterns for $\lambda = \infty$. A dislocation in $u_x$ corresponds to shear movement on a fracture surface parallel with the direction of propagation, and a dislocation in $u_z$ corresponds to the sudden propagating expansion (or collapse if multiplied by -1) of a lenticular cavity, the expansion (or collapse) taking place in the direction of the normal to the plane of the cavity walls. The dislocation in $u_z$ could correspond to a tensile rupture in which case nearly all first motions would be compression, or it could correspond to the collapse of fractured rock in the excavation and in which case nearly all first motions would be rarefaction.

The sudden failure of a volume of rock can be regarded as the application of strain dislocations between two surfaces. Knopoff and Gilbert[32] have given the theory for two dislocations separated by a small distance, but have only applied it to dislocations in $u_x$ and $e_{xz}$ since they

/ considered ....

considered the other dislocations unlikely in earthquake mechanisms. By applying the theory to laminar or double dislocations in $e_{xx}$, $e_{yy}$ and $e_{zz}$, it is found that the first motions in all directions are rarefaction and the pattern is shown in Figure 41.

$$A' e_{xx} = A' e_{yy} = A' e_{zz} = -\gamma_z^2$$

When the theory is applied to double dislocations in $e_{xz}$ and $e_{yz}$ a four lobed pattern results as for $u_y$ in Figure 38. Thus, in general, when a volume of rock suddenly fails, the first motion pattern consists of a summation of the patterns for all five strain components. The resulting pattern is therefore predominantly rarefation and is independent of the velocity of propagation.

Theory shows that four distinctive first motion radiation patterns can arise, and they are summarised as follows:

i) First motion compression in nearly all directions. This pattern can result from a tensile rupture.

ii) First motion rarefaction in nearly all directions. This pattern can result from the brittle failure of a volume of rock, or the collapse of fractured rock in the excavation.

iii) Two-lobed pattern resulting from simple strain dislocations or dislocations in $u_x$ and $u_z$ when $\lambda$ is very small.

iv) Four-lobed pattern with alternating lobes of compression and rarefaction, associated with shearing effects.

/ FIGURE 41

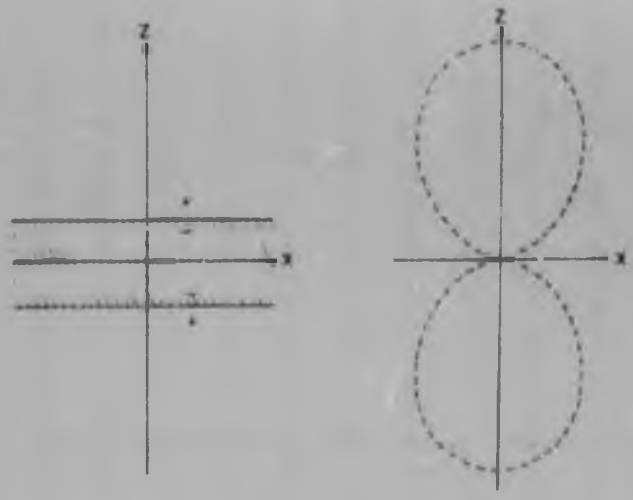


$$A'_{e_{xx}} = A'_{e_{yy}} = A'_{e_{zz}} = -\gamma_z^2$$

FIGURE 4[illegible] FIRST MOTION PATTERN FOR DOUBLE STRAIN DISLOCATIONS IN $e_{xx}$, $e_{yy}$ and $e_{zz}$. ALL FIRST MOTIONS ARE RAREFACTION.

First Motion Results

About 30 percent of the first motions had an emergent character which could not be distinguished clearly. Only first motions that were perfectly distinct were used in this analysis.

It is possible that a seismic wave could follow a curved path so that the angle of incidence of the waves at a seismometer is somewhat uncertain, thus, whenever the angles of incidence were greater than $65^{o}$ the first motion data were rejected. In the original seismic network, therefore, no more than six seismometers could be used for seismic events near the reef plane. Consequently the seismic network was modified to make more seismometers useful. The three vertical seismometers (2, 3 and 6) in the reef plane were replaced by horizontal seismometers orientated radially to the seismically most active parts of the mine. A second amplifying stage was introduced into the network at each seismometer so that the first motions would be more distinct. In addition five portable seismometer stations were set up on surface; each station had a low speed tape-recorder with high gain amplifiers such that the first motions from events of magnitude $10^{3}$ ft.-lbs. could be distinguished.

The original network with the six useful seismometers showed that in the case of the seismic events near the reef plane, the majority of the first motions was rarefaction, regardless of the magnitude or of the position of the event relative to the excavation. In 1952, Gane, Seligman and Stephen[8] found that in their surface array of six seismometers on a Witwatersrand mine 80 percent of the first motions were rarefaction.

/ In the ....

In the modified seismic network, the first motions could be determined with certainty on about 9 or 10 seismometers for each event. This network was in operation for a month and during this period 100 seismic events were analysed; they consisted of some events of magnitude $10^3$ and $10^4$ ft.-lbs., and all the events greater than $10^4$ ft.-lbs. For 40 percent of the seismic events, the distinct first motions were all rarefaction; a central projection of one of these events is shown in Figure 42. For 26 percent of the events, one seismometer showed distinct compression while the remainder of the distinct motions were rarefaction. In 23 percent of the cases, only two or three seismometers showed compression and these seismometers were spaced such that they lay within a cone with apex at the focus, Figure 43. In all cases, the cone of compressive motion lay at an angle of less than $30^\circ$ to the reef plane.

The distribution pattern of first motions fits neither the four-lobed pattern for shear movements, nor the nearly all compression pattern of a fast or symmetrical tensile rupture. Since the seismic network covers mainly the upper half-space, it could be argued that the radiation pattern is in fact two-lobed with the rarefaction lobe in the upper half-space and the compression lobe in the lower half-space where it would not be observed. The two-lobed pattern could be produced by a simple strain dislocation, a very slow tensile rupture propagating vertically downwards or a slow shear movement propagating horizontally and unilaterally. A simple strain dislocation is an unreasonable mechanism since it requires the extensive failure of the rock in the lower half-space. The two rupture mechanisms are also unlikely since a very slow tensile rupture would have a low seismic yield and the shear movement is required to take place in a direction in which the shear stress is at a minimum.


FIGURE 42 A CENTRAL PROJECTION OF THE FIRST MOTIONS OF A SEISMIC EVENT FOR WHICH ALL THE OBSERVED FIRST MOTIONS WERE RAREFACTION. THE + SIGN INDICATES THE SEISMOMETERS THAT WERE IN THE UPPER HALF SPACE AND THE CIRCLE REPRESENTS $\tan \phi = 1$.

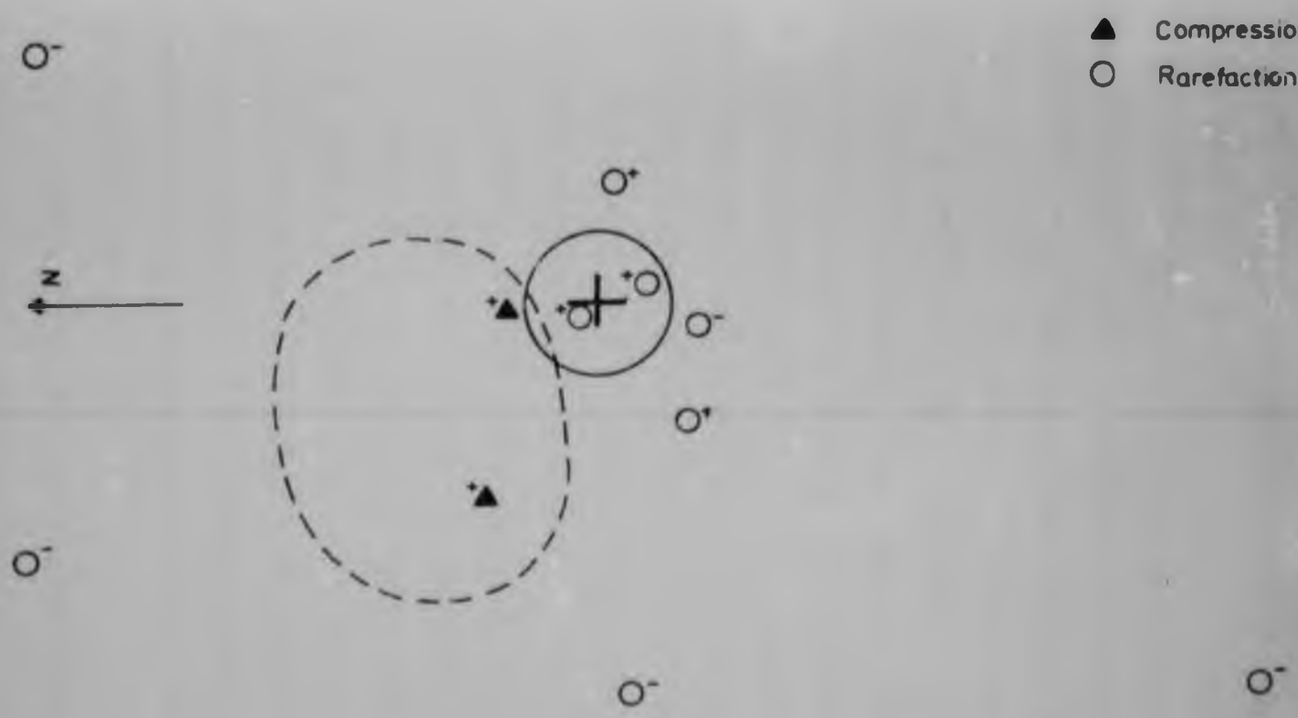


FIGURE 43 A CENTRAL PROJECTION OF THE FIRST MOTIONS RADIATED BY A SEISMIC EVENT FOR WHICH COMPRESSION WAS RADIATED IN A RESTRICTED DIRECTION. THE BROKEN LINE REPRESENTS THE PROJECTION OF A HYPOTHETICAL CONE AND THE CIRCLE REPRESENTS tan $\phi$ = 1.

Also it is most unl ... that a rupture propagates unilaterally, particularly at the start of the rupture, therefore it is expected that the two-lobed pattern for a rupture physically cannot exist.

The mechanism which fits the first motion pattern best is the sudden failure of a volume of rock (double strain dislocation) or the collapse of fractured rock in the excavation.

It was thought that for those events which radiated compression the direction in which the first motions were compression might show a consistent relationship to the excavation. Most of the seismic events occurred on remnants, so that no significance could be attached to the direction of compression; however, on any particular remnant the events tended to radiate compression in the same direction. About 15 events occurred on one dyke of which 7 radiated rarefaction only, the remainder radiated compression in a direction at about $45^{\circ}$ to the strike direction of the dyke.

Seven percent of the seismic events did not fit any of the standard patterns and a projection of one of these is shown in Figure 44. The first motions cannot be separated into four compartments containing compression and rarefaction by two straight lines. Since no straight lines can be found which could form the projections of two planes at right angles, the mechanism of these events cannot be a shear movement or rupture. It is noted that earthquakes that exhibit faulting, consistently radiate the four-lobed pattern of Figure 39 for $\lambda = \infty$.

During the period that the modified network was in operation, only three seismic events were located at the Harmony Sill.

/ FIGURE 44

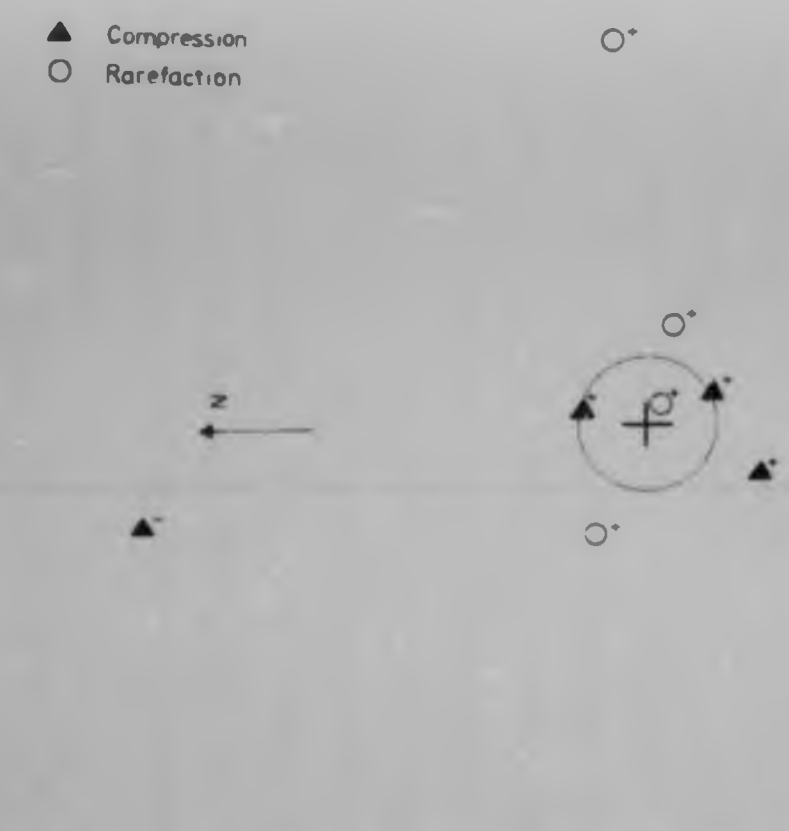


FIGURE 44 A CENTRAL PROJECTION OF THE FIRST MOTIONS RADIATED BY A SEISMIC EVENT FOR WHICH THE FIRST MOTION PATTERN DOES NOT FIT ANY STANDARD PATTERN. THE CIRCLE REPRESENTS tan $\phi = 1$.

These events were all of magnitude $10^3$ ft.-lbs., and a number of the first motions were indistinct so that the first motion radiation pattern was not conclusive. The distinct first motions of these events, however, were more frequently compressive than for the events near the excavation, and all could have fitted the four-lobed pattern. Similarly, for the events located near the Harmony Sill in the original network, about 50 percent of the distinct first motions were compressive, and in all the cases, the first motions could have fitted the four-lobed pattern. Thus the mechanism of the events at the Sill may have been a shear movement.

Cook and Hodgson[33] have suggested that in a steadily increasing compressive stress field in rock, a compressive pulse is attenuated more rapidly than a rarefactive pulse. If the attenuation is sufficiently greater in compression, all first motions would appear as rarefaction. However, there were a few cases in which two seismometers were in line with the focus and with one seismometer much closer to the focus than the other. Both seismometers always showed the same motion, and in the case of compression, the motion was as distinct at the far seismometer as at the near seismometer. Therefore it is thought that the difference in attenuation between compressive and rarefactive pulses is not sufficient to nullify the first motion patterns.

In conclusion it can be said that the mechanism of seismic events is not a tensile or shear rupture, but a volumetric collapse of either fractured rock or rock that suddenly fails.

/ Spectral Analysis ....

Spectral Analysis

The theory of Hirasawa and Stauder[17] cannot be applied to the seismic events, since the mechanism is not a simple unilaterally propagating rupture. A more detailed analysis for a propagating volumetric collapse was not attempted since small deviations from the ideal case seriously affect the spectrum, which for the ideal case would be complex. The spectrum can, however, still be used to determine the duration of an event by making assumptions about the velocity of propagation and the dimensions of the source mechanism.

Since a seismic event has finite duration, its time behaviour can be regarded as the product of a rectangular pulse and some other function of time, thus

$$f(t) = \left\{ U\left(t + \tfrac{1}{2}\tau\right) - U\left(t - \tfrac{1}{2}\tau\right) \right\} \times h(t)$$

where $U(t)$ = unit step function

$h(t)$ = a function of time related to the velocity of propagation and the dimensions of the source.

$\tau$ = duration of the source mechanism.

The velocity of propagation may differ in different directions, but if it is assumed that it remains constant in each direction, then $h(t)$ is independent of time. Also, if the source dimensions are small in relation to the wave length of elastic waves, interference of waves radiated from different parts of the source can be ignored For example, if the dimensions of the source are 100 feet, P waves of frequency less than 100 c/s appear as though radiated from almost a point source, since $\alpha$ is 19,000 ft./sec. Thus for a small source and $\lambda$ = constant, at a

/ distant ....

distant point, the time behaviour of the source appears as

$$f(t) = A \left\{ U\left(t + \tfrac{1}{2}\tau\right) - U\left(t - \tfrac{1}{2}\tau\right) \right\}$$

where A = constant.

The Fourier transform of this function is

$$F(\omega) = \frac{A\tau}{\sqrt{2\pi}} \frac{\operatorname{Sin} \tfrac{1}{2}\tau\omega}{\tfrac{1}{2}\tau\omega}$$

The minima in this amplitude spectrum occur at intervals of $\Delta\omega = 2\pi\,\Delta f$, therefore

$$\tau = \frac{1}{\Delta f}$$

Figure 45a shows a "missilgram" of two seismic events that occurred within 2½ seconds of each other. It can be seen that the low frequencies persist for longer than the high frequencies; the missilgrams do not have sufficient resolution to yield any further information. Figure 45b shows typical spectra or "sections" of the P waves of an event of magnitude $10^7$ ft.-lbs., and of an event of magnitude $10^4$ ft.-lbs. It can be seen that there is very little spectral content above 200 c/s, and that in the case of the $10^7$ ft.-lbs. event, the minima are so closely spaced that they are almost indistinguishable (the bandwidth of the spectrograph is about 5 c/s).

/ FIGURE 45

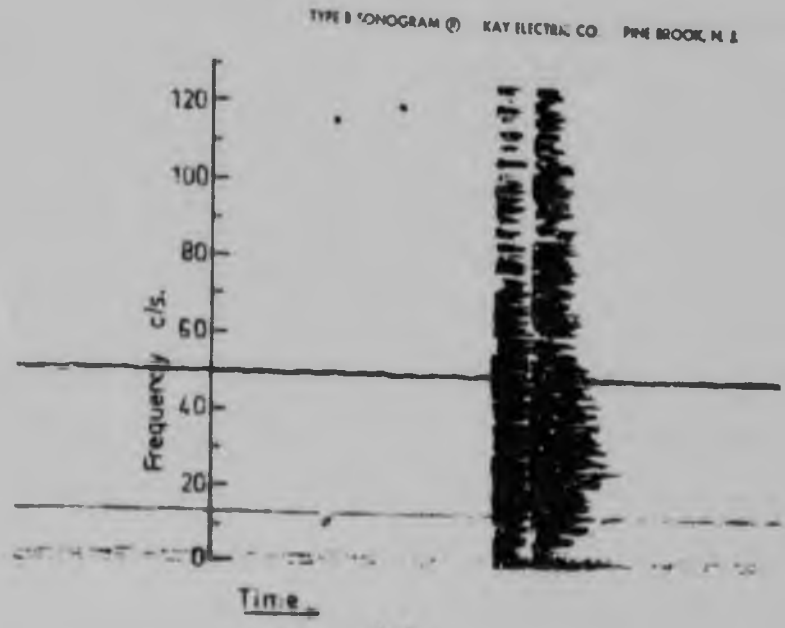


(a)

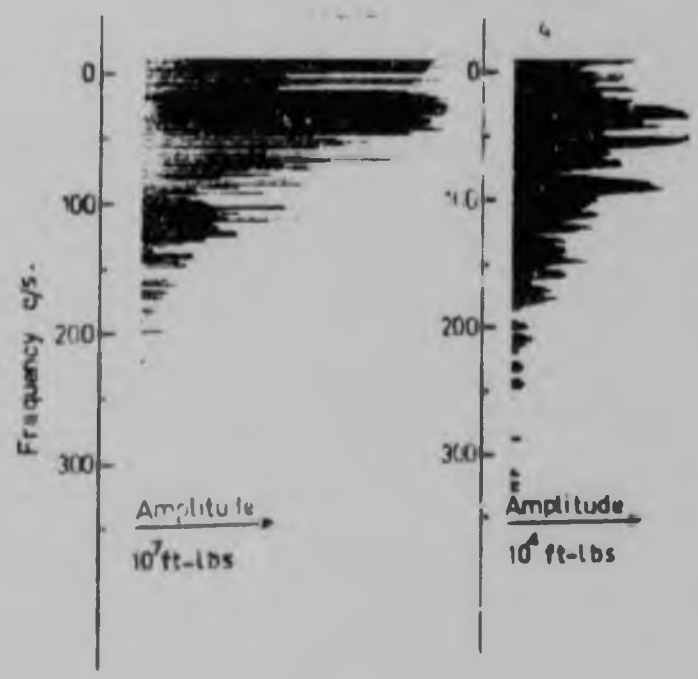


(b)

FIGURE 45

(a) A "MISSILGRAM" OF TWO SEISMIC EVENTS THAT OCCURRED WITHIN 2½ SECONDS OF EACH OTHER.

(b) "SECTIONS" IN THE P WAVES OF TWO SEISMIC EVENTS OF MAGNITUDE $10^7$ ft.-lbs. AND $10^4$ ft.-lbs.

In Figures 46, 47 and 48, sections through the P waves (between the P and S arrivals) of some typical seismic events are shown on an expanded frequency scale; the sections are for different seismometers surrounding the focus. Figure 46 is for a seismic event of magnitude $10^4$ ft.-lbs. that occurred 100 feet above the reef and for which all observed first motions were rarefaction. Figure 47 is for an event of magnitude $10^6$ ft.-lbs., 200 feet above the reef and for which all observed first motions were rarefaction. Figure 48 is for an event of magnitude $5 \times 10^4$ ft.-lbs. that occurred near the Harmony Sill and for which 3 of the 6 distinct first motions were compression.

The spectra are not the same at the different seismometers, thus h(t) is not constant and the source mechanism is not spherically symmetrical. The spectra are only crudely similar to that of a rectangular pulse; however, they do show some distinct minima and it is possible to make an estimate of the frequency interval between minima. In Figure 46, $\Delta f$ is about 10 c/s corresponding to a duration of $\tau = 1/10$ sec., in Figure 47 $\Delta f$ is about 3 c/s, therefore $\tau = 1/3$ sec., and in Figure 48 $\Delta f$ is about 6 c/s, therefore $\tau = 1/6$ sec. These crude estimates of the duration of the source mechanism correspond roughly with the duration of the high amplitude part of the P wave on the seismic record. Since the dimensions of the source mechanism are necessarily limited to dimensions of the order of 100 feet, the velocity of propagation must be very low. Intuitively, a low velocity of propagation is expected in a volumetric collapse.

/ FIGURE 46

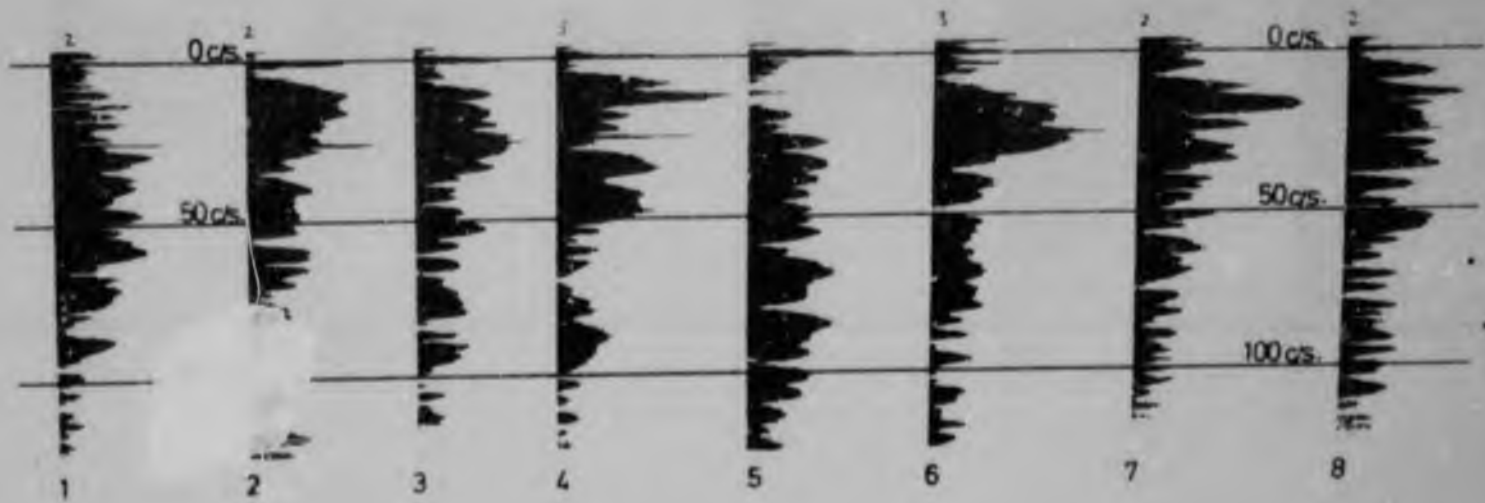


FIGURE 46 SECTIONS OR SPECTRA THROUGH THE P WAVES OF A SEISMIC EVENT OF MAGNITUDE $10^4$ ft.-lbs. THAT OCCURRED NEAR THE REEF PLANE. THE NUMBER BELOW EACH SECTION IS THE NUMBER OF THE SEISMOMETER FOR WHICH THE SECTION WAS MADE.

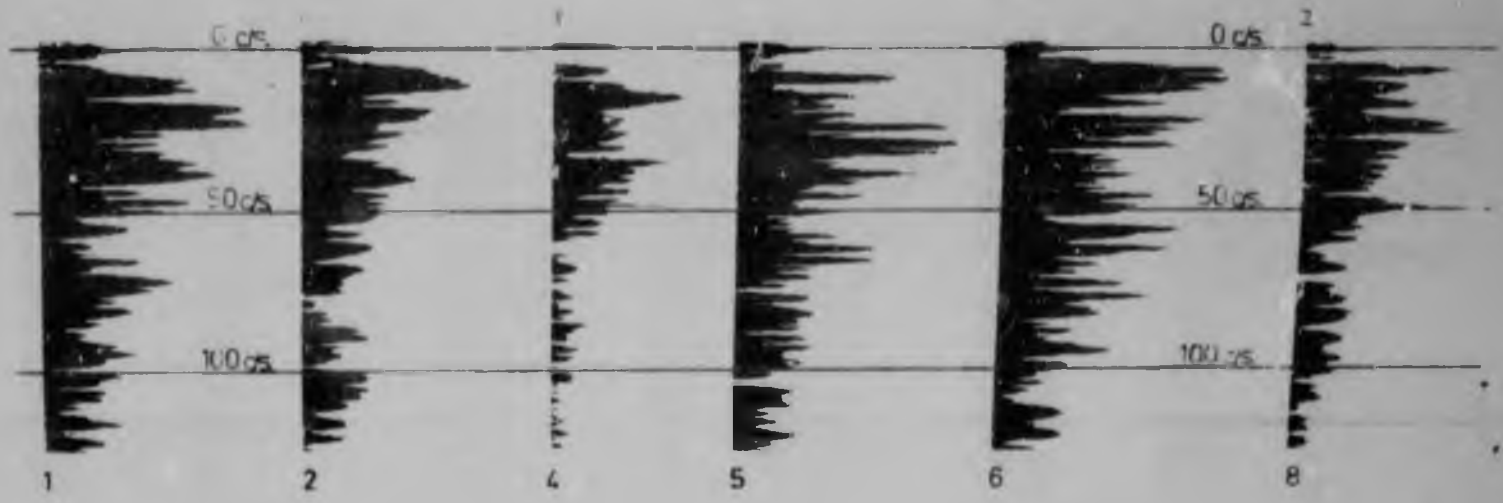


FIGURE 47 SECTIONS OR SPECTRA THROUGH THE P WAVES OF A SEISMIC EVENT OF MAGNITUDE $10^6$ ft.-lbs. THAT OCCURRED NEAR THE REEF PLANE. THE NUMBER BELOW EACH SECTION IS THE NUMBER OF THE SEISMOMETER FOR WHICH THE SECTION WAS MADE.

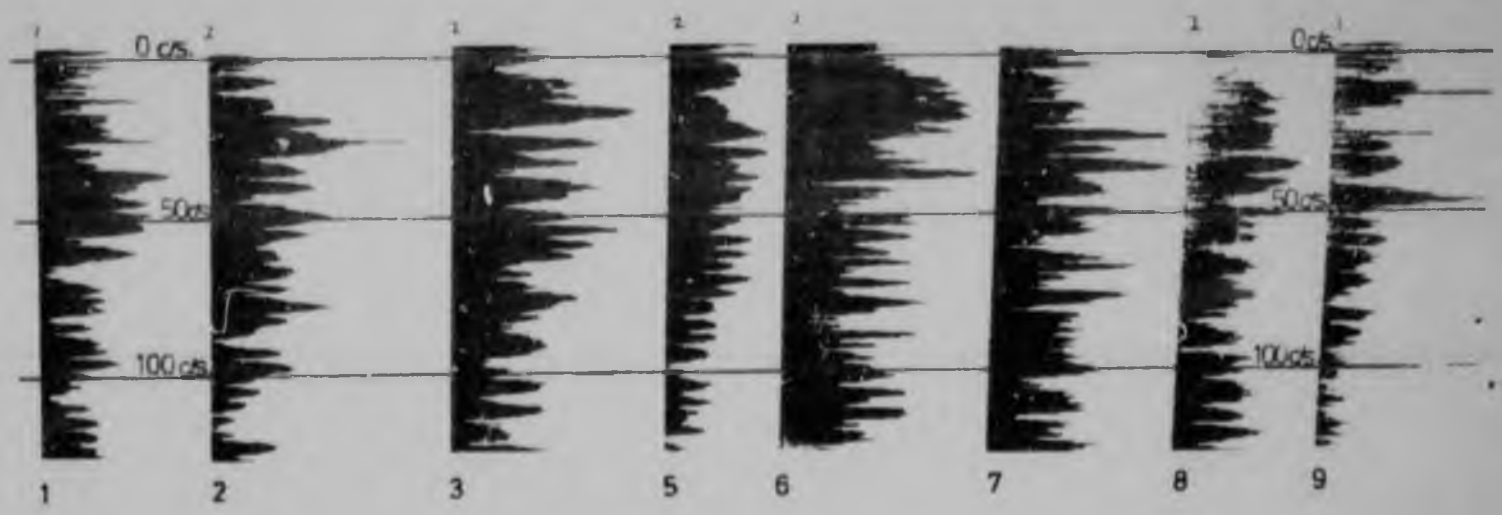


FIGURE 48 SECTIONS OR SPECTRA THROUGH THE P WAVES OF A SEISMIC EVENT OF MAGNITUDE 5 x $10^4$ ft.-lbs., THAT OCCURRED NEAR THE HARMONY SILL. THE NUMBER BELOW EACH SECTION IS THE NUMBER OF THE SEISMOMETER FOR WHICH THE SECTION WAS MADE.

In conclusion, the mechanism of seismic events is not sufficiently simple for thespectral analysis technique to reveal the dimensions of the source.

/ SUMMARY OF CONCLUSIONS.

## SUMMARY OF CONCLUSIONS

The seismic technique has proved to be a most rewarding method of investigating violent rock failure underground. During the first year of recording 3100 seismic events ranging in magnitude from $10^3$ ft.-lbs. to $10^8$ ft.-lbs. were located, and the accuracy with which the events could be located was $\pm$ 100 feet with 90 percent confidence.

It was found that there were two distinct groups of seismic events. 95 percent of the events occurred between the reef plane and a weak band of rock 300 feet above the reef plane, while the remainder occurred near the Harmony Sill approximately 2400 feet above the reef plane. The seismic observations were compared with some earlier strain measurements in the Ventilation Shaft. This comparison showed that the elevation of th seismic events coincided with the elevation of regions where measured extensional strains in the rock exceeded the original compressive strain in the rock. It was concluded that rock failure was limited to a zone extending to a height of approximately 300 feet above the excavation and that the zone extending laterally as the face advanced; however, rock failure also occurred in a confined region at the Harmony Sill.

A large proportion of the seismic events and damage due to rock failure occurred in the parts of the mine which were highly stressed. The energy released per unit area increase in the size of the mine excavation was compared with damage due to rock failure, seismicity and the stope labour requirements. All these factors showed a marked increase as the energy release rate increased. It was concluded that the rate of energy release is a significant parameter in predicting the magnitude of problems arising

/ from .....

from rock failure and that these problems are easily manageable when the rate of energy release is less than $10^8$ ft.-lbs. per fathom$^2$.

There was no difference in the behaviour of seismic events of different size, except that all the events of magnitude $10^7$ ft.-lbs. and $10^8$ ft.-lbs. occurred at dykes. Although blasting triggered a large number of events, more than 50 percent occurred well outside blasting time, and the rate at which seismic events occurred fluctuated quite widely, even when the rate of mining was nearly constant.

Only a small fraction of the damage was accompanied by seismic activity, which implies that the damage was due to falls of rock which had been fractured before the rockfalls occurred. The only manner in which this type of damage can be reduced is to reduce the extent of the fractured rock by reducing the energy release rate, or by improving the type of support in the stopes.

The total energy radiated by seismic events of a particular size exceeded the total energy radiated by events of a smaller size. Also, the total energy radiated by all the seismic events formed a very small fraction of the energy released by increasing the size of the excavation, therefore a mechanism must exist for dissipating large quantities of energy in a stable manner.

Cook[15] and Fairhurst and Cook[26] have shown that some rock types can fail violently or non-violently, depending on the manner in which the rock is loaded. It was shown that these theories may explain the stable development of the fracture zone; however the large quantities of energy that are dissipated stably can only be dissipated by friction in the fracture zone; a

/ relatively ....

relatively small fracture zone is required to dissipate this energy.

First motion studies of the mechanism of the seismic events showed that the mechanism was not a tensile or shear failure, but a volumetric collapse. The mechanism could therefore be a sudden growth in the fracture zone, or the collapse of fractured rock near the face or in the worked-out areas, or the sudden failure of a volume of rock slightly removed from the excavation. The mechanism of the seismic events near the Harmony Sill was not clearly resolved but could, however, have been a shear movement.

The spectral analysis did not reveal any useful information except that the velocity of propagation of the volumetric collapse was low.

/ SUMMARY

APPENDIX 1

Because the seismometers in the shafts, i.e., Nos.7 and 8, show velocities higher than those near the reef plane, there must be a layer of rock in the upper strata which has a higher P wave velocity. Also there must be a layer of rock with a very low propagation velocity near the surface, since seismometer 9 shows a low velocity. Obviously the apparent velocity of propagation from an event to a seismometer will then depend on the position of the event relative to the seismometer.

The following method is presented, which enables the elevation of a seismic event to be determined independently of the velocity calibration; the velocity calibration can also be used to determine the elevation of the seismic event by this method. Figure 1A shows a seismometer at A, and two layers having different P wave velocities. Say $V_1 > V_2$, then a wave travelling from C to A will have the path shown. The apparent velocity of the P wave from C to A will be higher than the apparent velocity from B to A, because the wave travels a comparatively greater distance in the higher velocity medium from C to A than from B to A. Figure 2A shows the variation of the apparent velocity as X (distance) changes; it will be noticed that the apparent velocity approaches a maximum as X increases. The general form of the curve in Figure 2A will be the same for any number of layers in an arbitrary order.

A number of seismic events were selected at random from asymmetrical positions relative to the two seismometers in the shafts. The following procedure was carried out for each event. Referring to Figure 3A, the plan position of the event was obtained on the locator by means of seismometers

/ 1 to .....

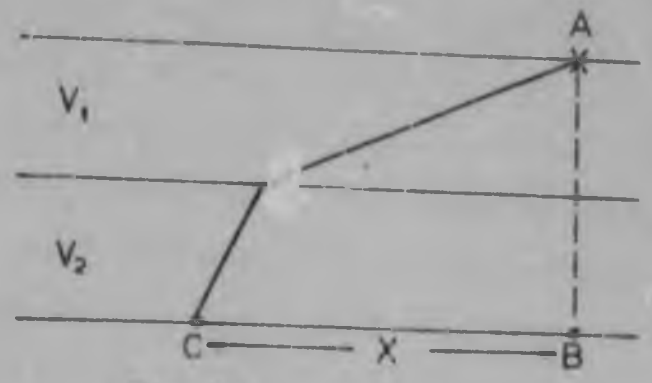


Fig 1A

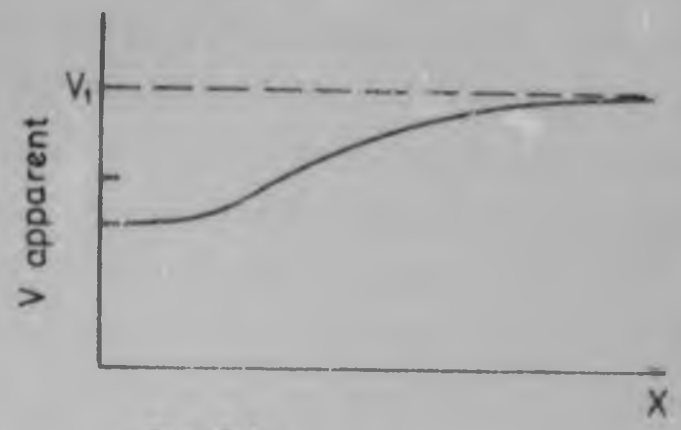


Fig. 2A.

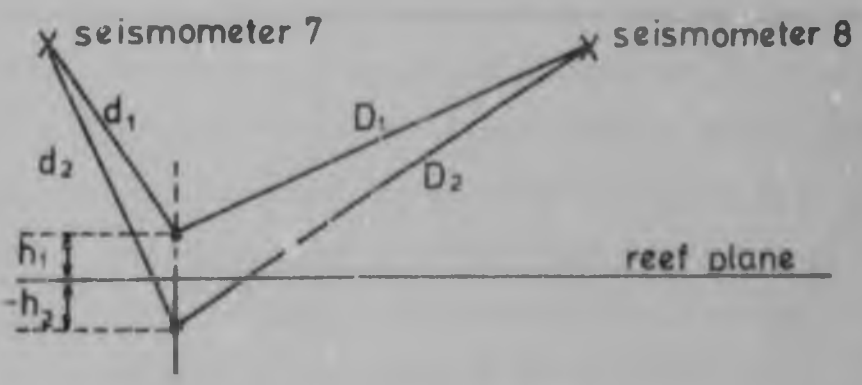


Fig. 3A.

1 to 6. The focus was deliberately made to appear above and below the reef plane, and for each elevation, $h_n$, the distances $d_n$ and $D_n$ were measured. The travel time from the focus to the seismometers can be found from the seismic record and the time of origin, determined on the locator. Hence, the apparent velocities $v_n$ and $V_n$ can be calculated for each elevation. For each event the apparent velocities to seismometers 7, 8 and 9 were obtained for a number of elevations. All the selected seismic events were analysed in this way, and Figures 4A to 13A show some of the plots of apparent velocity, V, versus elevation above reef, h. The curves marked near and far are for seismometers 7 and 8; the near curve is for the seismometer that is nearest to the focus of the seismic event.

There are two factors which permit the determination of the elevation of the event, namely,

a) The seismometer furthest from the focus of the seismic event must show an apparent velocity higher than the nearer one. Hence the elevation of the event must be to the right of the intersection of the near and far curves. This condition still applies even if the strata dip a little relative to the seismometers; however, the focal position for which the apparent velocities are equal, occurs at a slightly asymmetrical position. In practice, it may sometimes be necessary to choose an elevation slightly to the left of the intersection, since there is frequently a little uncertainty in the reading of the seismic records.

b) From the velocity calibration for seismometer 8, a velocity of 19,250 ft./sec. was obtained when the charge was fired in the reef plane directly below it, and 19,700 ft./sec. when the charge was in the reef plane

/ and a ....


Fig 4A

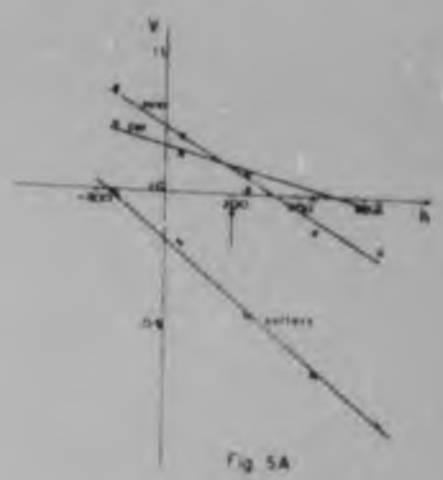


Fig 5A


Fig 6A


Fig 7A

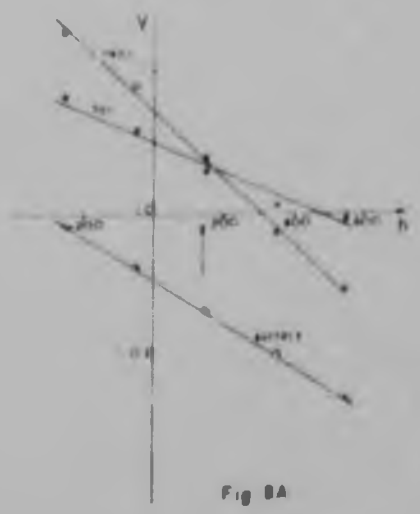


Fig 8A

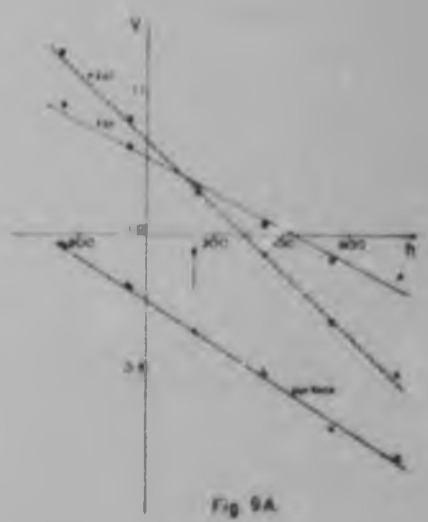


Fig 9A

FIGURES 4A-9A THE VARIATION OF APPARENT VELOCITY WITH ELEVATION ABOVE THE REEF PLANE.


Fig 10A


Fig 11A

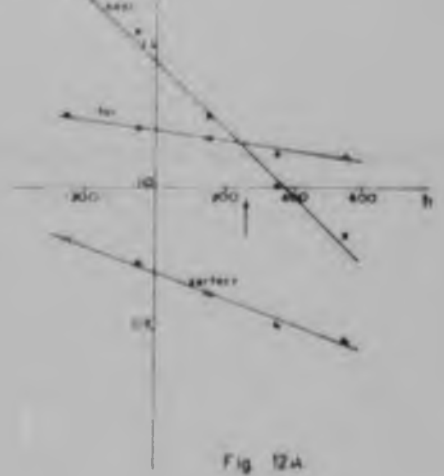


Fig 12A

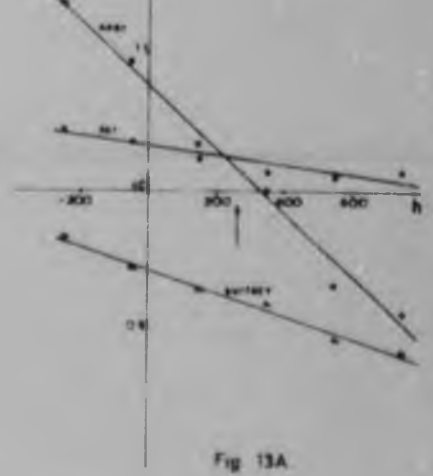


Fig 13A

FIGURES 10A-13A — THE VARIATION OF APPARENT VELOCITY WITH ELEVATION ABOVE THE REEF PLANE.

and a few thousand feet to the side. Thus when 19,000 ft./sec. is taken as the velocity near the reef plane, the apparent velocity to this seismometer should be 1 percent to 4 percent higher than 19,000 ft./sec. A similar argument applies to seismometer 7. Seismometer 9 on surface, however, should have an apparent velocity about 6 percent lower than 19,000 ft./sec.

In Figures 4A to 13A V = 1.0 represents a velocity of 19,000 ft./sec. The arrows indicate the most likely elevation satisfying these conditions. It can be seen that there is good agreement between the two conditions and that most of the events occurred well above the reef plane.

APPENDIX 2

In the Central Projection, planes passing through the focus project as straight lines. Two planes at right angles passing through the focus project as two intersecting straight lines at an angle $\theta$ to each other. The angles of dip, $\phi_1$ and $\phi_2$ of the two planes are related to $\theta$.

Let the projection plane be the plane $Z = 0$, with the focus at $(0, 0, -1)$, and let $l_1$, $m_1$, $n_1$, and $l_2$, $m_2$, $n_2$, be the direction cosines of the two planes, Figure 14A(a). Since the two planes are at right angles

$$l_1 l_2 + m_1 m_2 + n_1 n_2 = 0$$

The equations of the two planes are

$$l_1 x + m_1 y + n_1 (z + 1) = 0$$

and $$l_2 x + m_2 y + n_2 (z + 1) = 0$$

The intersections of these two planes with the projection plane $z = 0$ are

$$l_1 x + m_1 y + n_1 = 0$$

$$l_2 x + m_2 y + n_2 = 0$$

and are shown in Figure 14A(b).

Consider two points C and D on one projection line and two points E and F on the other line

$$C \left(0, -\frac{n_1}{m_1}, 0\right) \text{ and } D \left(-\frac{n_1}{l_1}, 0, 0\right)$$

$$E \left(0, -\frac{n_2}{m_2}, 0\right) \text{ and } F \left(-\frac{n_2}{l_2}, 0, 0\right)$$

then $$\underset{\sim}{CD} = \left\{ -\frac{n_1}{l_1}, \frac{n_1}{m_1}, 0 \right\}$$

$$\underset{\sim}{EF} = \left\{ -\frac{n_2}{l_2}, \frac{n_2}{m_2}, 0 \right\}$$

and $$\underset{\sim}{CD} \cdot \underset{\sim}{EF} = (CD) \times (EF) \cos \theta$$

/ ....

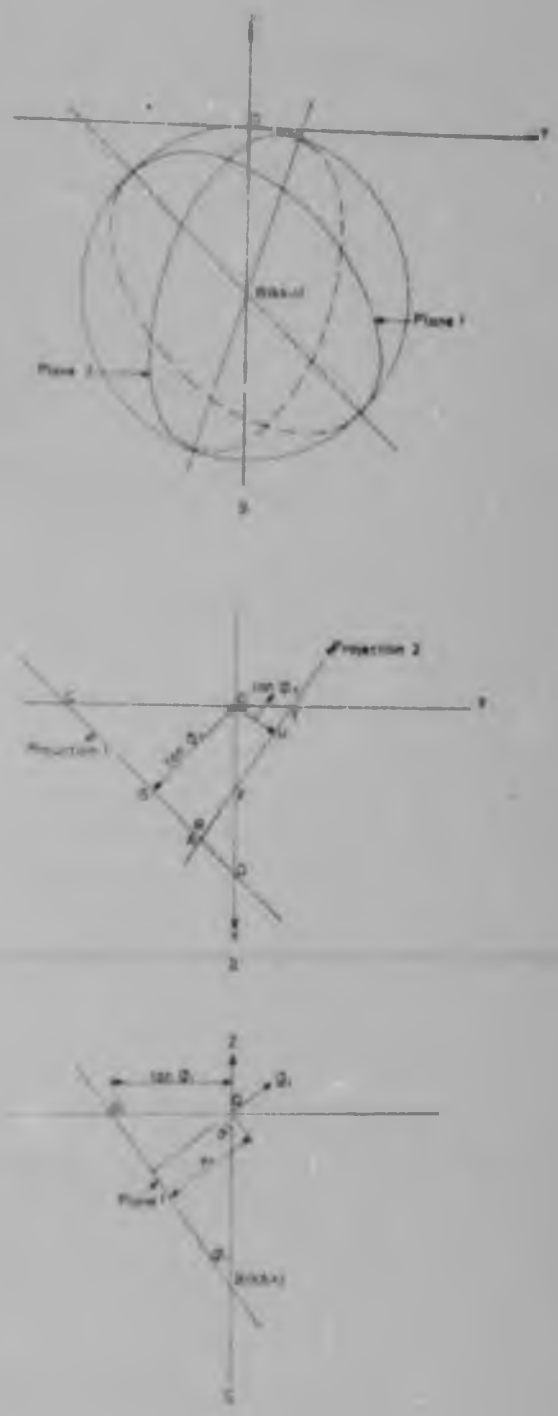

FIGURE 14A THE CENTRAL PROJECTION

$$\underset{\sim}{CD}\cdot\underset{\sim}{EF} = \sqrt{\frac{n_1^2}{\ell_1^2} + \frac{n_1^2}{m_1^2}}\ \sqrt{\frac{n_2^2}{\ell_2^2} + \frac{n_2^2}{m_2^2}}\ \text{Cos}\ \theta$$

$$= \frac{n_1\, n_2}{m_1 \ell_1 m_2 \ell_2}\ \sqrt{1 - n_1^2}\ \sqrt{1 - n_2^2}\ \text{Cos}\ \theta$$

Since $\ell_1^2 + m_1^2 + n_1^2 = 1$

and $\ell_2^2 + m_2^2 + n_2^2 = 1$

Also $\underset{\sim}{CD} \cdot \underset{\sim}{EF} = \frac{n_1}{\ell_1}\frac{n_2}{\ell_2} + \frac{n_1}{m_1}\frac{n_2}{m_2}$

$$= \frac{n_1\, n_2}{\ell_1 \ell_2 m_1 m_2}\ (m_1 m_2 + \ell_1 \ell_2)$$

$$= \frac{n_1\, n_2}{m_1 \ell_1 m_2 \ell_2}\ (-\, n_1 n_2)$$

Since $\ell_1 \ell_2 + m_1 m_2 + n_1 n_2 = 0$

thus

$$\text{Cos}\ \theta\ \frac{-\, n_1\, n_2}{\sqrt{1 - n_1^2}\ \sqrt{1 - n_2^2}}$$

In Figure 14A(c), consider the unit vector $\underset{\sim}{a}_1$ normal to plane 1.

$$\underset{\sim}{a}_1 = \{\ \ell_1,\ m_1,\ n_1\}$$

$$n_1 = \text{Cos}\ \alpha_1 = \text{Sin}\ \phi_1$$

$$\sqrt{1 - n_1^2} = \text{Cos}\ \phi_1$$

$$\therefore\ \frac{n_1}{\sqrt{1 - n_1^2}} = \tan\ \phi_1$$

Similarly $\frac{-\, n_2}{\sqrt{1 - n_2^2}} = \tan\ \phi_2$

$\therefore$ Cos $\theta$ = tan $\phi_1$ tan $\phi_2$

/ This ....

This conclusion provides an easy method for determining when two planes are at right angles. Tan $\phi_1$ and tan $\phi_2$ are the distances of the projection lines from the origin. These distances and $\theta$ can be measured directly from the Central Projection, and only when Cos $\theta$ = tan $\phi_1$ tan $\phi_2$ are the planes at right angles. Notice that the two projection lines must be on opposite sides of the origin.

APPENDIX 3

The transient spectrograph or "Missilyzer" is an audio and sub-audio spectrograph which produces permanent, visual records of complex waveforms. Two different analyses of the recorded data are possible with the "Missilyzer". The first analysis relates frequency and intensity to time and the record is called a "missilgram". The second analysis relates intensity to frequency at a particular instant of time (over a wider dynamic range than the first) and is referred to as a section.

The Missilyzer was used in the 5 to 500 c/s range and 15 to 1500 c/s range corresponding to 1.25 to 125 c/s and 3.75 to 375 c/s seismic signal frequency. The factor of 4 change in frequency arose because the replay deck of the seismic network ran at a speed 4 times faster than the record deck.

Figure 15A shows a general view of the "Missilyzer" and Figure 16A shows sections and missilgrams for a sine wave, a square wave and a triangular wave. The dynamic range in intensity for the missilgram is 6 db. while the dynamic range in amplitude for the section is 25 db.: the bandwidth is 5 c/s. The amplitude scale is not calibrated, so that it merely represents relative amplitude.

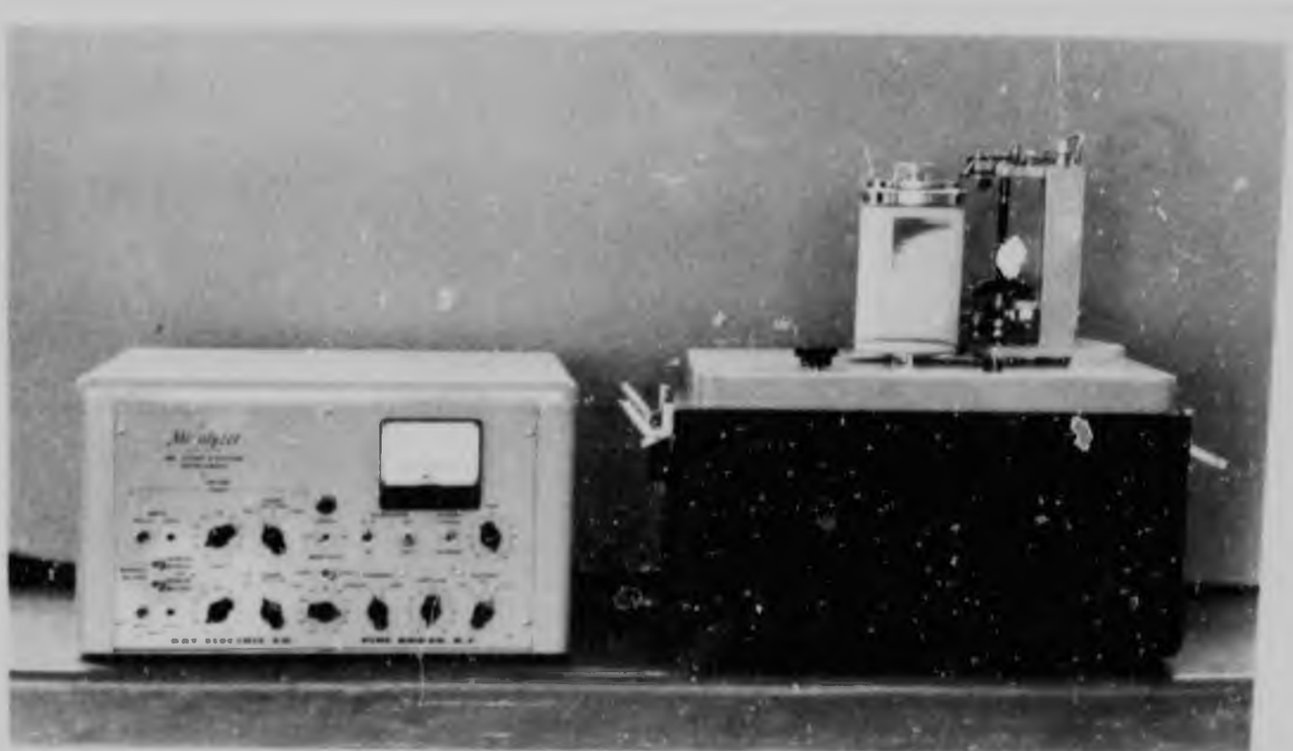

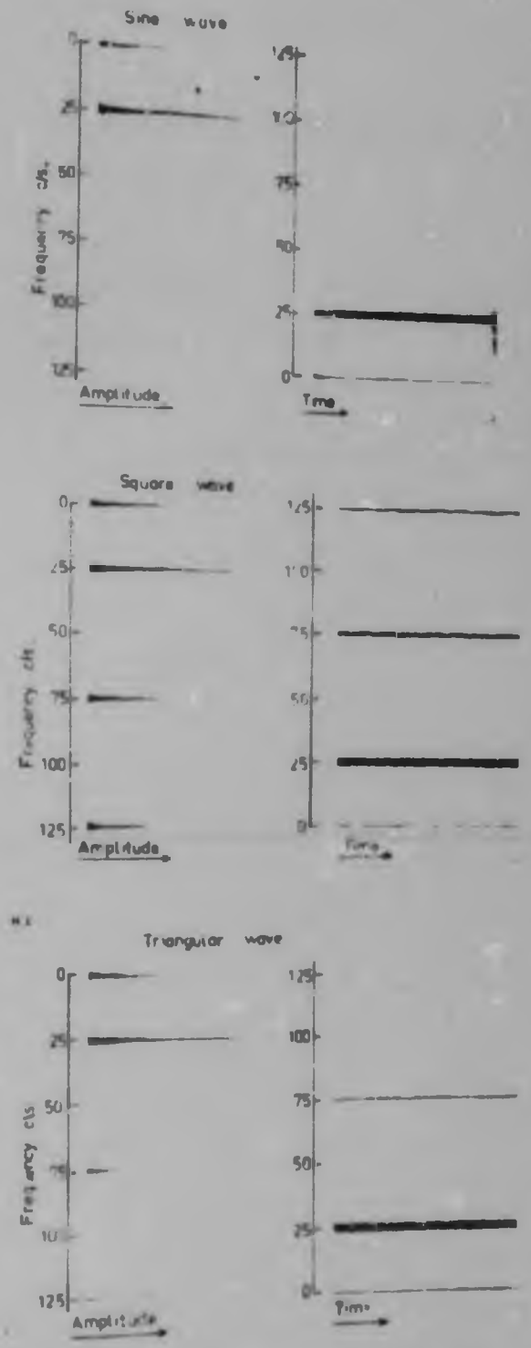


FIGURE 16A SPECTRAL ANALYSIS OF STANDARD 25 c/s WAVES BY THE TRANSIENT SPECTROGRAPH. THE GRAPHS ON THE LEFT ARE "SECTIONS" AND SHOW THE HARMONIC CONTENT OF THE WAVES. THE GRAPHS ON THE RIGHT ARE "MISSILGRAMS" AND SHOW THE HARMONIC CONTENT AS A FUNCTION OF TIME; THE INTENSITY OF THE TRACE REPRESENTS RELATIVE AMPLITUDE.

APPENDIX 4

Figure 17A The frequency response of the Hall-Sears model HS1 seismometer.

Figure 18A Circuit diagram of the record and replay amplifiers.

Figure 19A Circuit diagram of the device performing the operation $\int_0^T v^2 \, dt$.

Figure 20A Circuit diagram of the digital clock.

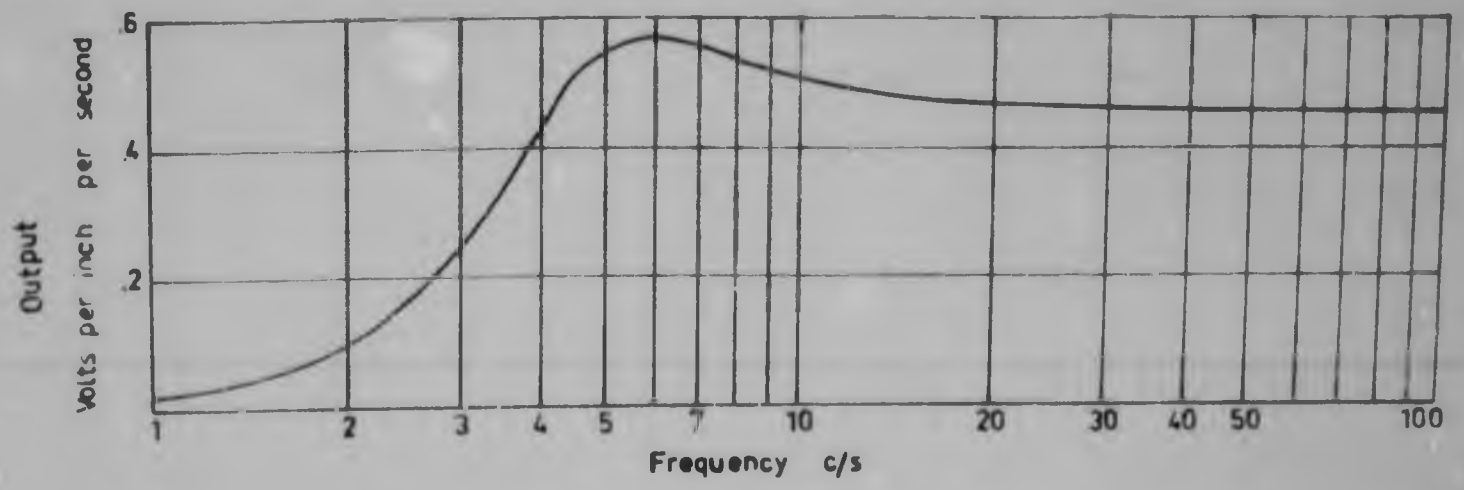


FIGURE 17A THE FREQUENCY RESPONSE OF THE HALL-SEARS MODEL HS1 SEISMOMETER

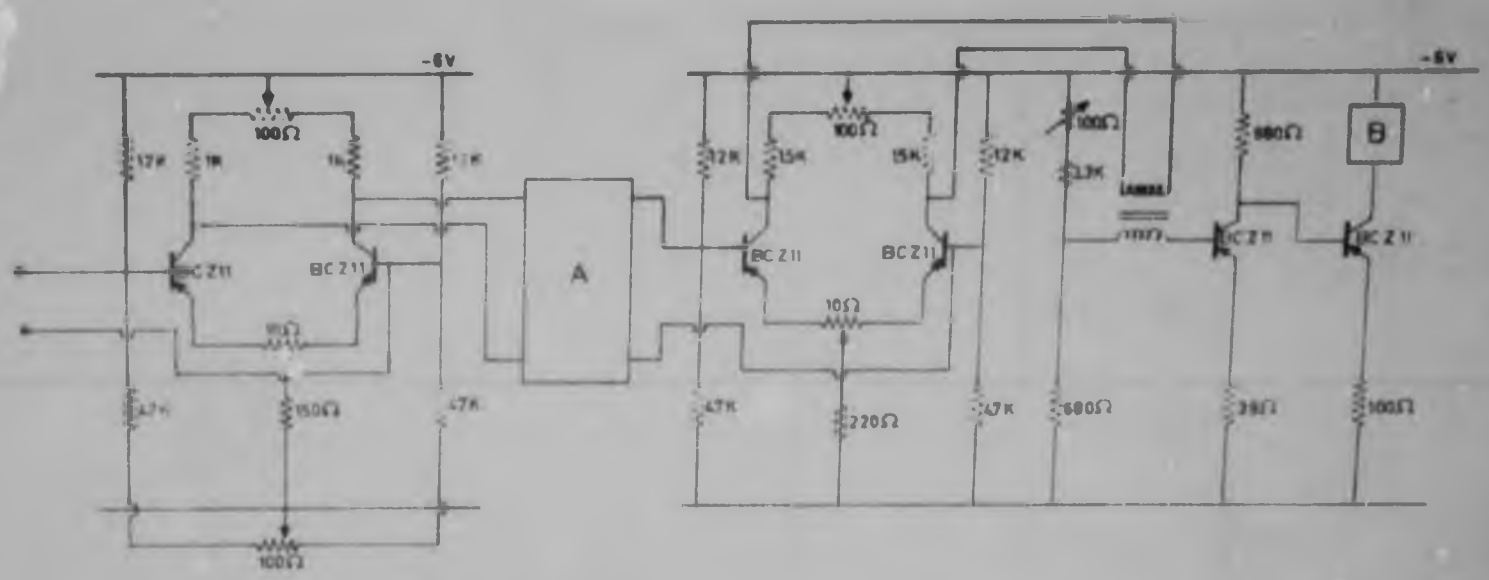


FIGURE 18A A CIRCUIT DIAGRAM OF THE RECORD AND REPLAY AMPLIFIERS. IN THE RECORD AMPLIFIER, A REPRESENTS THE CABLE FROM THE SEISMOMETER TO THE RECORDER AND AN ATTENUATOR, AND B REPRESENTS A 3 OHM RECORDING HEAD. IN THE REPLAY AMPLIFIER, A REPRESENTS AN EQUALIZING NETWORK AND B REPRESENTS A 15 OHM GALVANOMETER.

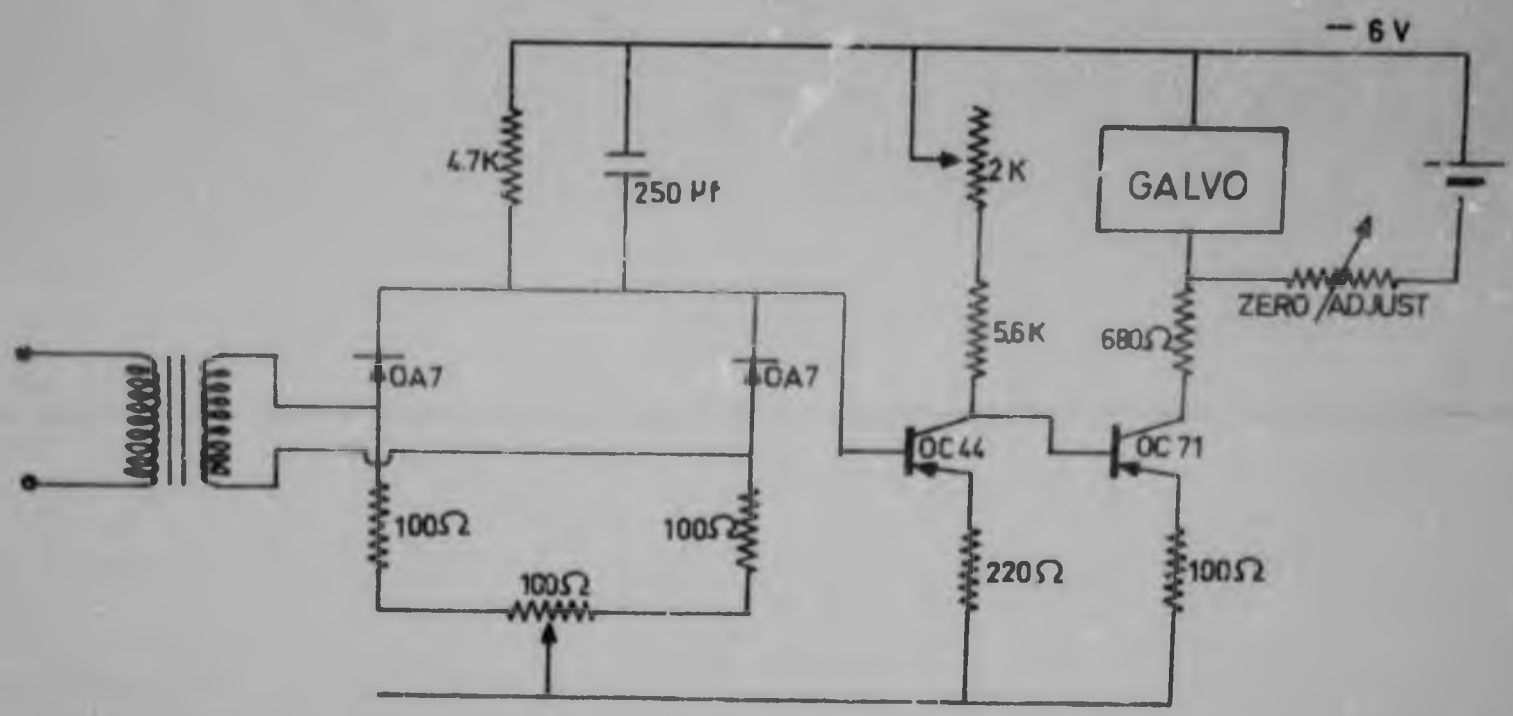


FIGURE 19A THE CIRCUIT DIAGRAM OF THE DEVICE WHICH PERFORMS THE OPERATION

$$\int_0^T v^2 \, dt$$

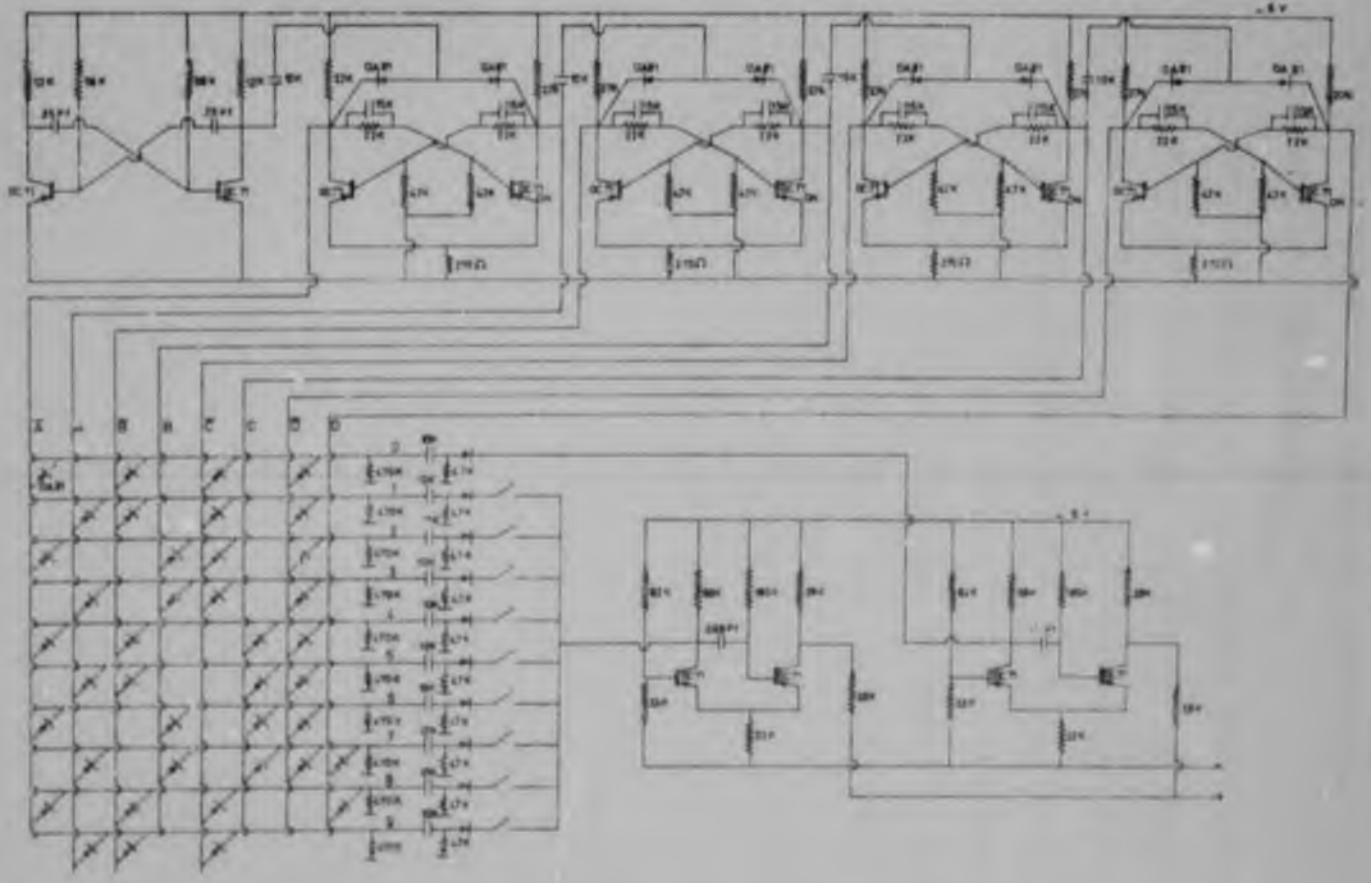

FIGURE 20A CIRCUIT DIAGRAM OF THE DIGITAL CLOCK. THE SERIES OF SWITCHES IS CONTROLLED BY A SERIES OF CAMS DRIVEN BY AN ELECTRIC CLOCK MOTOR.

ACKNOWLEDGEMENTS

Most of this work was carried out at the Bernard Price Institute of Geophysical Research and was sponsored by the Transvaal and Orange Free State Chamber of Mines. The work also forms part of the rock mechanics research conducted by the Mining Research Laboratory of the Transvaal and Orange Free State Chamber of Mines.

I would like to thank the Management and Staff of the Harmony Gold Mining Company, Limited and the Research and Ventilation Department of Rand Mines, Limited for their co-operation and assistance, and for permission to use the data.

I am indebted to Dr. N. .N. Cook for his help and guidance, and I wish to thank Mrs. M. Westcott, Mrs. A. Martinson, Miss R. Port, Mr. G.H.A. Klix and Mr. D. Stepto for their assistance.

REFERENCES

1. BICCARD JEPPE, C. "Gold Mining on the Witwatersrand" Vol.1. The Transvaal Chamber of Mines, 1946.

2. DENKHAUS, H.G. "The application of the mathematical theory of elasticity to problems of stress in hard rock at great depth." Pap. Ass. Min. Mangrs. S. Afr., 1958.

3. BARCZA, M. and VON WILLICH, G.P.R. Strata movement measurements at Harmony Gold Mine. Ass. Min. Mangrs. S. Afr., Circ.10, 1958.

4. DENKHAUS, H.G., HILL, F.G., and ROUX, A.J.A. A review of recent research into rockbursts and strata movement in deep level mining in South Africa. Ass. Min. Mangrs. S. Afr., Circ.8, 1958.

5. WIGGILL, R.B. The effects of different support methods on strata behaviour around stoping excavations. J.S.A.I.M.M., Vol.63, 1963, pp.391-425.

6. PRETORIUS, P.G.D. Some observations on rock pressure at depth on the East Rand Proprietary Mines, Ltd. Ass. Min. Mangrs. S. Afr., Circ.10, 1958.

7. LUTSCH, A., and SZENDREI, M.E. The experimental determination of the extent and degree of fracture of rockby means of sonic and ultrasonic methods. Ass. Min. Mangrs. S. Afr., Circ.10, 1958.

8. GANE, P.G., SELIGMAN, P., and STEPHEN, J.H. Focal Depths of Witwatersrand Tremors. Bull. Seis. Soc. Amer., Vol.43, No.3, July, 1952.

9. COOK, N.G.W. A study of failure in the rock surrounding underground excavations. Thesis presented to the Department of Geophysics of the University of the Witwatersrand, 1962.

/ ....

10. HOEK, E. Rock fracture under static stress conditions. C.S.I.R. (Pretoria) Report MEG 383, 1965.

11. ORTLEPP, W.D., and NICOLL, A. The elastic analysis of observed strata movement by means of an electrical analogue. J.S.A.I.M.M., Vol.65, No.4, 1964, pp.214-235.

12. RYDER, J.A., and OFFICER, N.C. An elastic analysis of strata movement in the vicinity of inclined excavations. J.S.A.I.M.M., Vol.64, No.6, 1964, pp.219-244.

13. COOK, N.G.W. The basic mechanics of rockbursts. J.S.A.I.M.M., Vol.64, No.3, 1963, pp.71-81

14. COOK, N.G.W. A note on rockbursts considered as a problem of stability. J.S.A.I.M.M., Vol.65, No.8, 1965, pp. [illegible]-446.

15. COOK, [illegible] W. The failure of rock. Int. J. Rock Mech. and [illegible] Sci., Vol.2, 1965, pp.389-403.

16. BEN-[illegible]d, A., and TOKSÖZ, M.N. Source-mechanism from spectra of long-period surface-waves.
(1) J. Geophys. Res., Vol.67, No.5, 1962, pp.1943-1955
(2) J. Geophys. Res., Vol.68, No.18, 1963, pp.5207-5222
(3) Bull. Seis. Soc. Amer., Vol.53, 1963, pp.905-919.

17. HIRASAWA, T., and STAUDER, W. [illegible]e seismic body waves from a finite moving source. Bull. Seis. Soc. Amer., Vol.55, No.2, 1965, pp.237-262.

18. COOK, N.G.W. The design of underground excavations. Eighth Rock Mechanics Symposium, Minneapolis, 1966.

19. COOK, N.G.W., and SCHÜMANN, E.H.R. An electrical resistance analogue for planning tabular mine excavations. Tvl. & O.F.S. Chamber of Mines Research Report No.72/65, 1965.

/ ....

20. ORTLEPP, W.D. Summary of strata movement observations by Rand Mines, Ltd. (1955-1963). Consulting Engineers' Mining Research and Ventilation Department, Report No.12, July, 1963.

21. COOK, N.G.W., HOEK, E., PRETORIUS, J.P.G., ORTLEPP, W.D., and SALAMON, M.D.G. Rock mechanics applied to the study of rockbursts. J.S.A.I.M.M., Vol.66, No.10, 1966, pp.435-528.

22. PETERSEN, A.C., and BOTHA, R.C. The use of concrete for stope support on Harmony Gold Mining Company, Limited. J.S.A.I.M.M., Vol.66, No.11, 1966, pp.565-624.

23. BRACE, W.F. Dependence of fracture strength of rocks on grain size. Penn. State Univ. Mineral Expt. Sta. Bull. No.76, 1961, pp.99-103.

24. BRACE, W.F., and BOMBOLAKIS, E.G. A note on brittle crack growth in compression. J. Geophys. Res., Vol.68, No.12, 1963, pp.3709-3713.

25. HOEK, E., and BIENIAWSKI, Z.T. Fracture propagation mechanism in hard rock. International Society of Rock Mechanics, First International Congress, Lisbon, 1966.

26. COOK, N.G.W., and FAIRHURST, C. The phenomenon of rock splitting parallel to a surface under a compressive stress. International Society of Rock Mechanics, First International Congress, Lisbon, 1966.

27. OROWAN, E. Fracture and strength of solids. The Phys. Soc. (London), Repts. on Progress in Physics, Vol.12, 1949, pp.185-232.

28. SACK, R.A. Extension of Griffith's theory of rupture to three dimensions. Phys. Soc. (London), Proc., Vol.58, 1946, pp.729-736.

/ ....

29. STARR, A.T. Slip in a crystal and rupture in a solid due to shear. Proc. Camb. Phil. Soc., Vol.24, 1928, p.489.

30. JAEGER, J.C. "Elasticity, Fracture and Flow" Methuen, London, 2nd Ed., 1962.

31. BARRON, K. C.S.I.R. (Pretoria) Contract Report MEG 425. Restricted - Not for publication.

32. KNOPOFF, L., and GILBERT, F. First motions from seismic sources. Bull. Seis. Soc. Amer., Vol.50, No.1, 1960, pp.117-134.

33. COOK, N.G.W., and HODGSON, K. Some detailed stress-strain curves for rock. Journ. Geophys. Res., Vol.70, No.12, 1965, pp.2883-2888.